Inhibition of Hox Function by the Cell Cycle Regulator Geminin

PhD Thesis

in partial fulfillment of the requirements
for the degree “Doctor of Philosophy (PhD)”
in the Molecular Biology Program
at the Georg August University Göttingen,
Faculty of Biology

submitted by

Lingfei Luo

born in
Chongqing, P.R.China

Göttingen 2004

Affidavit

Here I declare that my Ph.D. thesis entitled “Inhibition of Hox function by the cell cycle regulator Geminin” has been written independently and with no other sources and aids than quoted.

Lingfei Luo
August 4th, 2004
Göttingen

Publications:

Lingfei Luo, Xiaoping Yang, Yoshihiro Takihara, Hendrik Knoetgen and Michael Kessel. The cell-cycle regulator geminin inhibits Hox function through direct and polycomb-mediated interactions. *Nature*, **427(6976):** 749-753 (2004).

Lingfei Luo and Michael Kessel. Geminin coordinates cell cycle and developmental control. *Cell Cycle*, **3(6):** 711-714 (2004).

Lingfei Luo and Michael Kessel. Coordination between patterning and cell cycle control by Geminin. *MPIbpc News*, **10(5):** 1-4 (2004).

Acknowledgements

This work was done from October 2001 to July 2004 in the Research Group Developmental Biology, Department of Molecular Cell Biology in the Max-Planck-Institute for Biophysical Chemistry, under the direction of Prof. Dr. Michael Kessel.

Upon the accomplishment of my Ph.D. career, I would first like to sincerely acknowledge my supervisor, Prof. Dr. Michael Kessel, for his patient supervision as well as extensive support both in science and in everyday life. In the period of these three years, what I have learned from him are not only knowledges and techniques. More important, from his serious and strict scientific attitude, I have learned how to be a good scientist. I cannot be more grateful to him.

I would also like to cordially appreciate the members of my thesis committee, Prof. Dr. Herbert Jäckle and Prof. Dr. Tomas Pieler, as my co-supervisors. They have put great efforts into my Ph.D. project and provided me many valuable suggestions.

When I was a neophyte in the lab and knew almost nothing about developmental biology, it was Dr. Hendrik Knoetgen who first led me into this area. I would like to express my cordial appreciation to him.

Many thanks to the members in our department, especially Priv. Doz. Dr. Ahmed Mansouri, Dr. Lars Wittler, Dr. Ulrike Teichmann, Dr. Nicole Bäumer, Dr. Mara Pitulescu, Sven Pilarski (M.Sc.), and Yvonne Uerlings for suggestions and discussions. Thank Wiebke Behrens for her technical assistance and Sharif Mahsur for his help in cell culture.

I have benefited a lot from the Chinese community in the institute, Dr. Xiaoping Yang, Dr. Chaoshe Guo, Dr. Xunlei Zhou and other friends. I am very grateful to them.

I appreciate Prof. Dr. Peter Gruss and Prof. Dr. Dieter Gallwitz for their continuous support on my Ph.D. project.

I also acknowledge the coordination office and all the faculty members of our International M.Sc./Ph.D. Program “Molecular Biology”, especially Dr. Steffen Burkhardt, for their kind help and hard work.

For providing experimental materials, I would like to acknowledge D. Duboule, Y. Takihara, A. Dutta, C. J. Tabin, S. Potter, R. Mass, and H. Koseki for their generosities.

Finally, and importantly, I sincerely say thanks to my parents and my wife for their persistent warm support. When I was almost punched down by experiments or referees, it is them who gave me most of the consolations and encouragements. Without their support, I would not have finished my Ph.D. career successfully. Thank you.

1. Introduction

From fertilization to maturity, a unicellular zygote undergoes numerous cell divisions to form a multicellular organism. During each cell cycle, a single set of genetic information must be accurately passed on to each daughter cell. At the same time, in order to form complex and different functional structures, cells are specialized by activating different combinations of genes during embryonic development. The timing of the cellular fate acquisitions and structure allocations has to be strictly coordinated with the schedule of embryonic growth, ensuring the correct size, location, as well as function of structures. Therefore, there is a strict coordination between embryonic patterning and the cell cycle. From this point of view, dual roles or mutual interactions of typical proliferation and developmental control genes are likely. The aim of my work is to understand the roles of a typical cell cycle regulator, Geminin, in embryonic development, and to provide further insights into the molecular links between the cell cycle regulation and embryonic patterning.

1.1 DNA Replication Licensing

For the maintenance of the genetic integrity of all organisms, cells must receive a complete copy of their genome every time they divide. This purpose is achieved during two phases of cell cycle: the S phase, during which the genomic DNA is replicated, and the M phase or mitosis, during which the replicated DNA equally segregates into the two newly divided daughter cells. Complete and accurate DNA replication is critical to guarantee the genomic stability from mother to daughter cells. Therefore, replication of the chromosomes is tightly controlled, so that DNA duplicates only once in each cell cycle. This goal is enabled by a process called licensing, which ensures that chromatin becomes competent for the next round of DNA replication only after passage through mitosis (Blow and Laskey, 1988). Licensing involves the ordered assembly of a number of replication initiation factors including the origin recognition complex (ORC), Cdc6, Cdt1, and minichromosome maintenance (MCM) complex, at replication origins, thus resulting in the assembly of pre-replicative complex (pre-RC). The regulation of licensing and the consequent pre-RC formation is a key element of the mechanisms coordinating DNA replication with the cell cycle.

1.1.1 The Origin Recognition Complex

DNA replication licensing is initiated from the binding of ORC to chromatin and achieved after the loading of MCM onto DNA (Fig. 1-1). ORC is a six-subunit complex that acts as the initiator selecting the sites for subsequent replication initiation at eukaryotic origins of replication (Bell and Dutta, 2002). Although identified in *S. cerevisiae* as binding to origins of replication in the chromatin in an ATP-dependent manner (Bell and Stillman, 1992), ORC have been demonstrated in subsequent studies as a conserved key factor for chromosomal replication in all eukaryotes. In *Xenopus* egg extracts, immunodepletion of several ORC subunits individually blocks MCM loading and pre-RC formation, indicating the essential role of the ORC in licensing and the initiation of DNA replication (Rowles *et al.*, 1996; Carpenter *et al.*, 1996; Romanowski *et al.*, 1996). Similarly, recessive lethal mutations in multiple *Drosophila* ORC subunits each show dramatic reductions of BrdU incorporation in third instar larva (Pflumm and Botchan, 2001). The best-understood activity of ORC is its ability to bind DNA at replication origins (Chesnokov *et al.*, 2001). Although this chromatin binding of ORC itself does not accomplish the licensing process, it is necessary for the recruitments of other initiation factors.

1.1.2 Cdc6

Cdc6, one of the members recruited by ORC, was first identified in the original screen of *S. cerevisiae* mutants with changes in the cell division cycle (Hartwell, 1973). It plays a crucial role in the assembly of the pre-RC, since immunodepletion of *Xl*Cdc6 abolishes chromosomal replication, but not elongation, on single-stranded DNA templates. The direct association of Cdc6 with chromatin at the replication origins requires ORC and is in turn required for MCM chromatin association (Coleman *et al.*, 1996; Tanaka *et al.*, 1997), indicating that Cdc6 is involved in the licensing process at a step after ORC and before MCM complex loading. Binding of Cdc6 increases the DNA binding specificity of ORC by inhibiting its non-specific DNA binding (Mizushima *et al.*, 2000). In addition, Cdc6 is an ATPase, and ATP binding and hydrolysis by Cdc6 is strictly required for MCM loading and DNA replication (Perkins and Diffley, 1998; Weinreich *et al.*, 1999).

1.1.3 Cdt1

Cdt1, another initiation factor recruited by ORC, was originally identified in *S. pombe* and implicated as a key factor in chromosomal duplication, since its mutation results in an abolition of DNA replication and defects in the S-phase checkpoint (Hofmann and Beach, 1994). Furthermore, *Sp*Cdt1 was demonstrated to associate with *Sp*Cdc6 to cooperatively promote the loading of MCM onto chromatin (Nishitani *et al.*, 2000). Like other licensing factors, Cdt1 is conserved in other eukaryotes including *Xenopus*, humen and *Drosophila*. In *Xenopus* egg extracts, the chromatin association of Cdt1 requires ORC but not Cdc6. And as in *S. pombe*, *Xl*Cdt1 and *Xl*Cdc6 are also found to be collaboratively required for MCM loading (Maiorano *et al.*, 2000). In *Drosophila*, mutations of Cdt1 show a failure to undergo S phase during the postblastoderm divisions, and defects in DNA replication and amplification in the adult ovary. In common with a role in the pre-RC, *Dm*Cdt1 colocalized with *Dm*ORC at sites of DNA replication and requires *Dm*ORC for this localization (Whittaker *et al.*, 2000). In mammalian cells, Cdt1 and Cdc6 are also mutually dependent on one another for the loading of MCM onto chromatin. The recruitment of MCM by Cdt1 is carried out through direct binding of the C-terminal region of Cdt1 to MCM subunits. Interestingly, the association of Cdt1 with MCM is regulated by cell growth. MCM prepared from quiescent cells associates very weakly with Cdt1, whereas MCM from serum-stimulated cells associates with Cdt1 much more efficiently, correlating with the normal accumulation of Cdc6 as cells progress from quiescence into the G1 phase. Corroboratively, Cdc6 is capable of inducing the binding of MCM to Cdt1, when ectopically expressed in quiescent cells. Further studies have demonstrated that the MCM-Cdt1 association is facilitated by Cdc6 through a direct physical interaction between Cdc6 and Cdt1, which is essential for Cdc6 function as well. Mechanistically, this sheds lights on how Cdt1 and Cdc6 cooperate to promote the MCM loading (Cook *et al.*, 2004). In contrast to Cdc6, there is no enzymatic activity suggested for Cdt1. However, besides the interactions with ORC, Cdc6 and MCM, Cdt1 can also direct bind DNA in a sequence-, strand-, and conformation-independent manner. This DNA binding activity of Cdt1 may contribute to anchoring the MCM complex at the origins of replication (Yanagi *et al.*, 2002).

1.1.4 MCM Complex and the pre-RC Assembly

The genes that encode the MCM2-7 complex were originally identified in genetic screens for proteins involved in plasmid maintenance, cell cycle progression, and chromosome missegregation and were primarily group together based on their sequence similarity (Dutta and Bell, 1997). Each MCM protein is highly related to all others, but unique sequences distinguishing each of the subunit types are conserved across eukaryotes. And all eukaryotes appear to have strictly six MCM proteins that each fall into one of the existing classes (MCM2-7), which together suggest that each MCM member has a unique and critical function. This hypothesis was proved by the lethality that results from deleting any individual MCM gene in yeast (Kelly and Brown, 2000). Subsequently, the functional significance of MCM2-7 multiprotein complex in replication licensing system was confirmed in *Xenopus* egg extracts (Chong *et al.*, 1995; Madine *et al.*, 1995; Kubota *et al.*, 1997). Both biochemical and genetic studies strongly demonstrate that these MCM proteins function together as a complex in the cell. As described above, the assembly of the MCM complex onto chromatin requires the coordinated functions of ORC, Cdc6 and Cdt1. Consistent with these requirements, reexpression of MCM proteins in S phase fails to rescue the replication arrest in MCM mutant (Labib *et al.*, 2000). Once the MCM proteins are loaded on chromatin, ORC and Cdc6 can be removed from the chromatin without interfering subsequent DNA replication (Hua and Newport, 1998), indicating that the successful loading of MCM complex manifests the accomplishment of the licensing process and the pre-RC assembly.

One more point needs to be addressed on the path to replication licensing. There is ample evidence to support an important role of nucleotide binding in controlling the pre-RC assembly. Of the known members of the pre-RC, ten of fourteen proteins have consensus motifs for nucleotide binding (MCM2-7, Orc1, Orc4, Orc5, and Cdc6). Mutations in eight of these ten nucleotide binding motifs result in nonfunctional proteins, with only mutants in the Orc4 and Orc5 ATP binding sites still viable (Bell and Dutta, 2002). Recent studies have begun to elucidate the role of nucleotides in the pre-RC assembly. At least two ATP dependent steps are required on the way to the pre-RC formation. The first step is the association of ORC with the origin, which strictly requires ATP binding but not hydrolysis (Bell and Stillman, 1992; Klemm *et al.*, 1997; Chesnokov *et al.*, 2001). A second ATP dependent step is required for the recruitment of Cdc6 and MCM complex (Seki and Diffley, 2000). Especially during the recruitment of Cdc6, it is very well defined that the ATP binding configurations of

both ORC and Cdc6 are simultaneously required for their mutual interaction (Klemm and Bell, 2001; Mizushima et al., 2000).

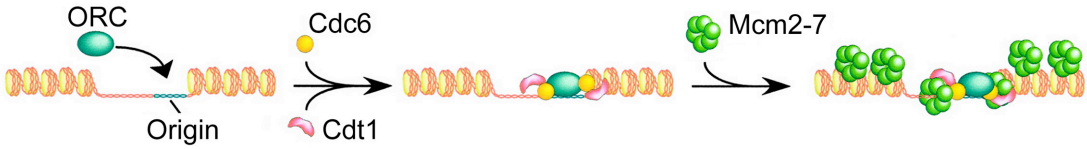

Figure 1-1: The process of DNA replication licensing. DNA replication licensing is initiated by the binding of ORC to chromatin, followed by Cdc6 and Cdt1 recruitment, and finally achieved after the loading of the MCM complex onto DNA (For further discussion, see body text 1.1) (Bell and Dutta, 2002).

In summary, the individual factors depicted above function together to direct the pre-RC formation, a key intermediate in the replication initiation process, and license subsequent DNA replication (Fig. 1-1). Association of ORC with the origin, which is required to recruit both Cdc6 and Cdt1, initiates the assembly of this structure. Cdc6 and Cdt1 associate with ORC-bound chromatin independent of one another (Nishitani *et al.*, 2000; Maiorano *et al.*, 2000). ORC, Cdc6, and Cdt1 together are required for the stable association of the MCM complex with the origin during G1 phase. Although the studies in several different organisms support the basic outline of these events, the molecular details of the recruitments of these different factors to the origin remain unclear.

The formation of pre-RC marks potential sites for the initiation of DNA replication, but multiple other proteins or protein complexes are further required to associate with the origins to initiate DNA synthesis. MCM complex is essential not only for the initiation but also for the elongation stages of DNA replication, since the MCM mutant alleles result in no replication if inactivated prior to S phase, and rapidly arrest the progression of the replication fork if inactivated during S phase (Labib *et al.*, 2000). Mechanistically, roles of the MCM complex are believed to play through either recruitment of further protein factors, or help to unwind DNA helix with its weak, nonprocessive, and intrinsic DNA helicase activity (Ishimi, 1997; You *et al.*, 1999), or interaction with histone and regulation of the local chromatin structures (Labib and Diffley, 2001). The transition from the pre-RC to the replication machinery will not be further discussed here. But, in general, the events occurring

during this transition can be divided into two main stages: the first leading to unwound DNA at origins and the second leading to the loading of DNA polymerase at the primer-template junctions, which together bring about a successful DNA duplication during S phase.

1.2 The Inhibition of DNA rereplication

After DNA replication initiation, it is very critical to ensure that the origins do not refire in the same cell cycle in order to maintain the genetic stability of the organism. Thus, eukaryotic cells have developed a number of redundant mechanisms to prevent DNA replication reinitiation by inhibiting new pre-RC formation, in which cyclin-dependent kinases (CDKs) play pivotal roles.

CDKs have a bipartite role in the regulation of eukaryotic DNA replication. On the one hand, increased CDK activity activates origins of replication when cell enters into S phase. On the other hand, the same elevated CDK activity is also required to prevent reinitiation from origins during S, G2, and M phases of the same cell cycle. The important role of CDKs in preventing rereplication was originally identified by genetic studies in yeast, in which inactivation of CDK activity in G2/M cells resulted in full rereplication of the genome. That the rereplication inhibition activity of CDKs is mediated by the inhibition of pre-RC formation is supported by findings in yeast as well as *Xenopus*, indicating that the elevation of CDK activity in G1 phase prevents the pre-RC formation (Dahmann *et al.*, 1995; Hua *et al.*, 1997; Detweiler and Li, 1998). All the four components of the pre-RC depicted above (ORC, Cdc6, Cdt1, and MCM) have been defined to be phosphorylated by CDKs to prevent rereplication and the pre-RC assembly.

1.2.1 ORC Phosphorylation

Although ORC appears to associate constitutively with origins throughout the cell cycle in yeast and *Drosophila* (Ogawa *et al.*, 1999; Pak et al., 1997), several subunits start to be phosphorylated in a CDK-dependent manner, when cells progress into S phase. This phosphorylation is required for preventing rereplication, since mutations of the phosphorylation sites on ORC lead to a rereplication of the genome (Nguyen *et al.*, 2001; Vas *et al.*, 2001). In contrast, *Xl*ORC is released from the chromatin and exported to the cytoplasm during M phase, which is a consequence of increased CDK activities (Romanowski *et al.*, 1996; Rowles *et al.*, 1999). In mammalian cells,

*Hs*Orc1 is dissociated from chromatin dependent on CDK activities and rapidly degraded after dissociation (Kreitz *et al.*, 2001). Together, CDK dependent ORC phosphorylation serves as one of the multiple, redundant mechanisms to prevent rereplication during the cell cycle.

1.2.2 Cdc6 Phosphorylation

The phosphorylation of Cdc6 by CDK activity is well documented both *in vitro* and *in vivo*, and this phosphorylation turns out to control either degradation or nuclear export of Cdc6 protein at the G1/S transition. In yeast, Cdc6 is targeted for ubiquitin-mediated proteolysis by the E3 ubiquitin ligase SCF (CDC4) from the end of G1 phase until mitosis, following a CDK-dependent phosphorylation. Mutations in several consensus CDK phosphorylation sites at the N-terminus of Cdc6 inhibit the degradation, suggesting that the elevated CDK activity promotes this proteolysis (Drury *et al.*, 1997; Elsasser *et al.*, 1999; Calzada *et al.*, 2000). In contrast, Cdc6 activity is controlled by a different mechnism in mammalian cells, but in a CDK-dependent manner as well. As cell enters S phase, phosphorylation of the *Hs*Cdc6 by CDK triggers the export of the protein from the nucleus. In subsequent mitosis, it is degraded by anaphase promoting complex (APC) mediated ubiquitination and proteolysis (Saha *et al.*, 1998; Jiang *et al.*, 1999; Petersen *et al.*, 2000). However, although mutations of all consensus CDK phosphorylation sites on Cdc6 result in either stabilization (yeast) or nuclear retention (mammals) of Cdc6, they are not sufficient to induce rereplication (Drury *et al.*, 1997; Delmolino *et al.*, 2001; Petersen *et al.*, 1999).

1.2.3 Inactivation of MCM Proteins

To prevent rereplication, CDK dependent phosphorylation also controls the function of the MCM proteins. It can phosphorylate at least Mcm2 and Mcm4 both *in vitro* and *in vivo* (Fujita *et al.*, 1998). Current scrutiny has proposed four possible mechanisms, not mutually exclusive, underlying the functional inhibition of MCM complex by CDK phosphorylation. One mode of regulation, especially in yeast, is likely to be through the regulation of the nuclear localization of the MCM proteins. *Sc*MCM proteins are localized in the nucleus in G1 and S phase, but are exported from the nucleus in G2 and M phase. Inactivation of CDK activity results in the stable maintenance of MCM proteins in the nucleus (Labib *et al.*, 1999; Nguyen *et al.*,

2000). Another possible mechanism is the direct inhibition of MCM complex activities. Phosphorylation of mouse Mcm4 at specific sites by CDK leads to a loss of Mcm4/6/7 helicase activity. In addition, Mcm4/6/7 purified from G1 and G1/S cells, but not from M phase cells, is active as a helicase (Ishimi *et al.*, 2000; Ishimi and Komamura-Kohno, 2001). A third proposed mechanism is that CDK phosphorylation induces release from chromatin and prevents MCM reassociation. In *Xenopus*, Mcm4 is one of the substrates for mitotic CDKs. Mcm4 is underphosphorylated in interphase, and its hyperphosphorylation is correlated with the release of MCM complex from chromatin. Furthermore, hyperphosphorylated MCM complex cannot be assembled onto chromatin any more (Hendrickson *et al.*, 1996; Findeisen *et al.*, 1999; Pereverzeva *et al.*, 2000). Recently, a novel metazoan-specific regulatory system, which serves as the fourth MCM inhibition mechnism during S phase of the cell cycle, was identified in *Xenopus*. In this system, MCM is removed from chromatin and sequestered by direct association with exportin-1/Crm1. This MCM-Crm1 complex formation is required for preventing rereplication, dependent on both Cdk2 activity and high Ran-GTP level. Lowering Ran-GTP within nuclei or nuclear extracts breaks the MCM-Crm1 complex, allows MCM to reassociate with chromatin during S or G2 phase and induces rereplication. Cdk2 kinase activity is a prerequisite and absolutely required for the Ran-GTP dependent MCM-Crm1 complex formation, since the association of MCM to chromatin is no longer inhibited by the addition of Cdk2 specific inhibitor p27/Kip, even in the presence of Ran-GTP. Importantly and intriguingly here, beyond the classic exportin function of Crm1, prevention of rereplication requires MCM-Crm1 association, but does not require export of MCM from the nucleus (Yamaguchi and Newport, 2003).

1.2.4 Controls of Cdt1 Activity

Controls of Cdt1 activity after the pre-RC assembly are also crucial for preventing rereplication. Human Cdt1 accumulates only during G1 phase. The level of the protein decreases after S phase onset, and becomes undetectable in later S phase and G2 (Nishitani *et al.*, 2001). At the G1/S transition, along with the expression of Cyclin A, human Cdt1 is phosphorylated by cyclin A-dependent kinases dependent on its cyclin-binding motif. This CDK phosphorylation results in a physical interaction between Cdt1 and SCF (Skp2) ubiquitin ligase, followed by an SCF (Skp2) mediated ubiquitination and proteolysis of Cdt1. Inhibition of CDK activity by overexpressed

p21 or p27 and the consequent Cdt1 dephosphorylation lead to a disruption of the Cdt1-Skp2 interaction, thus the Cdt1 stabilization and chromatin reassociation. A downregulation of Skp2 by siRNA also brings about a similar Cdt1 accumulation effect in S phase (Li *et al.*, 2003; Sugimoto *et al.*, 2004; Liu *et al.*, 2004). In addition, the DNA binding activity of Cdt1 is also inhibited by CDK phosphorylation, which may contribute to the Cdt1 functional inactivation (Sugimoto *et al.*, 2004). In *C. elegans*, Cdt-1 is present in G1 phase nuclei, but degraded through Cul-4 ubiquitin ligase mediated ubiquitination and proteolysis as cells enter S phase to prevent aberrant DNA replication reinitiation. Inactivation of Cul-4 causes massive DNA re-replication, and Cdt-1 levels fail to decrease during S phase and instead remain constant in the rereplicating cells. Removal of one genomic copy of *Cdt1* suppresses the *Cul-4* mutant rereplication phenotype (Zhong *et al.*, 2003). All these studies have suggested that functional inactivation of Cdt1 appears to be one of the redundant mechanisms to prevent rereplication. Interestingly, in metazoans such as fly, fish, frog, mouse and human, but not in yeast, one more significant protein has been discovered to sequestrate Cdt1 and ensure a complete inhibition of rereplication — Geminin.

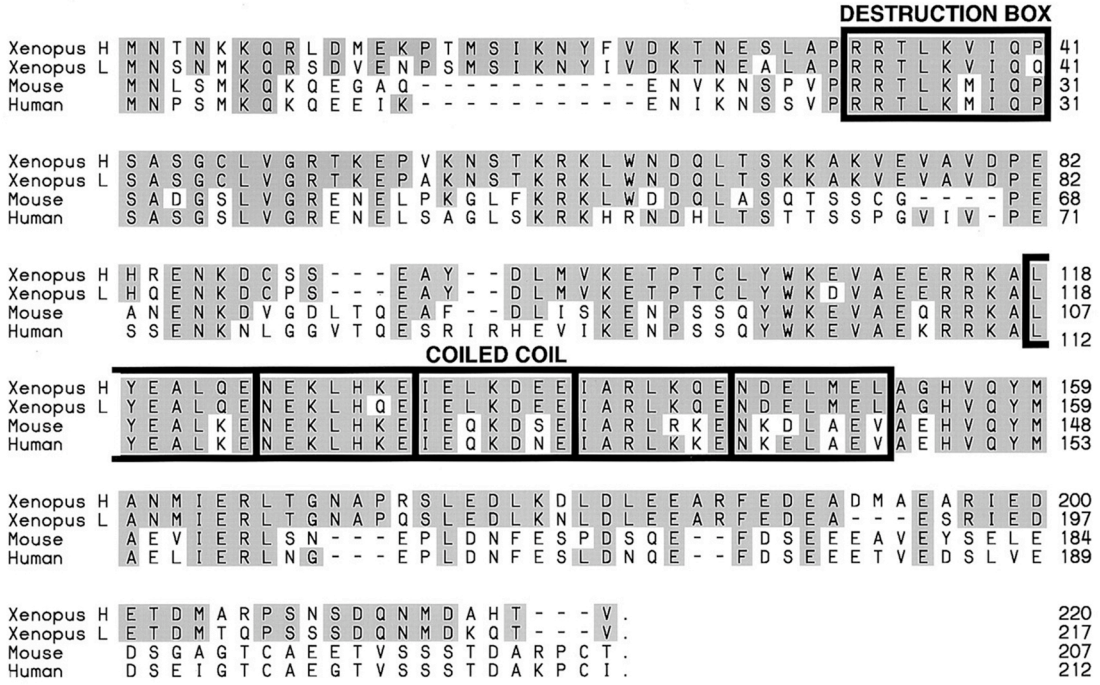

Figure 1-2: The amino acid sequence and conserved structural motifs of Geminin protein. Note that the N-terminal portion contains a consensus destruction box sequence and the central portion contains a conserved coiled-coil domain (McGarry and Kirschner, 1998).

1.3 The Involvement of Geminin in Preventing Rereplication

Geminin was first discovered in a screen for proteins that are degraded by mitotic *Xenopus* egg extracts but not by interphase egg extracts. Except for B-type cyclins, the cDNA encoding Geminin was most abundant in the screen. Several structural motifs have been identified by inspection of the amino acid sequence of Geminin (Fig. 1-2). The N-terminal portion contains a short sequence that has homology to the consensus destruction box of mitotic cyclins and appears to be an ubiquitination signal. The central portion of Geminin contains five heptad amino acid repeats predicted to form a coiled-coil domain that is commonly used in protein dimerization (amino acids 118-152 of *Xl*Geminin). There are clusters of basic amino acids between the destruction box and the coiled-coil domain. They may serve as a nuclear localization signal of the Geminin protein.

1.3.1 The Inhibition Role of Geminin on Cdt1

As discussed above, during G1 phase, Cdc6 and Cdt1 are recruited by ORC to the replication origins and in turn required for the loading of MCM complex onto DNA to form the pre-RC. The formation of pre-RC is essential for the assembly of replication machinery and subsequent DNA replication initiation at S phase onset. Geminin starts to accumulate in the nucleus at this point of the cell cycle after DNA replication is initiated, and maintains its nuclear presence until the end of mitosis. Geminin physically interacts with Cdt1, and sequesters Cdt1 from its role in the pre-RC assembly, thus preventing DNA rereplication. In the cell-free *Xenopus* egg extracts system, the supply of recombinant Geminin protein disrupts the pre-RC assembly by inhibiting the loading of MCM proteins, without affecting the chromotin association of ORC and Cdc6. Consequently, this unloading of MCM proteins leads to an inhibition of nuclear DNA replication. All these inhibitory effects resulted from recombinant Geminin can be efficiently rescued by the addition of excess Cdt1 (McGarry and Kirschner, 1998; Wohlschlegel *et al.*, 2000). Immunodepletion of endogenous Geminin from metaphase *Xenopus* egg extracts allows MCM complex to associate with replication origins and promotes DNA replication. This gain of licensing activity in the absence of Geminin is not due to the loss of CDK activity. Conversely, the inhibition of CDKs in metaphase extracts stimulates origin assembly only after the depletion of Geminin, further suggesting that Geminin is the major inhibitor of rereplication in metaphase (Tada *et al.*, 2001).

The inhibition of rereplication by Geminin through Cdt1 sequestration is conserved in metazoans. The *Drosophila* Geminin homolog also inhibits DNA replication *in vitro* by preventing binding of MCMs to chromatin (Quinn *et al.*, 2001). The *in vivo* overexpression of Geminin in *Drosophila* embryos results in a general decrease of BrdU-labeling cells in mitotic and endoreplicating tissues, that is, an inhibition of DNA replication. The DNA replication inhibition phenotype is accompanied by a dramatic decrease of S phase cells, increased numbers of metaphase cells and apoptosis. In addition, Geminin overexpression during the early proliferative phase of the eye-antennal imaginal disc also results in an extraordinary decrease of S phase cells, thus the size of third instar larvae eye discs and adult eye. In agreement with the overexpression phenotypes and the inhibitory role of Geminin in DNA replication, Drosophila Geminin mutants exhibit overreplication defects late in embryogenesis and in oogenesis. For an instance, in most stage-12 wild type ovaries, DNA amplification is only observed in the anterior region in one focus per cell, whereas 100% of Geminin mutant stage-12 ovaries show strong BrdU labeling of four amplification loci in all follicle cells. By stage-14, all follicle cells of wild type ovaries have ceased DNA amplification, whereas many follicle cells from Geminin mutant ovaries still continue amplification. Mechanistically, Geminin not only physically associates with Cdt1 like in other species, which is clarified by an immunoprecipitation from *Drosophila* embryos, but also interacts genetically with Cdt1. A similar phenotype of Geminin overexpression is observed in Cdt1 mutants, suggesting their opposite roles in regulating DNA replication. Halving the dosage of Cdt1 enhances the Geminin overexpression eye phenotype, leading to a smaller and rougher eye. Vice versa, the Cdt1 mutant phenotypes can be suppressed by a Geminin mutant (Quinn *et al.*, 2001). Therefore, it seems that the regulatory role of Geminin in DNA replication and the mechanism are conserved among metazoans.

Direct elimination of Geminin by antisense techniques in developing *Xenopus* embryos provide further insight into the roles and mechanisms of Geminin in preventing rereplication. The Geminin eliminated embryos have a unique early embryonic lethal phenotype. These embryos arrest in G2 phase immediately after the midblastula transition, the point in development when the cell cycle slows and zygotic gene expression begins. The cells in the deficient embryos show overreplicated DNA content, which confirms the role of Geminin in preventing rereplication. The mechanisms of Geminin loss of function to arrest the embryos in G2 phase partly

assign to a hyperphosphorylation of Chk1 protein kinase, an effector to implement checkpoint response. The activated Chk1 by increased phosphorylation prevents entry into mitosis in part by inhibiting Cdc25C, the phosphatase that removes the phosphates from T14 and Y15 of the mitotic cyclin-dependent kinase Cdc2 and consequently activates Cdc2 at the onset of mitosis. Cdc2 is always hyperphosphorylated on Y15 and maintained as an inactive form in the absence of Geminin. Bypassing of Chk1 pathway by injecting either Cdc25C mutant or Chk1 mutant individually rescues G2 arrest phenotype (McGarry, 2002). Similarly, in support to the rereplication inhibition role of Geminin, silencing of Geminin by siRNA in *Drosophila* Schneider D2 cells leads to a cessation of mitosis and asynchronous overrreplication of the genome, with cells containing single giant nuclei and partial ploidy between 4N and 8N DNA content (Mihaylov *et al.*, 2002). This phenotype of Geminin deficiency is completely rescued by cosilencing of Cdt1, in agreement with the mechanism discussed above that Geminin prevents rereplication by direct sequestering Cdt1. In addition, the phenotype induced by Geminin knock down is also partially rescued by coablation of Chk1, again indicating the involvement of Chk1 in the checkpoint control in response to DNA overreplication (Mihaylov *et al.*, 2002). Together, loss of function phenotypes in both *Xenopus* embryos and *Drosophila* cells reinforce our understandings that Geminin plays a pivotal role in DNA rereplication inhibition through Cdt1 binding and sequestration.

The Cdt1 interaction domain is mapped into the coiled-coil domain of Geminin. A fragment of *Xl*Geminin consisting only of amino acids 87-168, which includes the coiled-coil domain, is sufficient to inhibit DNA replication (McGarry and Kirschner, 1998). By contrast, the N-terminal domain, which does not interact with Cdt1 but accounts for the neuralizing activity of Geminin (see below), has no effect on DNA replication or cell cycle progression. In mammals, the Geminin binding region of Cdt1 has also been characterized. The Cdt1 central region (amino acids 177-380) is demonstrated to be the Geminin binding domain, whereas Mcm6 interacts with the Cdt1 C-terminal region (amino acids 407-477). Interestingly, the C-terminal region of Cdt1 is conserved among all eukaryotes including yeast, whereas the central Geminin binding region is only conserved in metazoans, which exactly correlates with that Geminin is a metazoan specific protein.

Recent studies provide further insight into the molecular basis of the Geminin-Cdt1 regulatory mechanisms in mammalian cells. The DNA binding domain of Cdt1

partly overlaps with its Geminin association domain. Therefore, the tight Geminin-Cdt1 interaction masks the DNA binding region of Cdt1 and inhibits the association of Cdt1 to replication origins in the chromatin. Furthermore, the Geminin-Cdt1 interaction blocks the binding of Cdt1 to Mcm2/6 as well as Cdc6, thus inhibiting the association of Cdt1 into pre-RC and the subsequent MCM complex recruitment. Although the Geminin and MCM interaction domains of Cdt1 are independent and the mechanisms underlying the inhibition of Cdt1-MCM association by Geminin still remain unclear, it is plausible to speculate that the binding of Geminin to the Cdt1 central region leads to a conformational change in the overall structure of Cdt1, which concomitantly results in its C-terminal MCM binding domain to be masked. Together, by means of interacting with and sequestering Cdt1, Geminin blocks the bindings of Cdt1 to DNA, Cdc6 and MCM proteins, thus inhibiting the assembly of pre-RC and preventing DNA rereplication (Yanagi *et al.*, 2002; Cook *et al.*, 2004). In addition, the CDK dependent phosphorylation of Cdt1 during S phase does not interfere with its binding to Geminin, suggesting that the phosphorylation and Geminin binding of Cdt1 are independent but function synergically to ensure a thorough inactivation of Cdt1, thus a complete DNA rereplication inhibition (Sugimoto *et al.*, 2004).

1.3.2 Inactivation of Geminin

After being expressed at early S-phase, the nuclear presence of Geminin is maintained in the following S, G2, and M phases of cell cycle until the anaphase-telophase transition, during which the nuclear Geminin protein needs to be inactivated to release Cdt1, hence making the Cdt1 protein available for the pre-RC assembly and licensing the DNA replication in the next round of cell cycle. At the end of mitosis, the nuclear Geminin protein is inactivated in a number of pathways in different organisms. In agreement with the N-terminal consensus destruction box sequence, the mitotic degradation of Geminin was first identified in *Xenopus* egg extracts and it was suggested to be through the APC mediated ubiquitination and proteolysis (McGarry and Kirschner, 1998). The *in vitro* transcribed/translated Geminin protein is stable in interphase egg extracts, whereas it is ubiquitinated and disappeared with a half-life of 15 minutes in mitotic egg extracts. This Geminin degradation is dependent on APC activity, since the co-incubation of cyclinB destruction box peptide (D-box peptide) as a dominant-negative APC inhibitor restrains the formation of Geminin-ubiquitin conjugates and stabilizes Geminin in mitotic extracts. If the destruction box is deleted

from the protein sequence, the resulted mutant Geminin^{DEL} recombinant protein is then stable in mitotic extracts but retains the wild type DNA replication inhibition activity. This correlates with the characterization of the coiled-coil domain as the DNA replication inhibition domain of Geminin. An injection of the mutant Geminin^{DEL} protein into one cell of a two-cell *Xenopus* embryo does not affect the process of cytokinesis and cell cleavage. However, the injected embryos fail to replicate their chromosomal DNA properly, thus the cells produced by cleavage are completely anucleated. Consequently, these embryos do not develop normally with a cessation at the blastula stage and never proceed into gastrulation. In contrast, embryos injected with the same concentration of wild type Geminin have small, misshapen nuclei instead of anucleated cells, indicating much weaker or even no DNA replication inhibition (McGarry and Kirschner, 1998). The APC mediated ubiquitination and degradation also turns out to be a substantial mechanism to inactivate Geminin in mammalian cells. In synchronized Hela cells, the dynamics of endogenous Geminin indicates that Geminin starts to disappear at the end of mitosis and accumulates again during the next early S phase. Although a transient overexpression of wild type Geminin in U2OS cells, an osteosarcoma cell line, does not result in a cell cycle progression defect, an overexpression of the nondegradable mutant Geminin^{DEL} arrests cell proliferation (Wohlschlegel *et al.*, 2002; Shreeram *et al.*, 2002). A recent study characterizes the roles of the Geminin destruction box in regulating cell cycle in details by knocking out the N-terminal 27 amino acids of Geminin, including most of the destruction box, through homologous recombination in HCT116 human cancer cell line (Yoshida *et al.*, 2004). The excision of the destruction box stabilizes the endogenous Geminin protein in all phases of cell cycle without elevating the total amount of Geminin, simultaneously eliminating the pleiotropic effects due to the overexpression of an exogenous protein. The G1 stabilization of Geminin diminishes chromatin loading of MCM complex, thus inhibiting the assembly of pre-RC and subsequent DNA replication. The DNA replication inhibition phenotype of mutated cells is accompanied by an activation of DNA damage checkpoint pathway with increased levels of p53 and p21 proteins, but without triggering apoptosis that normally happens in cases of Geminin overexpressions (Quinn *et al.*, 2001; Shreeram *et al.*, 2002). In addition, since the mutated Geminin inhibits cell proliferation, the *in vivo* tumorigenesis capacity of the HCT116 cell line is suppressed in mutant cells. All these deficits resulted from the

deletion of Geminin destruction box can be efficiently rescued by overexpression of Cdt1, which further supports the inhibition role of Geminin on Cdt1 (Yoshida *et al.*, 2004). The *Drosophila* Geminin also contains the destruction box and is degraded at the end of mitosis, although there is no direct evidence showing that this *Dm*Geminin degradation is APC dependent (Quinn *et al.*, 2001; Mihaylov *et al.*, 2002). Therefore, the degradation of Geminin during the anaphase is significant for DNA replication licensing and normal cell cycle progression. Alteration of the cell cycle dependent regulation of Geminin inhibits DNA replication and suppresses tumor growth. However, besides the APC mediated degradation, redundant mechanisms to inactivate Geminin were also discovered.

In *Xenopus* egg extracts, although some Geminin degradation is clearly observed upon exit from mitosis, 30-60% of endogenous Geminin resists degradation and maintains its existence after released into interphase. The presence of Geminin protein in the interphase extracts does not prohibit the loading of MCM complex onto chromatin (Hodgson *et al.*, 2002). For the licensing system to be activated, the remaining Geminin has to be inactivated. One of mechanisms involves the CDK dependent transient polyubiquitination without proteolysis, in which the destruction box sequence also serves as the ubiquitination signal. This transiently ubiquitinated Geminin loses its affinity to Cdt1, and cannot form a complex during the interphase. Thus, MCM complex can be successfully loaded onto chromatin to license the DNA replication in S phase. The inhibitors blocking APC mediated ubiquitination such as the D-box peptide result in a recomplex of Geminin and Cdt1, preventing activation of the licensing system. In contrast, inhibitors of the 26S proteasome, in which the APC ubiquitinated proteins are digested, do not interfere with the inactivation of Geminin. The mitotic CDK inhibitors lead to a derepression of Geminin and a consequent loss of licensing activity, suggesting the inactivation of Geminin is CDK dependent. Nevertheless, Geminin is only transiently ubquitinated on exit from mitosis, with deubiquitination leaving Geminin still locked into an inactive form. One possible way is through a second covalent modification that is dependent on earlier ubiquitination of Geminin. Alternatively, ubiquitination may force Geminin into an inactive conformation. Together, although some of the ubiquitinated Geminin is degraded, this is not essential for activation of the licensing system. In order to ensure the activation of the licensing system, the CDK dependent transient ubiquitination is

essentially required to inactivate the remaining Geminin protein during interphase (Li and Blow, 2004).

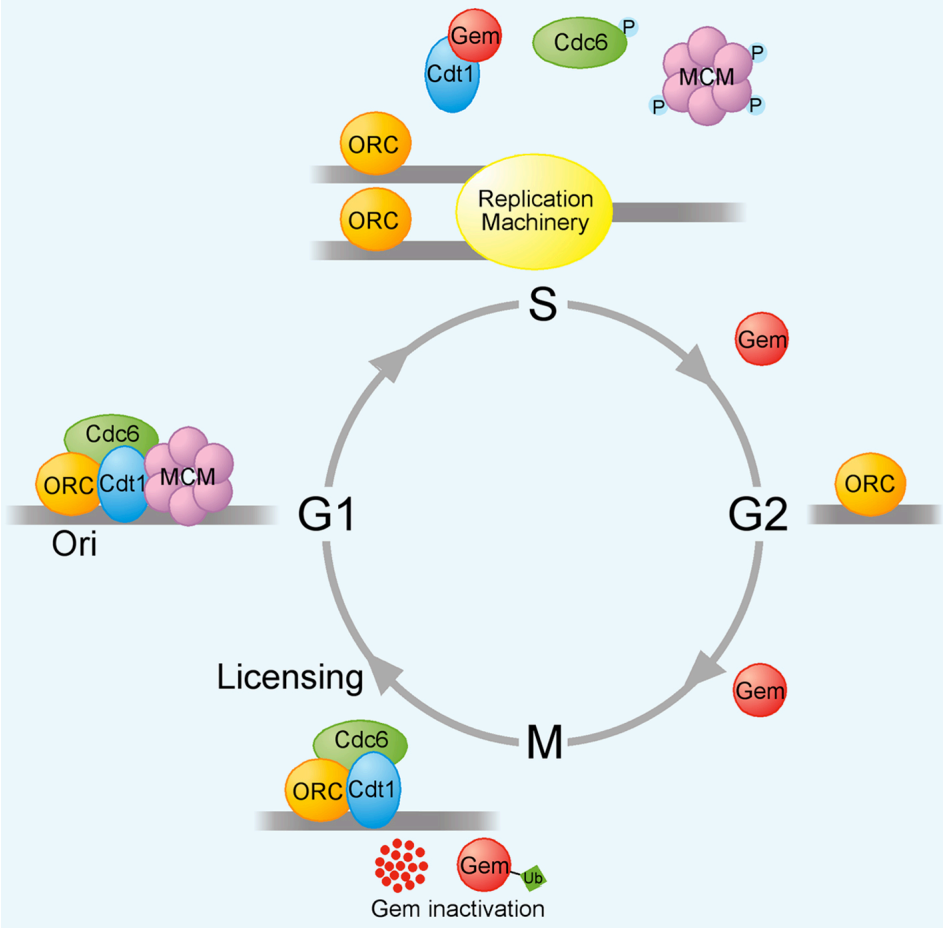

Figure 1-3: The regulatory role of Geminin in DNA replication. Geminin starts to accumulate in nucleus immediately after DNA replication initiation at early S phase, and inhibits DNA rereplication by direct interaction with and sequestration of Cdt1. The presence of active Geminin in the nucleus is maintained throughout S and G2 phases until the end of mitosis, during which Geminin is inactivated through degradation or ubiquitination to license the next round of DNA replication. P: phosphorylation. Ub: ubiquitination (Lygerou and Nurse, 2000; Luo and Kessel, 2004a).

Further inactivation mechanism attributes to the nuclear export of Geminin, since Geminin has been found to be re-activated following a nuclear import process in *Xenopus* egg extracts. Both nuclear assembly and nuclear transport are required for the generation of the inhibitory activity of Geminin (Hodgson *et al.*, 2002). Like multiple redundant mechanisms have developed to guarantee a complete inhibition of rereplication at early S phase, a number of Geminin inactivation mechanisms may also be applied to license the next round of DNA replication during late mitosis and

G1 phase. It is also possible that different organisms use different dominant Geminin inactivation mechanism, since the APC mediated proteolysis of Geminin appears to be essential in mammalian cells to inactivate Geminin comparing to *Xenopus* eggs.

All together, the role of Geminin in DNA replication regulation is very well characterized (Fig. 1-3). Immediately after DNA replication initiation at early S phase, Geminin accumulates in nucleus and serves as an important molecule to inhibit DNA rereplication by direct interacting with Cdt1. The Geminin-Cdt1 interaction inhibits the bindings of Cdt1 to DNA, Cdc6 and Mcms, prevents the loading of MCM complex onto chromatin, thus inhibiting rereplication. The presence of active Geminin in the nucleus is maintained throughout S and G2 phases until the end of mitosis, during which Geminin is inactivated through various pathways including APC mediated degradation, ubiquitination without proteolysis, and nuclear export. The complete inactivation of Geminin ensures the DNA replication licensing for the next round of cell cycle.

1.4 The Roles of Geminin in Embryonic Development

The role of Geminin in embryonic development was first discovered as its overexpression expands the neural plate at the expense of adjacent neural crest and epidermis in *Xenopus* embryos (Kroll *et al.*, 1998). Therefore, in addition to preventing DNA rereplication in cell cycle, Geminin has also been defined as a neuralizing molecule that demarcates the future neural plate at the onset of gastrulation. The injection of Geminin mRNA into one cell of the two-cell stage embryo leads to a hypertrophy of neural tissue at early neurula stage. The injected embryos exhibit an increased primary neuron density, or an expansion of N-tubulin expressing tissue. Downregulation of bone morphogenetic protein 4 (BMP4) levels is the primary means by which Geminin neuralizes ectoderm. Misexpression of Geminin in gastrula ectoderm suppresses BMP4 and epidermal keratin expressions, thus converting prospective epidermis into neural tissue. On the contrary, BMP4 has neither a stimulatory nor inhibitory effect on Geminin transcription. The neuralizing domain of Geminin is mapped to its N-terminal region (amino acids 38-90), which is independent of its cell cycle regulation domain and sufficient to evoke neural hypertrophy and ectopic neurogenesis. Furthermore, two secreted proteins expressed *in vivo* as BMP inhibitors in gastrula organizer mesoderm, chordin and noggin, can directly bind BMPs to prevent their receptor binding. Both chordin and noggin can

strongly induce Geminin expression (Kroll *et al.*, 1998). Similarly, in *Drosophila*, ectopic overexpression of Geminin results in the formation of ectopic neuronal cells, while a percentage of Geminin mutant embryos have a reduction of the dorsal most peripheral neurons (Quinn *et al.*, 2001). Therefore, both in *Xenopus* and *Drosophila*, Geminin plays an important role in inducing neural differentiation.

Hence, Geminin is a bifunctional protein that prevents DNA rereplication in the cell cycle, also regulates processes of embryonic development such as neurogenesis. This is how the name "Geminin" comes from, for gemini meaning twins, to denote its functional duality.

The involvement of Geminin in eye development was first suggested from phenotypes of the *Drosophila* embryos with Geminin overexpressed. In these embryos, overexpression of Geminin leads to a decrease in the size of third instar larvae eye discs as well as the size of adult eyes. Recently, the role of Geminin in eye development has been further investigated in Medaka fish (Del Bene *et al.*, 2004). Different overdoses of Geminin in the embryo by mRNA injection resulted in smaller eyes, cyclopia, or loss of the entire forebrain structure. These eye phenotypes were accompanied by or resulted from a decreased number of proliferative cells and premature neural induction in the optic vesicles, which correlated with the roles of the Geminin in cell cycle regulation and neurogenesis. Furthermore, in support to the overexpression effect of Geminin in cultured cells, the injection of Geminin mRNA also led to apoptosis in Medaka embryos. Vice versa, Geminin knock down by morpholino increased the number of mitotically active cells, thus enlarging the size of the optic vesicles (Del Bene *et al.*, 2004).

1.5 Homeosis and *Hox* Genes

More than one hundred years ago, the term "homeosis", also called homeotic transformation nowadays, was first proposed by William Bateson to qualify morphological variations transforming "something into the likeness of something else" (Fig. 1-4; Bateson, 1894). In the late 1940s, scientists began a study of mutations that produced homeotic transformations in fly, such as flies with four wings instead of two at the expense of balance organs, the halteres. Over the past twenty years, genes involved in such transformations have been isolated from all kinds of metazoans.

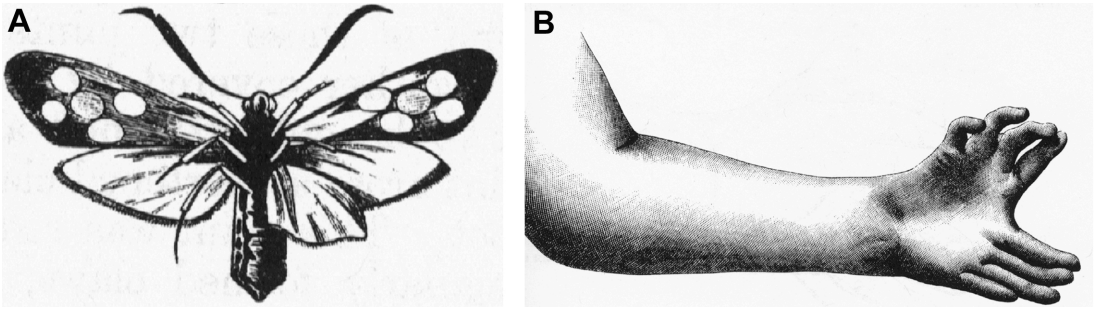

Figure 1-4: Homeosis: transformations of "something to the likeness of something else". (A) One example of homeosis in a moth: the transformation of a leg to a wing. (B) Another example of homeosis on a human autopod: the transformation of a thumb into a set of four fingers (Bateson, 1894).

1.5.1 Homeodomain and Homeobox

Homeodomain proteins are a family of transcription factors characterized by a 60-amino acid DNA binding domain, the homeodomain, which is encoded by a 180-base pair DNA sequence known as the homeobox. The highly conserved homeobox motif was first discovered in homeotic genes of the *Drosophila* homeotic complexes (*HOM-C*) (McGinnis *et al.*, 1984a; McGinnis *et al.*, 1984b; Scott and Weiner, 1984). The homeodomain folds into three α-helices, the latter two folding into a helix-turn-helix conformation that is characteristic of transcription factors that bind DNA in the major groove of the double helix. The third helix is the recognition helix, making contact with the bases of the DNA. A four-base motif, TAAT, is conserved in nearly all sites recognized by homeodomains, which probably distinguishes those sites to that

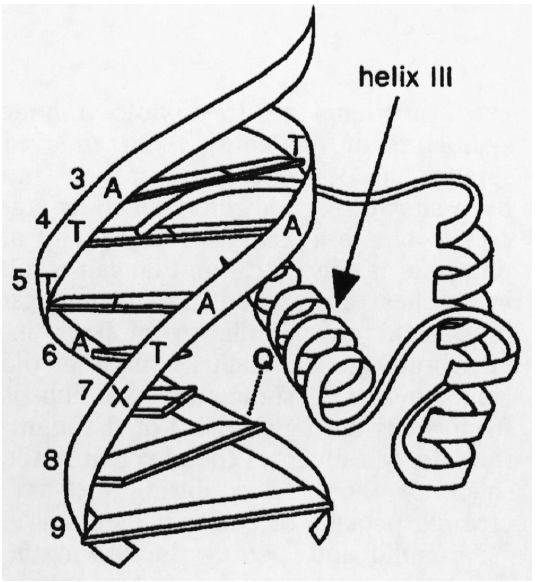

Figure 1-5: Homeodomain-DNA interactions. The helix-turn-helix motif of the homeodomain binds to DNA in the major groove of double helix, in which the four-base motif TAAT serves as the conserved core recognition sequence (Riddihough, 1992).

homeodomain proteins can bind (Fig. 1-5). The 5' terminal T appears to be critical in this recognition, as mutating it destroys all homeodomain binding. The base pairs following the TAAT motif have been demonstrated to be important in distinguishing between similar recognition sites (Riddihough, 1992).

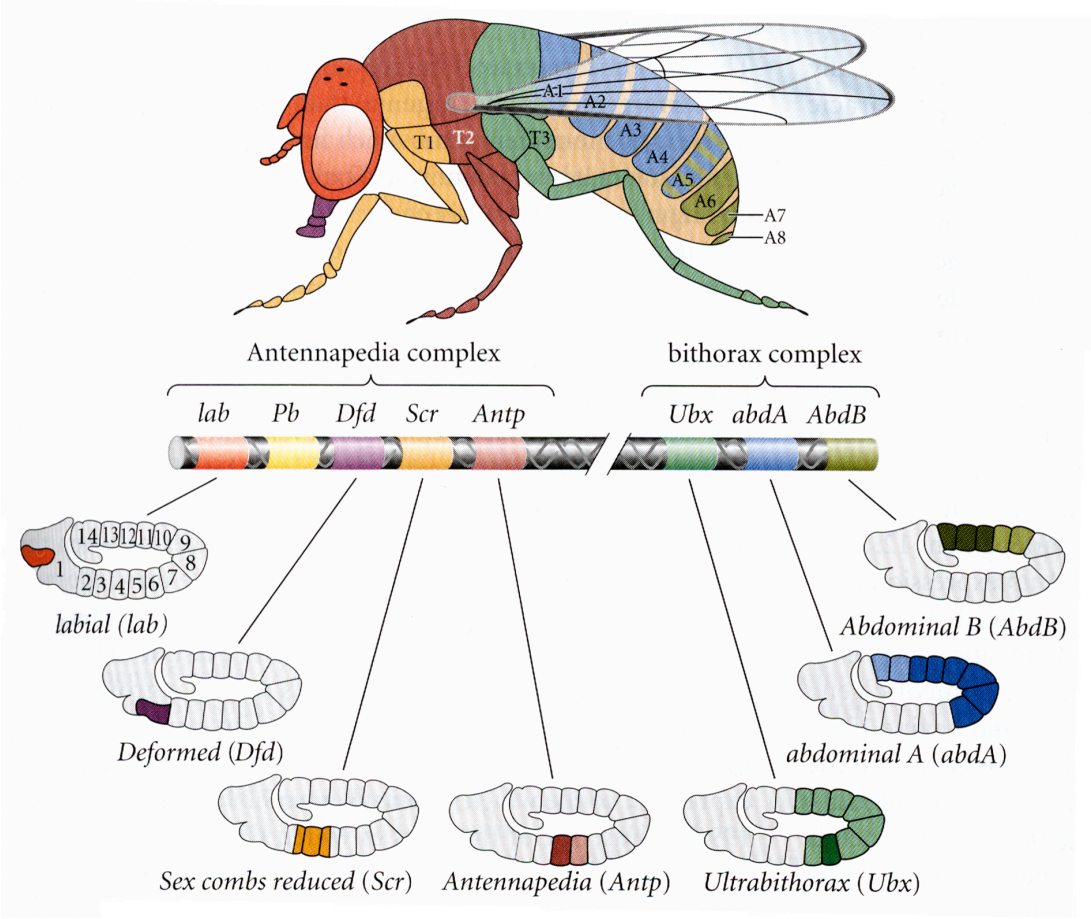

Figure 1-6: Homeotic gene expression in *Drosophila*. In the center are the genes of the Antennapedia and bithorax complexes and their functional domains. Below and above the gene map, the regions of homeotic gene expression in the blastoderm of the *Drosophila* embryo and the regions that form from them in the adult fly are shown. The dark shaded areas represent those segments and parasegments with the most product.

1.5.2 *Drosophila* Homeotic Genes

The wild-type functions of homeotic genes are individually restricted to a specific region of the developing insect and specify the segmental identities. Two regions of *Drosophila* chromosome 3 contain most of these homeotic genes (Fig. 1-6). One of these, the Antennapedia complex, includes the homeotic genes *labial* (*lab*),

proboscipedia (*pb*), *Deformed* (*Dfd*), *Sex combs reduced* (*Scr*), and *Antennapedia* (*Antp*). The second region of homeotic genes is the bithorax complex, in which three genes, *Ultrabithorax* (*Ubx*), *abdominal A* (*abdA*), and *Abdominal B* (*AbdB*), are found. The chromosome region containing both the Antennapedia complex and the bithorax complex is often referred to as the homeotic complex (*HOM-C*). In *Drosophila*, transcripts from each homeotic gene can be detected in specific regions of the embryo, especially prominent in the central nervous system (Harding *et al.*, 1985; Akam, 1987). The current prevalent view is that different homeotic genes in different segments along the body axis can select for different developmental programs, for example by activating or repressing incompletely overlapping sets of target genes, thereby leading to the formation of different structures, such as antenna, leg, haltere, or wing (Lawrence and Morata, 1994). The *lab* and *Dfd* genes specify the head segments, while the *Scr* and *Antp* contribute to the identities of the first and second thoracic segments. More posterior, *Ubx* is required for the identity of the third thoracic segment, while *abdA* and *AbdB* are responsible for the positional identities of the abdominal segments (Fig. 1-6; Wakimoto *et al.*, 1984; Kaufman *et al.*, 1990; Sánchez-Herrero *et al.*, 1985).

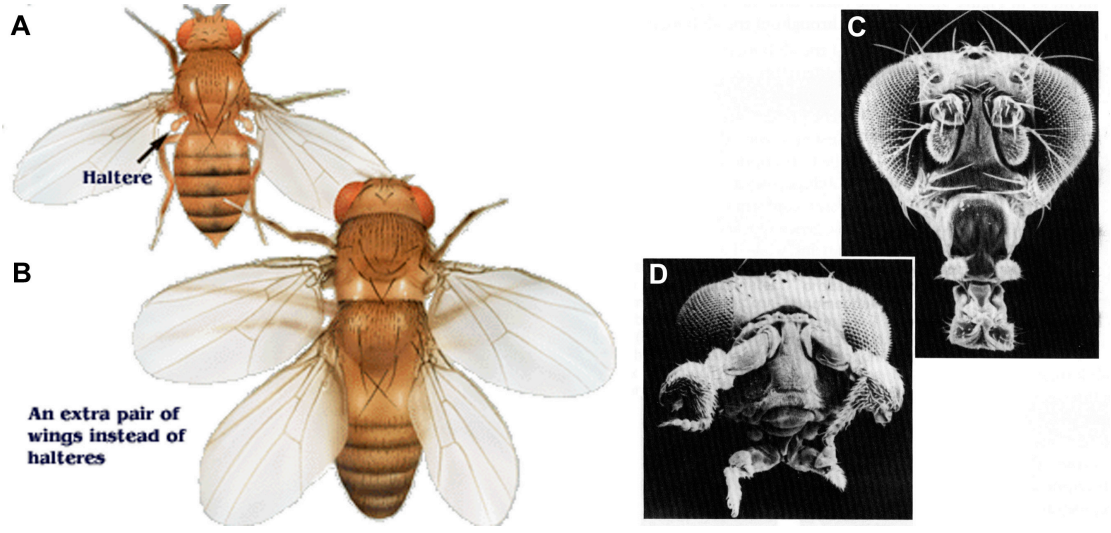

Figure 1-7: Homeotic transformation phenotypes resulted from mutations of homeotic genes in *Drosophila*. When the *Ubx* gene is deleted, the third thoracic segment is transformed into another second thoracic segment that is a fly with four wings at the expense of halteres (B) in contrast to the wild type fly (A). When *Antp* gene is misexpressed in the head, legs sprout from the head sockets (D) instead of antenna in wild type flys (C) (Kaufman *et al.*, 1990).

Since the homeotic genes provide the positional specific information to define the embryonic structures along the body axis, mutations in them lead to bizarre homeotic transformation phenotypes. When the *Ubx* gene is deleted, the third thoracic segment is transformed into another second thoracic segment, resulting in a fly with four wings but without halteres (Fig. 1-7A, B). Similarly, *Antp* usually specifies the second thoracic segment of the fly. When flies carry the mutation wherein the *Antp* gene is misexpressed in the head in addition to the thorax, legs sprout from the head sockets instead of antenna (Fig. 1-7C, D; Kaufman *et al.*, 1990). In larvae lacking the whole bithorax complex, every segment from 5-13 develops similar to segment 4, which is an embryonic lethal phenotype (Casanova *et al.*, 1987)

However, although the structure and biochemistry of these homeotic genes and proteins have been rapidly deciphered, the mechanism by which such genes can identify or transform the morphologies of given segments or metameres is poorly understood.

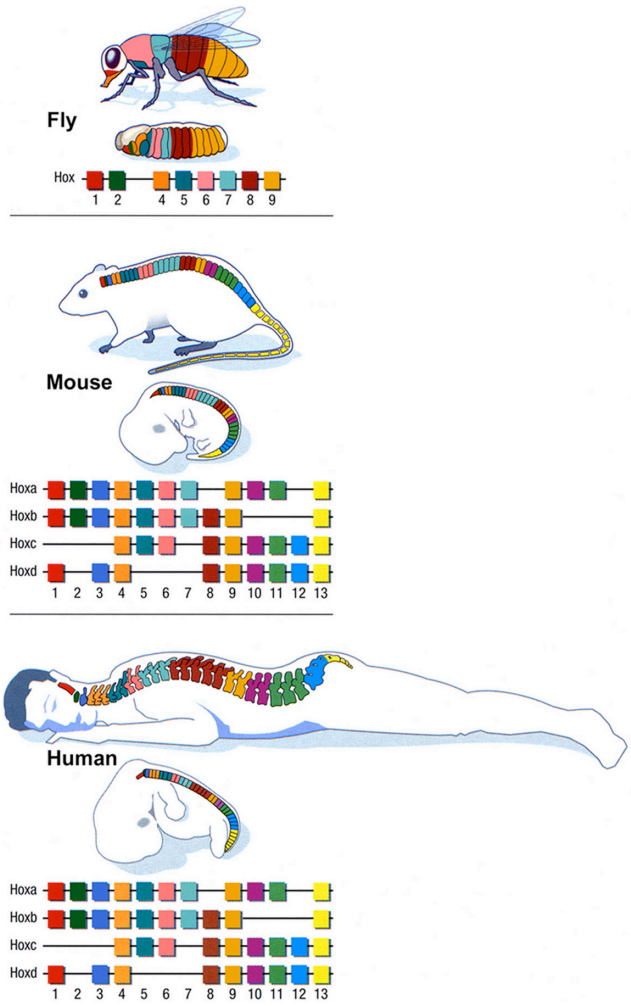

Figure 1-8: *Hox* gene clusters: the vertebrate homologs of *Drosophila* homeotic genes. There are four clusters of *Hox* genes in vertebrates, subdivided into 13 paralogous groups. Note that genes belonging to the same paralogous group and their *Drosophila* homolog are depicted with the same color.

1.5.3 Vertebrate *Hox* Genes: Clustering and Colinearity

In vertebrates, there are four *Hox* gene clusters organized into four complexes on four different chromosomes, totally containing 39 *Hox* genes. Analyses in mouse, human and all other vertebrates indicate an identical *Hox* gene organization, and that the genes in each cluster are all oriented in the same direction of transcription. *Hox* gene clusters are the vertebrate homologs of *Drosophila HOM-C*. Based on the multiple domains of sequence identity including the homeodomain itself, and on the relative position of the genes within the respective complexes, the 39 *Hox* genes can be grouped into 13 paralogous groups with the corresponding genes in each cluster (such as *Hoxa9*, *Hoxb9*, *Hoxc9* and *Hoxd9*) defined as a paralogous group. Furthermore, the organization and homology relationship between *Hox* gene clusters and *HOM-C* can be mapped (Fig. 1-8).

Hox gene expression can be seen along the dorsal axis in the neural tube, neural crest, paraxial mesoderm, and surface ectoderm from the anterior boundary of the hindbrain through the tail, also in the limb, gut, and gonadal tissue (Krumlauf, 1994). A distinguishing hallmark of the *Hox*/*HOM-C* clusters is the correlation between the physical order of genes along the chromosome and their expression as well as function along the anteroposterior axis of the embryo. This characteristic was originally recognized by Lewis in *Drosophila* bithorax complex and referred to as spatial colinearity (Lewis, 1978). It was postulated at that time that the bithorax complex could represent a mechanism for translating genetic information into a combinatorial code for the regulation of regional identity. This property is extended to vertebrate *Hox* genes, where also a spatial colinear relationship between gene order and their expressions along the anteroposterior axis of vertebrate embryos exists. The more 3' the gene located in the cluster along chromosome, the more anterior it expresses along the body axis (Graham *et al.*, 1989; Duboule and Dollé, 1989). There is also a relationship between the organization of the genes along the chromosome and the time of the appearance of gene expression during embryogenesis, named temporal colinearity (Izpisua-Belmonte *et al.*, 1991). Therefore, the famous "colinearities", both spatial and temporal, refer to the prominent characteristics of *Hox* genes that genes located at the 3' extremity are activated earliest and have most anterior boundaries of expression, whereas moving along the clusters in a 5' direction, the genes are transcribed progressively later in more posterior areas during embryonic development. In addition, there is also a colinear sensitivity in the level and time of

response of *Hox* genes to retinoic acid (RA) in cell lines and embryos. Again, the more 3' the gene located in the clusters, the higher sensitive to RA induction (Simeone *et al.*, 1990; Dekker *et al.*, 1993).

Although the biological relevances of *Hox* gene "clustering" and "colinearity" are well perceived and they are known to be critical for proper vertebrate development, the reasons and mechanisms behind this genomic organization and transcriptional progression remain as one of the major mysteries of *Hox* genes. Nevertheless, in the past decade, a good deal of effort has been put into the dissection of underlying mechanisms. Two issues should be mentioned here in attempts to decipher the molecular basis of clustering and colinearity. First, it is likely that not all the animals implement their colinearities in the same way. These alternatives are probably made necessary by the important divergence in developmental strategies between different animals, even though the outcome of the *Hox* system is identical throughout metazoans. Second, the problem of *Hox* gene clustering is related but not identical to that of colinearity. Understanding why and how *Hox* genes are clustered may not tell us about colinearity as this latter phenomenon may represent only one of the many reasons why *Hox* genes are clustered together (Duboule, 1998).

So far, what are the understandings nowadays? What is the rationale of spatial and temporal colinearities and how are they achieved? Unlike the situation in flies, where the activation mechanism depends on factors unequally distributed by the segmentation process, four classes of mechanisms have been evoked to implement colinearity in vertebrates, alone or in combination.

The first mechanism relies on the progressive transcriptional availability of *Hox* genes, from one end of the cluster to the other, a process that may or may not be independent of their own transcription. For example, repressive or silencing factors like promyelocytic leukemia zinc finger (Plzf) and the Polycomb complex (Barna *et al.*, 2002; Gould 1997) could be released through a passive transition in chromatin states (Kondo and Duboule, 1999). Alternatively, transcription of the genes themselves could help remodel chromatin to allow the next gene to be accessed. The latter possibility is supported by the failure of the posterior *HoxD* cluster to efficiently repress the early expressed *Hoxb1*/*lacZ* transgene, which suggests that an early gene can still recruit necessary factors to be activated in a timely manner, even though positioned within a "closed" domain (Kmita *et al.*, 2000). In this view, a chromatin dependent colinear process would involve a transcriptional entry point at one side of

the cluster that triggers the processing from a closed to an open configuration through a proximity effect. This would allow for progressively more genes to be transcribed toward the other extremity of the cluster.

The second scenario proposes that colinear activation in time and space is orchestrated by the integration of locally cis-acting control sequences. Since local enhancer functions are shared among subsets of neighboring *Hox* genes, they ultimately provide distinct expression features through unequal partitioning of their activities on the genes they control (Sharpe *et al.*, 1998). Although this strategy accounts for the rather precise activation of randomly integrated transgenes, it may not be a key factor in tightly maintaining genes in clusters. Hence, it is likely not a primary mechanistic basis for the colinearity.

The third mechanism involves the existence of global enhancer sequence, located outside the clusters, which can regulate several *Hox* genes in a relatively promoter unspecific manner. The positions of these enhancers, close to either end of a *Hox* cluster, introduce an intrinsic regulatory asymmetry that can be subsequently translated into a colinear mechanism. For an instance, the cycling expression of *Hoxd* genes in the presomitic mesoderm, in coordination with segmentation, involves a regulatory element located outside the cluster, which can act over several genes at different times. This regulatory element may be the outcome of the segmentation process, setting up the pace of the temporal and spatial colinear activation of *Hox* genes and thereby keeping these two key aspects of patterning in phase with each other (Zàkàny *et al*., 2001; Dubrulle *et al.*, 2001). Likewise, colinearity in developing limbs relies on the existence of a global digit enhancer element located far upstream on the other side of the cluster (Spitz *et al.*, 2003). Sequence specific enhancer tropism, as well as promoter competition, eventually induces the terminal genes to be expressed in the most distal structures, with a progressively decreasing efficiency (Kmita *et al.*, 2002). In these cases, colinearity is determined by the action of global enhancers.

As known in the genome, nearly 1% of the predicted mammalian genes encode microRNAs (miRNAs). Then, the fourth colinear possibility involves the participation of miRNAs in *Hox* gene regulation. RNA interference is the process of sequence specific, post-transcriptional gene silencing in animal and plants, initiated by a double-stranded RNA that is homologous in sequence to the silenced gene. The mediators of sequence specific mRNA degradation are 21- or 22-nucleotide duplex

siRNAs (Elbashir *et al.*, 2001). The involvement of miRNAs in *Hox* gene regulation was first hinted from discoveries that several miRNA encoding sequences are located in the introns or intergenetic regions within *Hox* clusters (Fig. 1-9; Lagos-Quintana *et al.*, 2003). MiR-196, an miRNA encoded by sequences between *Hox-9* and *Hox-10* at three paralogous loci in the A, B, and C vertebrate *Hox* clusters, has extensive, evolutionarily conserved complementarity to messages of *Hoxb8, Hoxc8*, and *Hoxd8*. Furthermore, this miRNA can direct endogenous cleavage of *Hoxb8* mRNA in mouse embryos, and mediate the inhibition of Hoxc8, Hoxd8, and Hoxa7 expressions predominantly on a translational level (Yekta *et al.*, 2004). Because of the colinearity and progressive opening of *Hox* gene clusters, the transcription of *Hoxb8* precedes that of miR-196 spatially and temporally. Therefore, the colinear organization of *Hox* genes ensures the proper spatial domains and temporal phases of functional Hoxb8 during embryogenesis. In addition, this post-transcriptional inhibition serves as one of the possible mechanisms involved in posterior prevalence of *Hox* genes (see below).

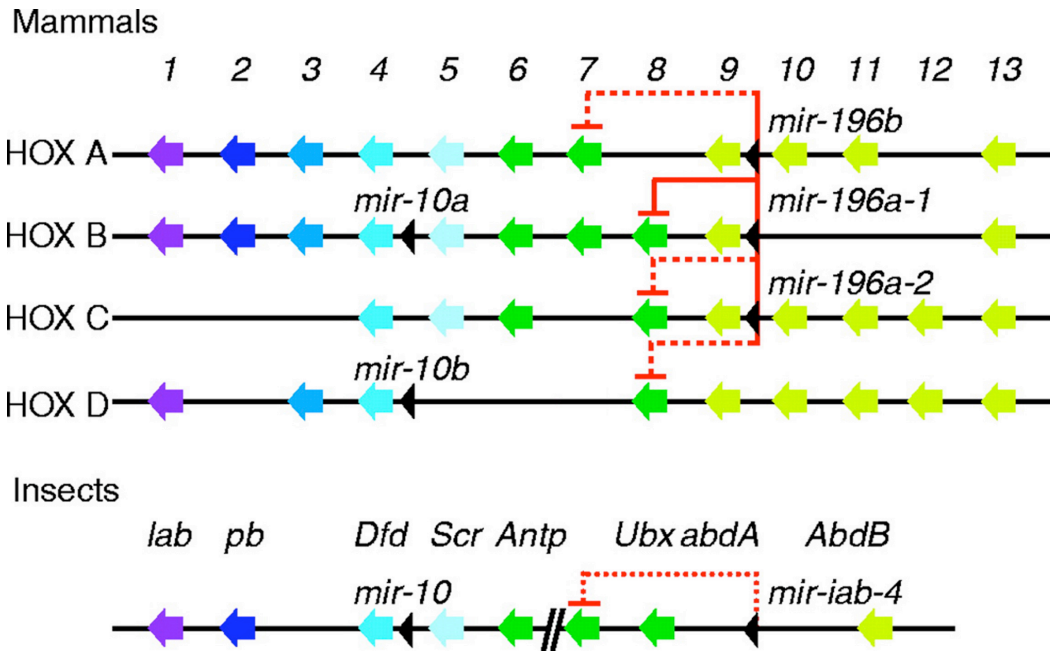

Figure 1-9: The involvement of miRNAs in *Hox* gene regulation and colinearity. Colored arrows indicate *Hox* genes representing 13 paralogous groups; black arrowheads depict miRNA genes. Repression supported by bioinformatic evidence only (dotted red line), cell-culture and bioinformatic evidence (dashed line), or *in vivo*, cell culture, and bioinformatic evidence (solid line) are indicated. The vertical red line indicates that miRNAs from any of the three loci could repress the targets (Yekta *et al.*, 2004).

1.5.4 Patterning the Anteroposterior Axis: The *Hox* Code

Once gastrulation begins, anterior-posterior polarity in all vertebrates becomes specified by the expression of *Hox* genes. As discussed above, during embryonic development *Hox* genes are activated in nonidentical, overlapping expression domains along the body axis of vertebrates, exhibiting a temporal and spatial colinearity with their genomic organization. The expression patterns of murine *Hox* genes suggest a code whereby a certain combination of *Hox* genes specifies a particular regional identity along the anteroposterior axis (Kessel and Gruss, 1991; Hunt and Krumlauf, 1991). Therefore, the term "*Hox* code" was proposed, so that each segment along the body axis has a special combination of functional active *Hox* genes, that is, a special *Hox* code, to provide its positional identity (Fig. 1-10). Evidence for such a code comes from the following three sources.

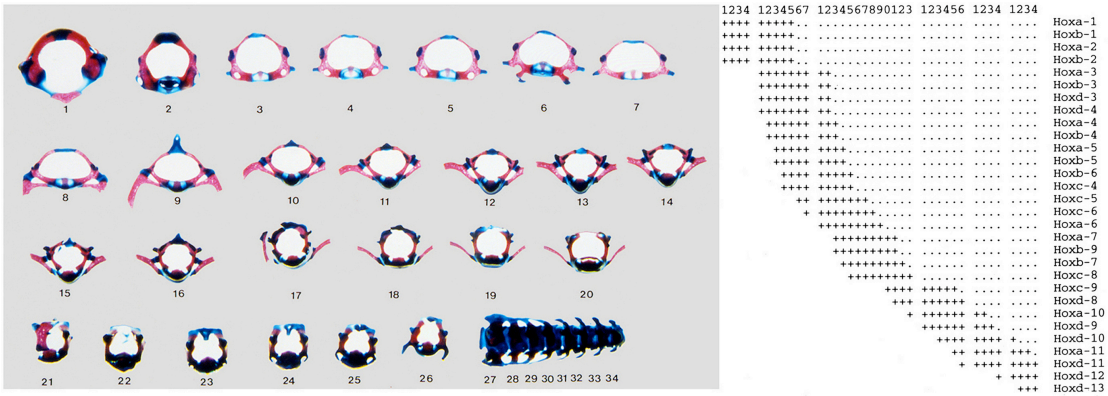

Figure 1-10: *Hox* code: each segment along the anteroposterior axis has a special combination of functionally active *Hox* genes. The left side shows the morphological identities of each vertebra, whereas the right side indicates the *Hox* gene combinations of each vertebral segment that determine their identities during embryogenesis.

The first evidence comes from knockout experiments of murine *Hox* genes. Absence of a *Hox* gene affects patterning in a way in agreement with the idea that *Hox* code provides the cells with positional identity. For an instance, mouse loss-of-function mutants of *Hoxa2*, *Hoxd3*, *Hoxb4*, *Hoxa5*, *Hoxc8*, *Hoxa11*, *Hoxd13* all display various forms of anterior or posterior homeotic transformations in the axial skeleton or neural crest (Reviewed by Krumlauf, 1994). These mutations illustrate that altering a single gene can cause changes of the *Hox* code in given segments, resulting in changes in cell fate and consequent homeotic transformations. The

correlation between changes of *Hox* code and transformations of segment identities can be clearly demonstrated, exampled by *Hoxb4* loss-of-function mutant (Ramirez-Solis *et al.*, 1993). Knockout of *Hoxb4* gene leads to a switch of the *Hox* code of the second cervical segment into that of the first cervical segment, which exactly correlates with the morphological transformation of axis (the second cervical vertebra) into another atlas (the first cervical vertebra).

The second evidence comes from the RA induced teratogenesis. Many *Hox* genes have RA receptor binding sites in their enhancers, and a gradient of RA has been established by day 7 of development that is high in the posterior regions and low in the anterior portions of the embryo (Sakai *et al.*, 2001). This gradient appears to be controlled by the differential synthesis or degradation of RA in different parts of the embryo. Exogenous RA applied to mouse embryos in uteri can lead to certain *Hox* genes to become expressed in groups of cells that usually do not express them. These ectopically expressed *Hox* genes cause alterations of *Hox* codes and concomitant homeotic transformations of vertebrae and axons, again demonstrating the biological relevance of *Hox* code in the specification of embryonic structures along the anteroposterior axis (Kessel and Gruss, 1991; Kessel, 1992; Kessel, 1993).

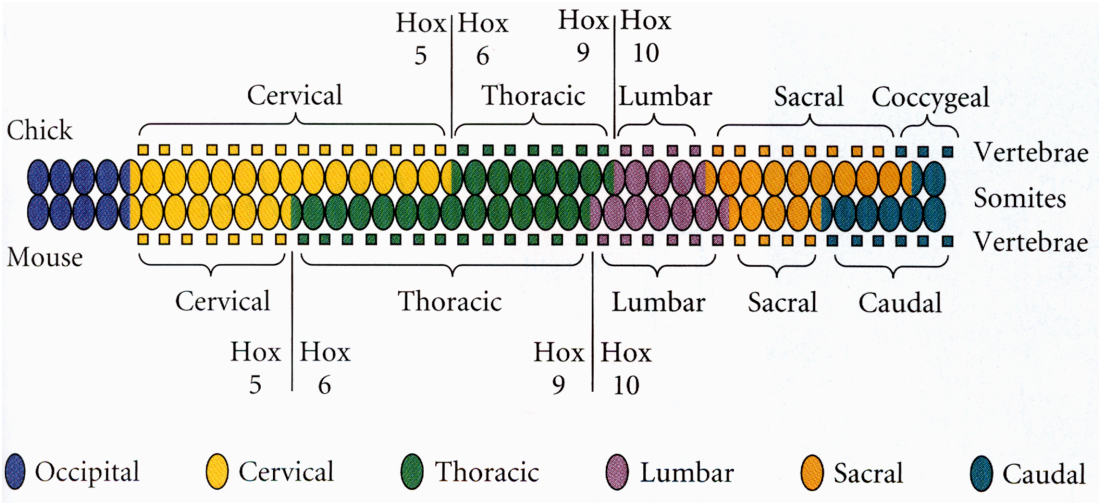

Figure 1-11: Schematic representation of the mouse and chick vertebral pattern along the anteroposterior axis. The boundaries of expression of certain *Hox* gene paralogous groups have been mapped onto these domains (For further explanation, see body text) (Burke *et al.*, 1995).

The third evidence comes from the comparative anatomy of mouse and chick vertebrae. Although mouse and chick have a similar number of vertebrae, they

apportion them differently. The constellation of expressed *Hox* genes predicts the type of vertebrae formed rather than the relative position of the vertebrae (Fig. 1-11). For an instance, in the mouse, the transition between cervical and thoracic vertebrae is between 7 and 8, whereas in the chick it is between vertebrae 14 and 15. In both cases, the *Hox-5* paralogous are expressed in the last cervical vertebra, while the anterior boundary of the *Hox-6* paralogous extends to the first thoracic vertebra. Similarly, in both animals, the thoracic-lumbar transition is seen at the boundary between the *Hox-9* and *Hox-10* paralogous groups. Therefore, it appears that there is a code of differing *Hox* gene expression along the anteroposterior axis, and that *Hox* code determines the type of vertebra formed (Burke *et al.*, 1995).

Hox gene clusters have 39 genes consisting of 13 groups of paralogous genes, which are highly related to each other in the sequences of the encoded homeodomain. The resulting functional overlaps between paralogous proteins, highlighted as their functional redundancies (Wellik and Capecchi, 2003), suggest that the developmental pathways concerned may rely on strong quantitative parameters. Likewise, the subtle morphological differences of some vertebral structures along the body axis also suggest that the qualitative combination of *Hox* genes in anteroposterior patterning is not the sole underlying mechanism. For an instance, mouse homozygous for null alleles at *Hoxa3* are characterized by perinatal lethality, absence of the thymus, and malformation of the hyoid bone. However, in mice lacking any Hoxa3 protein but instead expressing Hoxd3 protein from both *Hoxa3* and *Hoxd3* loci, the *Hoxa3* null mutant phenotypes are dramatically rescued, indicating that the Hoxd3 protein complements the absence of Hoxa3 protein when expressed at the *Hoxa3* locus. Vice versa, the expression of Hoxa3 protein from *Hoxd3* locus complements the Hoxd3 function and rescues *Hoxd3* null mutant phenotypes. Hence, the proteins encoded by the paralogous genes, *Hoxa3* and *Hoxd3*, can carry out identical biological functions, and that the different roles attributed to these genes are the result of quantitative modulations in gene expression (Greer *et al.*, 2000).

In vertebrates, successively more caudal body levels tend to show an increasing amount and diversity of Hox products, resulting from the expression strategy. Yet segmented structures do not become more elaborate toward the caudal end of the embryo, nor do they display a greater potential for variation after gene inactivation experiments, thus excluding a strict combinatorial input. The most posteriorly expressed gene usually imposes its function over that of more anterior genes through

a suppressive mechanism that does not involve transcriptional repression (Schock *et al.*, 2000). This so-called posterior prevalence (Duboule, 1991) explains why the phenotypes induced by vertebrate *Hox* mutations are restricted either to a few body segments or to the upper morphological window in which a given group of paralogs is at work (Horan *et al.*, 1995; van den Akker *et al.*, 2001). Posterior prevalence is an interesting property for morphological evolution, given that an anterior shift in the expression of a caudal gene would lead to the functional inactivation of more rostral components. Therefore, the functional interplay between Hox proteins is the result of their colinear distribution along the body, and is the essential constraint of the system. Consequently, any mechanism generating this protein distribution may have been evolutionarily selected and implemented in the numerous instances in which this strategy is used.

Together, during embryonic development, vertebrate *Hox* genes are activated in nonidentical, overlapping expression domains along the anteroposterior axis, exhibiting a temporal and spatial colinearity with their genomic organization. Qualitative and quantitative combinatorial distributions of Hox proteins along the body axis provide positional specific information, thus defining embryonic structures.

1.5.5 Maintenance of *Hox* Gene Transcription or Inhibition

The initial domains of homeotic gene expressions are established by the gap genes and pair-rule genes in *Drosophila*. However, gap gene and pair-rule gene proteins are transient, whereas the identities of segments must be stabilized during development. Thus, once the transcription patterns of homeotic genes have become set up, they are locked into an active or repressive state epigenetically by the transcriptional memory system.

On the basis of reciprocal homeotic phenotypes, two classes of genes have been identified to involve in the epigenetic maintenance of *Hox*/*HOM-C* gene transcription. The *trithorax* group (*trxG*) is responsible for sustaining the active state of *Hox*/*HOM-C* gene transcription, while the *Polycomb* group (*PcG*) encodes a stable repressor system (Schumacher and Magnuson, 1997). Activation of a eukaryotic gene depends upon the coordinated action of chromatin remodeling factors, histone modifying enzymes, gene specific and general transcription factors, and RNA polymerase. Chromatin remodeling complexes and histone modifying enzymes play significant roles in maintaining on or off state of transcription after an initial gene expression

decision is made. Polycomb and trithorax group proteins are evolutionarily conserved chromatin components that maintain spatial patterns of *Hox*/*HOM-C* gene transcription. Several lines of evidence indicate that numerous members of *trxG* and *PcG* products (Tab. 1-1) form multiprotein complexes, which are required to keep *Hox*/*HOM-C* and other potential target genes activated or repressed.

Murine gene	Class	Identification	Drosophila homologs	Vertebrate homologs	Conserved domains
Bmi1	PcG	Proviral integration site in Mo-MLV-induced B-cell lymphomas	*Psc, Su(z)2*	Human *BMI1* *Xenopus Xbmil*	Ring-finger motif, C-terminal proline/serine-rich, putative transactivation domain
Mel18	PcG	Expression cloning using mouse melanoma B16 cells	*Psc, Su(z)2*	Human *MEL18*	Ring-finger motif, C-terminal proline/ serine-rich, putative transactivation domain
Cbx2 (M33)	PcG	Homology screen using *Drosophila Polycomb*	*Pc*	Human *CBX2* *Xenopus Xpolycomb*	Chromodomain, C-terminus
Rae28 (Mph1)	PcG	Induced in retinoic acid treated F9 cells, and in yeast two-hybrid screen with *Bmi1*	*ph-p, ph-d*	Not identified	Zinc finger, glutamine rich region, a-helical domain, SPM (SEP) domain
Enx1b	PcG	Homology screen using human *ENX1*, which was isolated by yeast two-hybrid screen with *VAV* proto-oncogene	*E(z)*	Human *EZH2*	SET domain, CXC domain
Ezh1	PcG	Homology screen using *Drosophila E(z)*	*E(z)*	Human *EZH1*	SET domain, CXC domain

Eed	PcG	Positional cloning	*Esc*	Human *EED*	High conservation throughout protein, five WD motifs
Mll	trxG	Homology screen using human *ALL1*, which was isolated from translocation breakpoints in human acute leukemias	*trx*	Human *ALL*	AT hook domain, DNA methyltransferase domain, PHD finger, SET domain
Brg1	trxG	Homology screen using human *BRG1,* which was isolated by homology screen *using Drosophila brm*	*brm*	Human *BRG1* Chicken *BRG1*	DNA helicase domain, bromodomain, P/Q domain
Not identified	trxG	*SNF2L2* isolated by homology screen using *Drosophila brm*	*brm*	Human *SNF2L2*, Chicken *SNF2L2*	DNA helicase domain, bromodomain, P/Q domain

Tabel 1-1: Murine Polycomb- and trithorax-group members and their *Drosophila* homologs

Four different complexes contain trxG proteins and at least two of them are demonstrated as pivotal components to maintain active *Hox* gene transcription. Trithorax acetyltransferase complex 1 (TAC1) contains Trx, Sbf1, and dCBP, a member of the CBP/p300 family of acetyltransferase. TAC1 acetylates all four core histones as well as mononucleosomes and nucleosome arrays. Trx, dCBP, and Sbf1 colocalize at many sites on polytene chromosomes, including a trithorax response element (TRE) at the regulatory region of *Ubx*. *Trx* and *dCBP* mutations reduce expression of both endogenous *Ubx* gene and reporter genes under TRE control. Therefore, the role of TAC1 complex in the maintenance of active *Hox* gene transcription is carried out through promoting histone acetylation in the vicinity of TREs (Petruk *et al.*, 2001). Another substantial trithorax complex, BRM complex, contains the trxG proteins Brahma, Moira, OSA, and SNR1. This complex is highly related to SWI/SNF, a chromatin remodeling complex, and catalyzes ATP dependent alterations of nucleosome organization. Other trxG proteins may target the BRM complex to specific promoters or modulate its activity. Thus, the BRM complex facilitates transcriptional activation on nucleosomal templates by remodeling chromatin structure at a step subsequent to activator binding (Kal *et al.*, 2000).

Two distinct Polycomb complexes have been identified and exhibit high conservation among metazoans: Polycomb repressive complex 1 (PRC1) and ESC-

E(Z) complex. The inhibition of *Hox*/*HOM-C* gene transcription by PRC1 is achieved through blocking of nucleosome remodeling. And the binding of PRC1 to chromatin occludes subsequent SWI/SNF or trithorax complex binding, further suggesting that the remodeling block is due to reduced positive regulator access to common or overlapping template sites (Francis *et al.*, 2001). The second Polycomb ESC-E(Z) complex is physically linked to histone deacetylases (HDACs). HDAC1 and HDAC2 co-fractionate and co-immunoprecipitate with EED and EZH2, the human homologs of ESC and E(Z). The immunoprecipitants contain HDAC enzyme activity and EED mediated repression in cells is sensitive to an HDAC inhibitor trichostatin A, indicating that ESC-E(Z) complex inhibits *Hox*/*HOM-C* gene transcription through recruiting HDACs and thereby modifying chromatin structures (van der Vlag and Otte, 1999). In mouse, PRC1 contains Bmi1, Mel18, Rae28 (also known as Mph1), M33, sex comb on midleg homolog 1 (Scmh1), Ring1A, Ring1B etc., while ESC-E(Z) complex contains EED1, EZH1, Enx1B, and yin yang 1 (YY1). Most of these PcG member loss-of-function mutants exhibit derepressions of *Hox* gene transcription, concomitant with posterior homeotic transformations of embryonic structures along the anteroposterior body axis (Akasaka *et al.*, 1996; Coré *et al.*, 1997; Suzuki *et al.*, 2002), further demonstrating the maintenance of *Hox* gene transcription inhibition by Polycomb complexes.

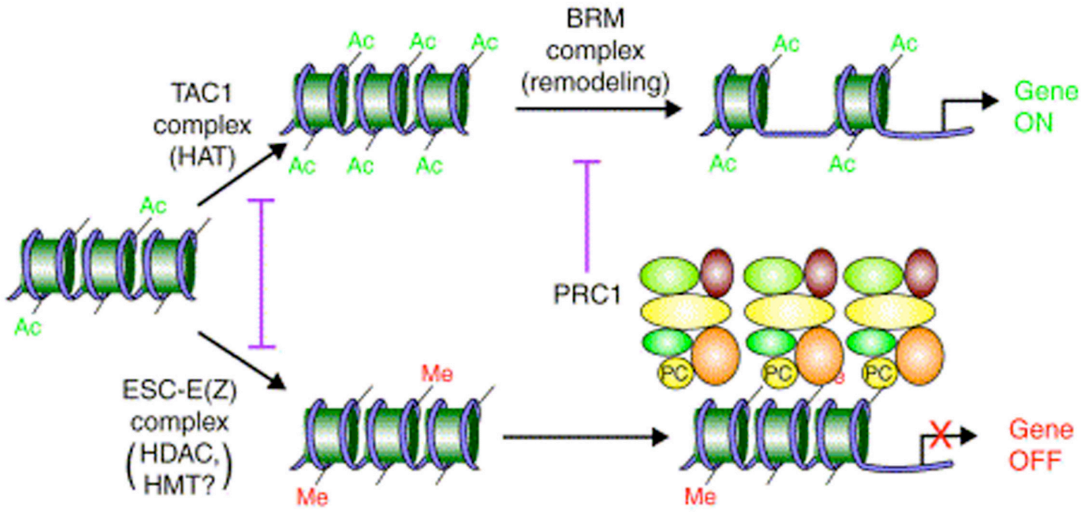

Figure 1-12: Model for multistep mechanisms of trxG and PcG chromatin complexes. The cartoon depicts a nucleosome array at a target *Hox* gene under trxG/PcG control. The activating pathway through trxG is shown at the top and the alternative repressive pathway mediated by PcG is shown below. "Ac" represents acetylation on histone tails and "Me" represents methylation. In the model,

TAC1 acetylates nucleosomes and ESC-E(Z) deacetylates. “HMT?” indicates the possibility that ESC-E(Z) might also harbor or recruit a histone methyltransferase. Distinct histone codes created in the first step then help attract either the BRM complex (trxG pathway) or PRC1 (PcG pathway), whose actions produce the indicated *Hox* gene transcription outcomes (For further explanation, see body text). Vertical purple bars indicate opposing effects of complexes at each step (Simon and Tamkun, 2002).

Together, the maintenance of *Hox*/*HOM-C* gene transcription state by trithorax or Polycomb complexes is accomplished through multistep mechanisms that involve nucleosome modification and chromatin remodeling (Fig. 1-12).

1.6 Aims of the Work

Growth and patterning are two major themes in embryogenesis. Embryonic patterning has to be strictly coordinated with cell cycle in order to guarantee correct timing and allocation of cells as well as structures during development. Geminin is a bifunctional protein, which is involved in both cell cycle regulation and embryonic development. On one hand, it directly binds to Cdt1 thereby inhibits DNA rereplication from early S phase to the end of mitosis. On the other hand, it is also functional in neuralization and eye development. The aim of my work is to investigate further roles of Geminin in embryonic development especially in patterning, then to understand the relationship between Geminin as a cell cycle regulator and as a developmental controller, that is, how Geminin coordinates cell cycle and embryonic development.

2. Materials and Methods

2.1 Isolation of Nucleic Acids

2.1.1 Plasmid DNA Isolation from *E. coli*

E. coli containing a certain plasmid were inoculated into 3.5 ml (Miniprep) or 90 ml (Maxiprep) LB Standard Medium (1% Bacto-Tryptone (Gibco BRL), 0.5% Bacto-Yeast Extract (Gibco BRL), 1% NaCl in Millipore water) with 50 μg/ml ampicillin or kanamycin, and incubated at 37 °C shaking for 16 hours. Then, the plasmid was extracted using Plasmid Mini or Maxi Kit (Qiagen) as described by the manufacturer and the concentration was measured using a BioPhotometer (Eppendorf). For cell transfection or embryo electroporation, the maxiprep DNA should be further extracted with 1 volume of phenol/chloroform/isoamylalcohol (25:24:1) once or twice, followed by 13,500 rpm centrifugation using Centrifuge C5417 (Eppendorf) for 2 minutes. The supernatant was carefully collected and subjected to 1 volume of chloroform extraction once, again followed by centrifugation and supernatant collection. Then, the DNA was precipitated with 0.7-1 volume of isopropanol and 0.1 volume of 3 M NaAc, pH 5.2 at –20 °C for 15 minutes. Afterwards, the DNA was pelleted by centrifugation at 13,500 rpm for 15 minutes, washed with 300 μl 70% ethanol, centrifuged at 13,500 rpm for another 5 minutes, air dried, and dissolved in a proper volume of Millipore H_2O.

2.1.2 Genomic DNA Extraction from Mammalian Cells or Mouse Tissue

The cultured mammalian cells in an 8.5 cm dish were trypsinized and washed with PBS twice. Then, the cell pellet was resuspended in 1 ml Cell Lysis Buffer (100 mM Tris, pH 8.0, 200 mM NaCl, 5 mM EDTA, 0.2% SDS, freshly added 100 μg/ml Proteinase K) and incubated at 50 °C shaking for 6 hours. Then, the lysis product was extracted with 1 volume of phenol/chloroform/isoamylalcohol (25:24:1) twice, and precipitated with 1 volume of isopropanol plus 0.1 volume of 3 M NaAc, pH 5.2. The precipitated pellet was washed with 500 μl 70% ethanol, air dried, and dissolved in 50 μl Millipore H_2O.

The mouse tissue was washed once with PBS before digestion in 500 μl Tissue Lysis Buffer (100 mM Tris, pH 8.5, 200 mM NaCl, 5 mM EDTA, 0.2% SDS, freshly

added 250 μg/ml Proteinase K) at 55 °C shaking overnight. Then, the treatments were the same as described above in mammalian cells.

2.1.3 DNA Electrophoresis and Purification from Agarose Gel

0.5-2% agarose gel was prepared by melting agarose (Invitrogen) in 1×TBE Buffer (90 mM Tris-borate, 2 mM EDTA, pH 8.0) and subsequently adding ethidium bromide to a final concentration of 0.3 μg/ml. DNA sample was mixed with 5×DNA Loading Buffer (25% Ficoll, 100 mM EDTA, 0.05% Bromophenol Blue), and electrophoresis was performed under 1-7 V/cm in 1×TBE buffer. For fragment purification, the band cut down was put into a small dialyse membrane pocket with 500 μl 0.5×TBE buffer. Then, the gel in the sealed pocket underwent electroelution in 0.5×TBE buffer under 7.5 V/cm for 20 minutes, followed by 20 seconds with opposite polarity of electricity. After that the eluted DNA solution in the pocket was collected, 500 μl 0.5×TBE buffer was used to wash the pocket and merged with 500 μl elution. This 1 ml solution was extracted by phenol/chloroform/isoamylalcohol (25:24:1) once, precipitated with isopropanol plus 3 M NaAc plus 1 μl 10 mg/ml glycogen, and washed with 70% ethanol as described above. The dried pellet was finally dissolved in 15 μl H_2O.

2.1.4 Total RNA Isolation from Eukaryotic Cells or Embryos

Total RNA from cultured cells or mouse embryos was isolated using RNeasy Mini Kit (Qiagen) as described by the manufacturer.

2.1.5 Labeled Nucleic Acids Purification

The labeled nucleic acids were purified using ProbeQuant G-50 Sephadex Micro Column (Amersham) (Tab. 2-1).

1. Resuspend the resin in the column by vortexing.
2. Loosen the cap one-fourth turn and snap off the bottom closure of the column.
3. Place the column in a 1.5 ml screw-cap microcentrifuge tube for support, and prespin the column at 770× g for 1 minute to generate the sample-loading surface.
4. Place the column in a new 1.5 ml tube and slowly apply 50 μl labeling reaction

product (20 μl labeling reaction plus 30 μl H_2O) to the loading surface.
5. Spin the column at 770× g for 2 minutes, and the purified sample was collected in the support tube.

Tabel 2-1: Purification of labeled nucleic acids using ProbeQuant G-50 Sephadex Micro Column.

2.2 Modifications and Manipulations of Nucleic Acids

2.2.1 DNA Digestion with Restriction Enzymes

For DNA analysis, 200-500 ng DNA was digested with 5-10 U restriction enzymes by treating with 800 W microwave for 12 seconds twice, then incubating at 37 °C for 10 minutes. For DNA preparation, 1-10 μg DNA was incubated with 20-80 U restriction enzymes at 37 °C for 4 hours. For end-cutting of PCR product, crude PCR product was purified with PCR Purification Kit (Qiagen) and then incubated with 30-60 U restriction enzymes at 37 °C overnight.

2.2.2 Dephosphorylating or Blunting the Ends of DNA Fragment

5'-ends of DNA fragment dephosphorylation was performed by directly adding 1 μl Alkaline Phophatase (1U/μl, Roche) into the restriction enzyme digestion mixture and incubating at 37 °C for 1 hour.

DNA polymerase I large fragment (Klenow fragment) (5U/μl, NEB) was used to fill-in the ends of 5'-overhang DNA fragment. DNA in restriction enzyme NEBuffer supplemented with 33 μM dNTPs was incubated with Klenow at a concentration of 1 U per μg DNA at 25 °C for 30 minutes.

3'-overhang DNA fragment was sharpened blunt using Pwo DNA Polymerase (5U/μl, Roche), 0.5 μl of which was mixed with 5 μl 10×conc. PCR Buffer with 20 mM $MgSO_4$ (Roche), 0.5 μl 20 mM dNTPs, 4 μl H_2O, and 40 μl DNA fragment elution in a total volume of 50 μl, then incubated at 72 °C for 15 minutes to achieve the reaction.

2.2.3 Annealing of Complementary Single-Stranded DNAs

The annealing mixture contains 5 μl each of the complementary DNA single strand (0.1 nmol/μl, IBA), 2 μl 10×Transcription Buffer (Roche), and 8 μl H_2O in a total volume of 20 μl. This annealing mixture was heated at 95 °C for 5 minutes and

slowly cooled down to 25 °C in an incubator (Eppendorf). Then, this annealed double-stranded DNA fragment can be directly used for ligation after a series of dilutions (1:1, 1:100, 1:1000).

2.2.4 Ligation

25-100 ng purified vector fragment was mixed with 3-10 folds (molecular ratio) of purified insert fragment, 1 µl 10×T4 DNA ligase buffer (MBI Fermentas), and 1 µl T4 DNA ligase (3 U/µl, MBI Fermentas) in a total volume of 10 µl. This ligation mixture was incubated at RT for at least 2 hours or overnight.

2.3 Polymerase Chain Reaction (PCR)

2.3.1 Standard and Genomic PCRs

The TaKaRa LA Tag system (TaKaRa) was used for standard and genomic PCR. In this system, primers should be 22-26 nucleotides with Tm higher than 68 °C. The reaction mixture contains 1 µl template DNA (10pg-1ng plasmid DNA, or 200 ng genomic DNA), 1 µl 10 pmol/µl forward primer, 1 µl 10 pmol/µl reverse primer, 5 µl 10×LA PCR Buffer, 5 µl 25 mM $MgCl_2$, 4-8 µl 2.5 mM dNTPs, and 0.5 µl LA Tag Polymerase (5U/µl) in a total volume of 50 µl. The thermocycling program (Tab. 2-2) was carried out using Mastercycler Gradient (Eppendorf). If the PCR product will be directly inserted into pGEM-T Easy T/A vector (Promega) or pCRII-TOPO vector (Invitrogen), 1 µl Tag polymerase (Gene Craft) was added into the reaction mixture immediately after the Step 5 final elongation and incubated at 72 °C for 30 minutes.

Step	Temperature	Duration
1. Initial Denaturation	94 °C	1 minute
2. Denaturation	98 °C	10 seconds
3. Annealing and Elongation	68 °C	1-10 minutes (about 1 minute/kb)
4. Go to Step 2, Repeat 29 to 39 times (30-40 cycles)		
5. Final Elongation	72 °C	3-15 minutes

Tabel 2-2: The thermocycling program for genomic PCR using LA Tag system.

2.3.2 RT-PCR

The One-Step RT-PCR Kit (Qiagen) was used to carry out RT-PCR thermocycling program (Tab. 2-3), in which the reaction mixture contains 1 µl Total RNA (0.1-0.5 µg/µl), 3 µl 10 pmol/µl forward primer, 3 µl 10 pmol/µl reverse primer, 10 µl 5×One-Step RT-PCR Buffer, 2 µl 10 mM dNTPs, 2 µl Enzyme Mix (Reverse Transcriptase plus Tag Polymerase), and 29 µl RNase-free H_2O to a total volume of 50 µl.

Step	Temperature	Duration
1. Reverse Transcription	50 °C	30 minutes
2. Reverse Transcriptase Inactivation	95 °C	15 minutes
3. Denaturation	94 °C	30 seconds
4. Annealing	55-65 °C	45 seconds
5. Elongation	72 °C	0.5-3 minutes (about 1 minute/kb)
6. Go to Step 3, Repeat 29-39 times (30-40 cycles)		
7. Final Elongation	72 °C	3-10 minutes

Tabel 2-3: The thermocycling program for one-step RT-PCR.

2.3.3 Detection and Purification of PCR Product

5 µl crude PCR product was loaded on the agarose gel and analyzed by electrophoresis. The left 45 µl PCR product can be purified by using PCR Purification Kit (Qiagen) as described by the manufacturer.

2.4 Transformation of *E. coli*

2.4.1 Preparation of Electrocompetent Cells

Preparation of electrocompetent cells was performed as described below (Tab. 2-4)

1. Inoculate two single colonies of *E. coli* (DH5α) into 2×10 ml LB medium and cultured at 37 °C shaking overnight (250 rpm).
2. Inoculate the 2×10 ml overnight cultures into 2×1 liter prewarmed LB medium and culture them at 37 °C shaking until the $O.D._{600}$ reached 0.6-0.8 (about 3

hours).
3. Chill the cells on ice for 10-30 minutes.
4. Centrifuge at 5,000 rpm at 4 °C for 20 minutes to harvest the cells.
5. Discard the supernatant, wash each pellet from 1 liter culture with 1 liter prechilled water (1:1 wash), then centrifuge at 5,000 rpm at 4 °C for 20 minutes.
6. Discard the supernatant, wash each pellet with 100 ml prechilled 10% glycerol (1:10 wash), then centrifuge at 6,000 rpm (Sorvall HS-4 rotor) at 4 °C for 10 minutes.
7. Discard the supernatant, wash each pellet with 20 ml prechilled 10% glycerol (1:50 wash), then centrifuge at 6,000 rpm at 4 °C for 10 minutes.
8. Discard the supernatant, wash each pellet with 2 ml prechilled 10% glycerol (1:500 wash), then centrifuge at 6,000 rpm at 4 °C for 5 minutes.
9. Aspirate the supernatant, resuspend each pellet in 2-3 ml 10% glycerol. 40 µl or 80 µl resuspension was aliquoted into each tube on ice, frozen in liquid nitrogen, and stored at –80 °C.

Tabel 2-4: Preparation of electrocompetent *E. coli* cells.

2.4.2 Preparation of Competent Cells for Heat Shock Transformation

The competent cells for heat shock transformation were prepared as described below (Tab. 2-5)

1. Inoculate a single colony of *E. coli* (DH5α or XL-1 Blue) into 50 ml LB medium and cultured at 37 °C shaking overnight (250 rpm).
2. Transfer 4 ml of the overnight culture into 400 ml LB medium and incubate at 37 °C shaking to an $O.D._{600}$ of 0.35-0.4.
3. Aliquot the culture into eight 50 ml prechilled sterile polypropylene tubes (BD Falcon), and incubate them on ice for 5-10 minutes.
4. Centrifuge at 1,600×g (3,000 rpm, Sorvall HS-4 rotor) at 4 °C for 7 minutes.
5. Discard the supernatants, gently resuspend each pellet in 10 ml prechilled $CaCl_2$ solution (60 mM $CaCl_2$, 15% glycerol, 10 mM PIPES, pH 7.0), and centrifuge at 1,100×g at 4 °C for 5 minutes.

6. Discard the supernatants, resuspend each pellet in another 10 ml prechilled $CaCl_2$ solution, and incubate them on ice for 30 minutes.
7. Centrifuge at 1,100×g at 4 °C for 5 minutes.
8. Discard the supernatants, and resuspend each pellet completely in 2 ml prechilled $CaCl_2$ solution.
9. Aliquot 200 µl into each tube on ice, freeze immediately in liquid nitrogen, and store them at –80 °C.

Tabel 2-5: Preparation of chemical competent *E. coli* cells.

2.4.3 Transformation of *E. coli* by Electroporation

40 µl competent cells were thawed on ice and transferred into a prechilled 0.1 cm electrode Gene Pulser Cuvette (Bio-Rad). 1 µl DNA solution (1 ng/µl) or 1.5 µl ligation product was added directly into the competent cells and mixed well by gently flicking. Then, the surface of the cuvette was completely dried and the electroporation was performed using Gene Pulser (Bio-Rad) under the condition of 1.8 kV voltage, 200 Ω resistance, 25 µF capacitance. Afterwards, 960 µl prewarmed LB medium was immediately supplied to the electroporated *E. coli* for recovery. The cells were recovered at 37 °C rotating for 1 hour, followed by plating 100 µl and 900 µl on separate plates.

2.4.4 Transformation of *E. coli* by Heat Shock

50-100 µl competent cells were thawed on ice and transferred into a Falcon 2059 polypropylene tube (BD Falcon). 10 ng pure DNA or 10 µl ligation product was directly added into the competent cells and mixed well by gently flicking. The mixture was incubated on ice for 30 minutes, heat shocked at 42 °C for 45 seconds, and incubated on ice for another 2 minutes. Then, 900 µl prewarmed LB or SOC medium (Invitrogen) was supplied to the heat shocked cells, and incubated at 37 °C rotating for 1 hour. The recovered cells were subsequently spun down at 3,000 rpm for 2 minutes, resuspended in 200 µl medium and plated.

2.5 Protein Purification and Analysis

2.5.1 GST-Fused Recombinant Protein Expression and Purification

GST-fused recombinant protein was expressed in *E. coli* and purified as described below (Tab. 2-6)

1. Mouse Geminin cDNA was inserted into pGEX-KG vector (Amersham) between B*amH*I and H*ind*III sites in frame with GST.
2. Heat shock transform the pGEX-KG-*Geminin* construct into BL21 DE3 C41 competent cells. Inoculate a single colony into 100 ml LB medium with 50 μg/ml ampicillin, and culture at 37 °C shaking overnight.
3. Add prewarmed LB medium with 50 μg/ml ampicillin into the 100 ml overnight culture up to 1 liter, and continuously incubate at 37 °C shaking to an $O.D._{600}$ of 0.7-0.8 (about 1 hour).
4. Add IPTG to a final concentration of 1 mM to induce the protein expression at 25 °C shaking for 6 hours (or at 37 °C shaking for 2 hours).
5. Centrifuge at 5,000 rpm at 4 °C for 25 minutes to harvest the cells.
6. Briefly discard the supernatant, resuspend the pellet with the remaining medium, and transfer the resuspension into a 50 ml Falcon tube.
7. Centrifuge at 4,000 rpm at 4 °C for 30 minutes. Discard the supernatant and freeze the pellet at –20 °C overnight.
8. Resuspend the pellet with 40 ml resuspension buffer (50 mM Tris, pH 7.5, 500 mM NaCl, 2 mM EDTA, freshly added protease inhibitor tablet (Roche)) on ice.
9. Sonicate the resuspension on ice for 5×1 minute with 1 cm tip using Cell Disruptor B15 (Branson Sonifier) under the condition of Output Option 7 and 50 % Duty Cycle.
10. Ultracentrifuge in a vacuum environment at 25,000 rpm at 4 °C for 25 minutes using L7 Ultracentrifuge (Beckman).
11. Collect the supernatant, add 500 μl prewashed Glutathione Sepharose 4B (Amersham), and incubate at 4 °C rotating for at least 1 hour.
12. Centrifuge at 800 rpm at 4 °C for 1 minute and discard the supernatant.
13. Wash with 15 ml prechilled washing buffer (50 mM Tris, pH 7.5, 1000 mM NaCl, 2 mM EDTA, freshly added protease inhibitor) twice. Centrifuge at 800 rpm at 4 °C for 1 minute and discard the supernatant in between.
14. Resuspend the beads with 5 ml washing buffer and transfer them into a 5 ml

column (Pierce). Flow through the buffer and wash the beads in the column once more with 4 ml washing buffer.
15. Elute the GST-Geminin fusion protein by incubating the beads with 1.2 ml 20 mM Glutathione (Sigma) at 4 °C rotating for 1 hour. Collect the elution.
16. Further elute the protein from the beads with another 2 ml 20 mM Glutathione at 4 °C rotating for another 1 hour. Collect the elution.
17. Measure the protein concentration with Bradford Assay (Bio-Rad), in which 1 µl of protein elution was mixed with 800 µl H_2O and 200 µl Bradford Reagent was added. Then, the $O.D._{595}$ of the sample was measured and the concentration of protein was determined according to the standard curve (Fig. 2-1).
18. Aliquot the purified protein, freeze them in liquid nitrogen and store at –80 °C.

Tabel 2-6: Expression and purification of GST-fused recombinant protein from *E. coli*.

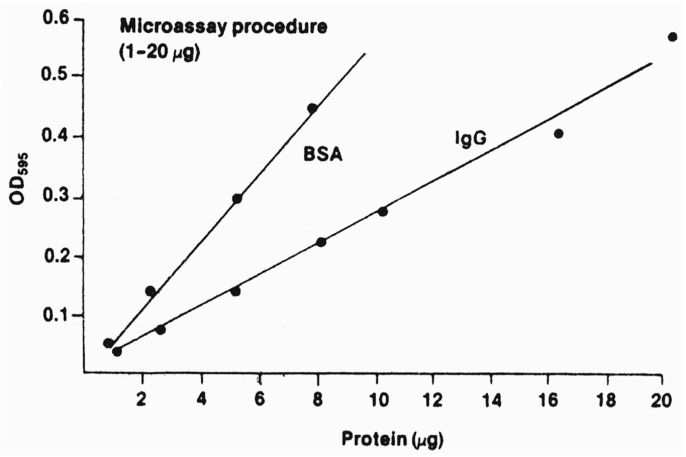

Figure 2-1: The standard curve for protein concentration determination. The BSA curve was used to determine protein concentrations, whereas the IgG curve was used for antibody concentration determination.

2.5.2 His-Tagged Recombinant Protein Expression and Purification

His-tagged recombinant protein was expressed in *E. coli* and purified as described below (Tab. 2-7).

1. Mouse Geminin cDNA was inserted into pQE30 vector (Qiagen) between B*amH*I and H*ind*III sites in frame with N-terminal His-tag.
2. Heat shock transform the pQE30-*Geminin* construct into XL-1 Blue competent cells. Inoculate a single colony into 100 ml LB medium with 50 µg/ml ampicillin,

and culture at 37 °C shaking overnight.
3. Add prewarmed LB medium with 50 μg/ml ampicillin into the 100 ml overnight culture up to 1 liter, and continuously incubate at 37 °C shaking to an $O.D._{600}$ of 0.7-0.8 (about 1 hour).
4. Add IPTG to a final concentration of 1 mM to induce the protein expression at 25 °C shaking for 6 hours (or at 37 °C shaking for 2 hours).
5. Centrifuge at 5,000 rpm at 4 °C for 25 minutes to harvest the cells.
6. Briefly discard the supernatant, resuspend the pellet with the remaining medium, and transfer the resuspension into a 50 ml Falcon tube.
7. Centrifuge at 4,000 rpm at 4 °C for 30 minutes. Discard the supernatant and freeze the pellet at –20 °C overnight.
8. Resuspend the pellet with 40 ml resuspension buffer (50 mM NaH_2PO_4-Na_2HPO_4, pH 8.0, 300 mM NaCl, 10 mM imidazole, 10% glycerol, freshly added protease inhibitor) on ice.
9. Sonicate the resuspension on ice for 5×1 minute with 1 cm tip using Cell Disruptor B15 under the condition of Output Option 7 and 50 % Duty Cycle.
10. Ultracentrifuge in a vacuum environment at 25,000 rpm at 4 °C for 25 minutes using L7 Ultracentrifuge.
11. Collect the supernatant, add 1 ml prewashed Ni-NTA beads (Qiagen), and incubate at 4 °C rotating for at least 1 hour.
12. Centrifuge at 800 rpm at 4 °C for 1 minute and discard the supernatant.
13. Wash with 15 ml prechilled washing buffer (50 mM NaH_2PO_4-Na_2HPO_4, pH 8.0, 300 mM NaCl, 20 mM imidazole, 10% glycerol, freshly added protease inhibitor) twice. Centrifuge at 800 rpm at 4 °C for 1 minute and discard the supernatant in between.
14. Resuspend the beads with 5 ml washing buffer and transfer them into a 5 ml column. Flow through the buffer and wash the beads in the column once more with 4 ml washing buffer.
15. Elute the protein with 2.5 ml 250 mM imidazole in washing buffer, collect the flow through immediately with 500 μl per tube.
16. Measure the protein concentration with Bradford Assay, in which 2 μl of protein elution was mixed with 800 μl H_2O and 200 μl Bradford Reagent was

added. Then, the $O.D._{595}$ of the sample was measured and the concentration of protein was determined according to the standard curve (Fig. 2-1).
17. Aliquot the purified protein, freeze them in liquid nitrogen and store at –80 °C.

Tabel 2-7: Expression and purification of His-tagged recombinant protein from *E. coli*.

2.5.3 Total Protein Extraction from Mouse Embryos

11.5 d.p.c. mouse embryos were dissected out from the uterus in PBS, and solubilized in 500 µl/embryo lysis buffer 1 (20 mM Tris, pH 7.5, 100 mM KCl, 2 mM EDTA, 1% Triton X-100, 1 mM β-mecaptoethanol, freshly added protease inhibitor) on ice, using glass homogenizer. The solubilized embryo extracts were centrifuged at 13,000 rpm at 4 °C for 15 minutes, and the supernatant was collected. The protein concentration of the soluble extracts was measure at absorbance of 280 nm by BioPhotometer (Eppendorf) and normalized by BSA standards. The total protein extracts were aliquoted, frozen in liquid nitrogen, and stored at –80 °C.

Alternatively, mouse embryos were homogenized briefly with pipette, and sonicated on ice with continuous pulses for 3-4×10 seconds in 400 µl/embryo lysis buffer 2 (20 mM HEPES, pH 7.85, 30 mM NaCl, 10% glycerol, 0.2 mM EDTA, 1 mM DTT, and freshly added protease inhibitor) using Cell Disruptor B15 and 3 mm tip. The following treatment was the same with using glass homogenizer.

2.5.4 *In Vitro* Transcription/Translation

For *in vitro* transcription/translation, cDNA fragment with single ATG was cloned into pSP64 or pSP65 vector (Promega) and maxipreped. The assay was performed using TNT Reticulocyte Lysate System (Promega). The reaction mixture containing 2 µg maxiprep DNA, 4 µl TNT reaction buffer, 2 µl amino acids mixture without methionine, 4 µl [^{35}S]-methionine, 1.5 µl RNasin, 1.5 µl TNT SP6 RNA polymerase, 50 µl reticulocyte lysate, and proper volume of DEPC treated H_2O in a total volume of 100 µl was mixed well by flicking and incubated at 30 °C for 2 hours.

2.5.5 Protein Gel Electrophoresis

SDS-polyacrylamide gels were prepared with protein gel preparation system (Bio-Rad). 12% separating gel and 6% stacking gel (Tab. 2-8) were applied to detect

proteins smaller than 50 kDa, while 10% separating gel and 5% stacking gel (Tab. 2-8) were used to analyze proteins larger than 50 kDa. A protein sample was mixed with the same volume of 2×SDS loading buffer (125 mM Tris, pH 6.8, 20% glycerol, 0.02% bromophenol blue, 2% β-mercaptoethanol, 4% SDS), and heated at 95 °C for 5 minutes or in boiling water for 3 minutes. A maximum of 25 µl sample was loaded into the slot and electrophoresis was performed in 1×SDS buffer (25 mM Tris-base, 0.1% SDS, 192 mM glycine, pH 8.75) under 20 mA/gel, following 30 minutes preelectrophoresis under the same condition. Then, the gel could be subjected to western blotting directly, or fixed in fixation solution (45% methanol, 7.5% acetate) for 5 minutes and stained with Coomassie blue staining solution (0.25% Coomassie brilliant blue R 250, 45% methanol, 10% acetate; or 0.1% Serva R 250, 50% methanol, 10% acetate) at RT for 0.5-1 hour. The Coomassie stained gel was subsequently destained with 10% acetate for several hours or overnight.

Separating Gel	10%	12%
1.5 M Tris, pH 8.8	7.5 ml	6 ml
30% Acrylamide-Bisacrylamide Solution (Roth)	10 ml	10 ml
H_2O	11.9 ml	7.5 ml
10% SDS	300 µl	240 µl
10% APS	300 µl	240 µl
TEMED	15 µl	12 µl
Total Volume	30 ml	24 ml

Stacking Gel	5%	6%
1 M Tris, pH 6.8	1.5 ml	1.25 ml
30% Acrylamide-Bisacrylamide Solution	2 ml	2 ml
H_2O	8.25 ml	6.38 ml
10% SDS	120 µl	100 µl
10% APS	120 µl	100 µl
TEMED	15 µl	12 µl
Total Volume	12 ml	10 ml

Tabel 2-8: The components of SDS-polyacrylamide gels.

2.5.6 Western Blotting

Western blotting and subsequent immunostaining were performed as described below (Tab. 2-9) using antibodies against Geminin (see 2.5.8), Rae28 (Tomotsune *et al.*, 1999), FGF2 (Chemicon), Cdt1 (Wohlschlegel *et al.*, 2000), Vimentin (Elbashir *et al.*, 2001), or His-tag (Novagen).

1. Cut a Protran Nitrocellulose Transfer Membrane (Schleicher & Schell BioScience) and 4 pieces of Whatman paper into a similar size to the gel, with the Whatman paper slightly larger. And presock them in blot buffer (48 mM Tris-base, 3.9 mM glycine, 0.037% SDS, 20% methanol).
2. Between two double-layered presocked Whatman paper, the SDS-polyacrylamide gel was placed tightly onto a presocked nitrocellulose membrane avoiding any air bubble in between, with the membrane close to the anode and the gel close to the cathode.
3. Press this sandwich including Whatman paper, gel, and membrane tightly together into a clamp. Electroblot was performed in blot buffer using western blotting system (Bio-Rad) under 15 V overnight or under 30 V for 1-2 hours with a cooling chamber.
4. Stop the membrane transfer, and stain the membrane with 0.1% Ponceau S to check the membrane transfer efficiency.
5. Destain the Ponceau S with water and then western buffer A (10 mM Tris, pH 7.4, 0.9% NaCl, 0.05% Tween 20).
6. Block the membrane in blocking solution (1-5% low fat milk powder in western buffer A) at RT for 1 hour, rocking on a rocky machine (Biometra).
7. Dilute the primary antibody 1:100-1:1000 in blocking solution, and incubate at 4 °C shaking overnight (preferred) or at RT rocking for 1-2 hours.
8. Wash with western buffer A at RT rocking for 5-10 minutes.
9. Wash with western buffer B (0.9% NaCl, 0.5% Triton X-100, 0.1% SDS, freshly added 0.1% BSA) twice at RT rocking for 5-10 minutes each.
10. Wash with western buffer A at RT rocking for 5-10 minutes.
11. Incubate the membrane with 1:5000 diluted Horseradish Peroxidase (HRP) conjugated anti-rabbit or mouse IgG secondary antibody (Amersham or Biotrend) in blocking solution at RT rocking for 45 minutes.

12. Repeat the washing steps 8-10.
13. Mix well 500 µl Renaissance Oxidizing Reagent and 500 µl Renaissance Enhanced Luminol Reagent (NEN) as the chemiluminescent substrate for HRP, and equally distribute the mixture onto the membrane. The chemiluminescence was observed by exposing the membrane to a Lumi-Imager (Boehringer Mannheim) for 10 seconds to 20 minutes.

Tabel 2-9: Western blotting onto nitrocellulose membranes and subsequent immunostainings

2.5.7 N-Terminal Coupling of Protein

His-Geminin recombinant protein was N-terminally coupled to agarose matrix at 4 °C using AminoLink Plus Coupling Gel Kit (Pierce) (Tab. 2-10).

1. Dialyse the purified His-Geminin protein against PBS at 4 °C overnight to exclude ammonia from the protein solution.
2. Resuspend the beads to mix well, take 4 ml (3 ml bed volume) into a 15 ml column, and flow through the buffer.
3. Wash the beads with 2.5 volumes (7.5 ml) of coupling buffer, pH 7.0.
4. Incubate the beads with 6 mg His-Geminin recombinant protein in 3 ml coupling buffer at 4 °C rotating overnight.
5. Add 50 µl (about 1/60-1/50 volume) 5 M Sodium Cyanoborohydride ($NaCNBH_3$) reduction reagent, and incubate at 4 °C rotating for 4 hours.
6. Flow through the liquid in the column and collect it. Wash the beads with 2.5 volumes (7.5 ml) of coupling buffer and collect the flow through.
7. Measure the protein concentration of the flow throughs (1.5 mg in 10 ml) and calculate the coupling efficiency (4.5 mg coupled, 75%).
8. Wash the protein coupled beads with 2 volumes (6 ml) of quench buffer.
9. Incubate the beads with 1 volume (3 ml) of quench buffer plus 50 µl reduction reagent (5 M $NaCNBH_3$) at 4 °C rotating for 1 hour.
10. Flow through the liquid and wash the beads with 2.5 volumes (7.5 ml) of 0.2 M glycine, pH 2.5.
11. Wash the beads with 2.5 volumes (7.5 ml) of 50 mM Tris, pH 7.5.

12. Resuspend the protein coupled beads with 1 volume (3 ml) of 50 mM Tris, pH 7.5 and store at 4 °C.

Tabel 2-10: N-terminal coupling of recombinant proteins to agarose matrix.

2.5.8 Antibody Purification from Crude Serum

The crude anti-Geminin antiserum was purified by chromatograph at 4 °C (Tab. 2-11), then aliquoted and stored at –80 °C.

1. Transfer the 4.5 mg N-terminally coupled His-Geminin recombinant protein (7 ml) into a 50 ml Falcon tube.
2. Wash the column with 2 ml 50 mM Tris, pH 7.5 and merge with the beads.
3. Incubate the beads with crude anti-Geminin antiserum at 4 °C rotating overnight to bind the antibody to the antigen.
4. Transfer the beads together with the serum into a 25 ml column, flow through the serum and collect it.
5. Wash the beads with 10 volumes (30 ml) of western buffer A.
6. Wash the beads with 10 volumes (30 ml) of western buffer B.
7. Wash the beads with 5 volumes (15 ml) of western buffer A.
8. Elute the anti-Geminin antibodies with 3 volumes (7.5 ml) of 200 mM glycine, pH 2.5, collect every 500 µl elution with tubes containing 75 µl 1.5 mM Tris, pH 8.8.
9. Measure the IgG concentration of each tube by Bradford Assay (Fig. 2-1).
10. Merge the tubes with high IgG concentration and dialyse against 1 liter PBS at 4 °C overnight. Measure the concentration again and aliquot it.

Tabel 2-11: Antibody purification from crude antiserum using chromatography.

2.6 Yeast Two-Hybrid Screen

The yeast two-hybrid screen was performed using ProQuest Two-Hybrid System (Gibco BRL).

2.6.1 Constructs for the Two-Hybrid Screen

The BanII/Pwo-NotI cDNA fragment encoding murine Geminin excised from pCMV3-*Geminin* eukaryotic expression construct was inserted into the MscI-NotI sites of pDBLeu vector (Gibco BRL) in frame with the GAL4 DNA binding domain. The resulted pDBLeu-*Geminin* construct was used as bait plasmid in the yeast two-hybrid screen.

The cDNA library from 8.5 d.p.c. mouse embryos has been cloned into pPC86 vector (Gibco BRL) in frame with the GAL4 activation domain. 2 μl *E. coli* containing the library DNA was inoculated into 100 ml LB medium with 50 μg/ml ampicillin and maxipreped.

2.6.2 Cotransformation Efficiency Evaluation of MaV203 Competent Cells

The cotransformation efficiency of MaV203 competent cells was evaluated as described below (Tab. 2-12).

1. Thaw the PEG/LiAc (Gibco BRL) solution at RT, mix the solution well before dispensation.
2. Thaw the MaV203 Competent Yeast Cells (Library Scale, Gibco BRL) in a 30 °C incubator for 90 seconds (or less). Invert the tube several times immediately, and transfer 100 μl into a 1.5 ml eppendorf tube.
3. Add 1 μg pDBLeu-*Geminin* and 1 μg pPC86 vector to the competent cells, mix well by flicking the tube.
4. Add 600 μl PEG/LiAc solution into the mixture, mix well by inverting the tube until the competent cells are totally homogenous.
5. Incubate in a 30 °C incubator for 30 minutes, inverting the tube every 10 minutes.
6. Add 35.5 μl DMSO and mix well by inverting the tube.
7. Heat shock the cells at 42 °C for 20 minutes, inverting the tube occasionally.
8. Centrifuge the tube at 2,000 rpm for 5 seconds and aspirate the supernatant.
9. Resuspend the pellet in 1 ml autoclaved H_2O and make 1:10, 1:100 and 1:1000 dilutions.
10. Plate 100 μl from crude resuspension and each dilution onto the selection

medium plate SD-L-W (21.36 g SD medium (Clontech), 0.512 g DO-Leu-Trp (Clontech), 17.6 g Agarose (Gibco BRL) in a total volume of 800 ml, autoclaved, 25 ml/dish).
11. Incubate the plate upside down at 30 °C for 72 hours.
12. After 72 hours incubation 100 µl 1:100 dilution generated 10 transformants, which means 1 µg DNA can generate 10^4 transformants. For library screen, 1 µg DNA should generate at least 10^5 transformants. So, the MaV203 Competent Yeast Cells was not suitable for library screen.

Tabel 2-12: The cotransformation efficiency evaluation of MaV203 yeast competent cells.

2.6.3 Determination of the 3AT Concentration

3AT was used to inhibit background colonies during the first round of library screen. 2 single yeast colonies each from five control strains A-E (Gibco BRL) as well as yeast cotransformed with pDBLeu-*Geminin* and pPC86 on SD-L-W plates were patched onto SD-L-W-H plates (8.01 g SD medium, 0.186 g DO-Leu-Trp-His (Clontech), 6.6 g agarose in a total volume of 300 ml, autoclaved, 25 ml/dish) supplemented with different concentrations of 3AT (0 mM, 10 mM, 25 mM, 50 mM, 60 mM, 75 mM, 100 mM, diluted from 2 M stock). After incubation for 18 hours at 30 °C, the highest 3AT concentration inhibiting the growth of control strain A and permitting the growths of other control strains was selected for the library screen, which is 60 mM.

2.6.4 Total Protein Extraction from Yeast

Total proteins of yeast were extracted as described below (Tab. 2-13).

1. Inoculate a single colony into 5 ml proper broth and incubate at 30 °C shaking overnight.
2. Check the $O.D._{600}$ of overnight culture, and apply 5 O.D. yeast cells for protein extraction (If $O.D._{600}$=1.0, use 5 ml cultured cells; If $O.D._{600}$=2.0, use 2.5 ml).
3. Centrifuge at 13,000 rpm for about 10 seconds to pellet the cells.
4. Aspirate the supernatant, resuspend the pellet in 180 µl 2 M NaOH containing 5% β-mercaptoethanol, and incubate on ice for 10 minutes.

5. Add 20 µl 110% TCA (w/v) to precipitate the proteins, incubate on ice for 10 minutes.
6. Centrifuge at 13,000 rpm for 1 minute and carefully remove the supernatant.
7. Neutralize the pellet by resuspending it in 100 µl 1 M Tris, pH 11.0.
8. Centrifuge at 13,000 rpm for 1 minute and carefully remove the supernatant.
9. Resuspend the pellet in 100 µl 2×SDS loading buffer, incubate at 95 °C for 5 minutes.
10. 5-10 µl (0.25-0.5 O.D.) sample was subjected to SDS-polyacrylamide gel electrophoresis and western blotting.

Tabel 2-13: Total protein extraction from yeast cells.

2.6.5 cDNA Library Screen on Histidine Minus Medium

The first round of cDNA library screen was performed on plates lacking leucine, tryptophan and histidine, and supplemented with 60 mM 3AT as described below (Tab. 2-14).

1. Heat shock transform the MaV203 competent yeast cells with pDBLeu-*Geminin* as described in 2.6.2, then plate on SD-L medium (8.01 g SD medium, 0.207 g DO-Leu (Clontech), 6.6 g agarose, autoclaved, 25 ml/dish) and incubate for 48 hours.
2. Inoculate a single pDBLeu-*Geminin* transformant into 100 ml SD-L broth, and incubate at 30 °C overnight.
3. Check the $O.D._{600}$ of the SC-L broth inoculated (1:5 dilution: $O.D._{600}$=0.604).
4. For good competent cells, the $O.D._{600}$ of the starting culture in YEPG broth (10 g Yeast extract, 20 g Peptone 140, 20 g D-glucose, 20 mg uracil, 20 mg adenine sulphate in a total volume of 1 liter, autoclaved) should be 0.2-0.3. Thus, centrifuge 20 ml overnight culture at 2,500 rpm for 2 minutes, discard the supernatant and resuspend the pellet in 1 ml YEPG broth. Add 200 ml YEPG broth to the resuspension and check $O.D._{600}$=0.316. So, add 50 ml more YEPG broth.
5. Incubate at 30 °C for 4.5 hours shaking. Check $O.D._{600}$=0.647. (The best range for preparing competent cells and transformation is 0.8-1.0. For one library scale transformation, we always use 100 ml 1 O.D. cells (about 10^9 cells). So, we used

200 ml O.D. 0.647 cells).
6. Centrifuge 200 ml culture at 2,500 rpm for 2 minutes, discard the supernatant and wash cells with 10 ml LTS buffer (10 mM Tris, pH 7.4, 1 mM EDTA, 0.1 M LiAc, 1M α-Sorbitol).
7. Centrifuge at 2,500 rpm for 2 minutes, discard the supernatant, resuspend the cells in 1.1 ml LTS buffer, and equally distribute it into 22 tubes with 50 µl each.
8. Centrifuge at 13,000 rpm for about 10 seconds, and aspirate the supernatants.
9. Add 250 µl 50% PEG 4000 (It is better to use PEG 3350), 36 µl 1 M LiAc, 20 µl 2 mg/ml carrier Salmon Sperm DNA (Stratagene) into each tube.
10. Add 50 µl DNA solution containing 5 µg maxipreped library DNA into each tube. Then use pipette to destroy the pellet slightly, and mix well by vortexing.
11. Incubate at 30 °C for 45 minutes, inverting the tubes occasionally.
12. Heat shock at 42 °C for 20 minutes, inverting the tubes occasionally.
13. Centrifuge at 13,000 rpm for about 10 seconds, and aspirate the supernatants.
14. Wash each pellet with 100 µl H_2O or TE buffer (10 mM Tris, pH 7.4, 1 mM EDTA) without destroying the pellets.
15. Resuspend each cell pellet in 500 µl YEPG broth and recover the transformed yeast cells at 30 °C for 3 hours shaking.
16. Centrifuge at 13,000 rpm for about 10 seconds, aspirate 300 µl medium, and resuspend the pellet in the left 200 µl medium.
17. Plate each resuspension onto a 15 cm SD-L-W-H plate supplemented with 60 mM 3AT (40 ml medium per 15 cm dish). Incubate the plates at 30 °C for 72 hours.
18. One tube was reserved to check the transformation efficiency before the last centrifugation. 20 µl from the 500 µl resuspension was diluted 1:10, 1:100, 1:1000, and 200 µl of these dilutions were plated onto SD-L-W plates.

Tabel 2-14: The first round of cDNA library screen on histidine minus medium.

2.6.6 cDNA Library Screen by X-gal assay

The second round of cDNA library screen, X-gal assay, was performed as described below (Tab. 2-15).

1. Inoculate 177 positive colonies from the first round of screen onto numbered SD-L-W plates. In the meantime, also inoculate all these colonies onto Nytran nylon transfer membranes (Schleicher&Schuell BioScience) that were wet and tightly attached to SD-L-W medium. Incubate the inoculated plates at 30 °C overnight.
2. Proper amount of X-gal (Applichem) was dissolved in 100 µl DMFA, and then diluted in 7 ml Z-Buffer (16.1 g $Na_2HPO_4 \cdot 7H_2O$ (or 10.7 g $Na_2HPO_4 \cdot 2H_2O$), 5.5 g $NaH_2PO_4 \cdot H_2O$, 0.75 g KCl, 0.25 g $MgSO_4 \cdot 7H_2O$ in a total volume of 1 liter) to a final concentration of 0.3-1 mg/ml.
3. Distribute the 7 ml X-gal in Z-Buffer onto a Whatman paper in a 9 cm dish.
4. Freeze the nylon membrane with yeast colonies inoculated in liquid nitrogen for 1 minute.
5. Place the frozen membrane onto the Whatman paper, and incubate at 30 °C.
6. Check the X-gal staining of the colonies after 10 minutes incubation to overnight.

Tabel 2-15: The second round of cDNA library screen using X-gal assay.

2.6.7 DNA Extraction from Yeast Cells

1.5 ml overnight culture was pelleted by centrifugation at 13,000 rpm for about 10 seconds, and resuspended in 30 µl STES buffer (100 mM Tris, pH 8.0, 1 mM EDTA, 100 mM NaCl, 0.1% SDS). The resuspension was vortexed, spun down at 13,000 rpm for about 10 seconds, and resuspended in another 30 µl STES buffer. Acid washed glass beads were added to 80% volume, followed by vortexing the sample for 5×1 minute. Then, 200 µl TE buffer was added, and DNA was recovered by phenol/chloroform/isoamylalcohol (25:24:1) extraction and isopropanol precipitation. For the isolation of a certain plasmid, the extracted DNA was transformed into *E. coli* and selected on an ampicillin or kanamycin plate.

2.7 Analysis of Protein-Protein Interactions

2.7.1 GST Pull-Down Assay

The *in vitro* protein-protein interactions were studied using GST pull-down assays (Tab. 2-16).

1. Prewash 50 µl Glutathione Sepharose 4B beads (40 µl bed volume) with 500 µl pull-down binding buffer (20 mM Tris, pH 7.5, 100 mM NaCl, 1 mM EDTA, 0.1% NP-40, freshly added 1 mM PMSF). Spin it down by brief centrifugation at less than 4,000 rpm for several seconds, and aspirate the supernatants.
2. For coupling, incubate the prewashed beads with 40-50 µg recombinant GST-Geminin or GST protein in 500 µl pull-down binding buffer at 4 °C rotating overnight.
3. Spin down the beads by brief centrifugation, and wash the beads once with 500 µl pull-down binding buffer at 4 °C rotating for 3 minutes to get rid of the unbound proteins.
4. Spin down the beads by brief centrifugation, aspirate the supernatants.
5. Incubate 45 µl *in vitro* transcription/translation product with GST-Geminin or GST coupled beads in 500 µl pull-down binding buffer at 4 °C rotating for 1-2 hours. Mix 10 µl *in vitro* transcription/translation product as control with 2×SDS loading buffer and heat at 95 °C for 5 minutes.
6. Spin down the beads, aspirate the supernatants, and wash the beads with pull-down binding buffer twice at 4 °C rotating for 3-5 minutes each.
7. Spin down the beads, aspirate the supernatants, and wash the beads with pull-down washing buffer (20 mM Tris, pH 7.5, 150 mM NaCl, 1 mM EDTA, 0.1% NP-40, freshly added 1 mM PMSF) twice at 4 °C rotating for 3-5 mintues each.
8. Spin down the beads and aspirate the supernatants.
9. Elute the protein from the beads with 40 µl 2×SDS loading buffer by heating at 95 °C for 5 minutes.
10. Spin down the beads, and load 20 µl supernatants and 10 µl control on the gel.
11. Put the gel on a wet Whatman paper and dry the gel with a vacuum gel drier (Biometra) at 60 °C for 3 hours.
12. Fix the gel together with the Whatman paper in the cassette, and expose to a BioMax film (Kodak) at –70 °C overnight.
13. Develop the film with Curix 60 developing machine (Agfa)

Tabel 2-16: Analysis of *in vitro* protein-protein interaction using GST pull-down assay.

2.7.2 Immunoprecipitation

The *in vivo* protein-protein interactions were studied using immunoprecipitations (Tab. 2-17).

1. Hydrate 30 mg Protein A Sepharose CL-4B (Amersham) beads with 500 µl PBS (about 150 µl bed volume), and wash the beads with 1 ml PBS twice.
2. Incubate 400 µg purified anti-Geminin antibodies (500 µl) or 100 µl pre-immune serum plus 400 µl PBS with washed beads at RT rotating overnight.
3. Wash the beads 4 times with 500 µl 0.2 M $Na_2B_4O_7$, pH 9.0 for 5 minutes each.
4. Resuspend the beads in 600 µl 0.2 M $Na_2B_4O_7$, pH 9.0 and save a 10 µl aliquot. Then, add 3.7 mg dimethylpimelimidate (about 20 mM) into the resuspension and incubate at RT rotating for 30 minutes to crosslink the antibody with beads.
5. Save another 10 µl aliquot, and stop the crosslinking reaction by washing with 500 µl 0.2 M ethanolamine, pH 8.0.
6. Incubate the beads with 500 µl 0.2 M ethanolamine, pH 8.0 at RT rotating for 2 hours.
7. Wash the beads with PBS 3 times for 5 minutes each, and incubate with 1.5 ml (40 mg/ml) 11.5 d.p.c. mouse embryonic extracts at 4 °C rotating for 2 hours.
8. Wash with 500 µl IP washing buffer (20 mM Tris, pH 7.5, 150 mM KCl, 1 mM EDTA, 1 mM β-mercaptoethanol, 1 mM PMSF, 0.1% Triton X-100) three times at 4 °C rotating for 5 minutes each.
9. Elute the co-precipitated proteins in 100 µl 2×SDS loading buffer by heating at 95 °C for 6 minutes.
10. 15-30 µl eluted co-precipitants were loaded on a 10% SDS-polyacrylamide gel, and western blotting was performed using anti-Rae28 antibodies. Alternatively, the eluted co-precipitants and save aliquots were loaded on a gel and stained by Coomassie.

Tabel 2-17: Analysis of *in vivo* protein-protein interaction by immunoprecipitation.

2.7.3 Peptide Array Analysis

Peptide array membranes were blocked with 10 ml blocking solution (1.5% BSA in western buffer A) at RT rocking for 1 hour. Then, His-Geminin recombinant protein was added into the blocking solution to a final concentration of 1 μg/ml, and incubated at 4 °C shaking overnight. Afterwards, membranes were sequentially washed with 10 ml western buffer A, western buffer B, western buffer B, and western buffer A for 10 minutes each. The following steps from primary antibody staining are the same with normal western blotting (see 2.5.6) except the blocking solution.

2.8 Analysis of Protein-Nuclei Acids Associations

2.8.1 Electrophoretic Mobility Shift Assays (EMSAs)

The *in vitro* protein-DNA interactions were studied using EMSAs (Tab. 2-18).

1. The DNA labeling mixture containing 1 μl sense strand oligonucleotide (0.1 nmol) including a certain protein binding site, 2 μl polynucleotide kinase buffer (Roche), 3 μl γ-32P-dATP (30 mCi), 1 μl polynucleotide kinase, and 13 μl H_2O in a total volume of 20 μl was incubated at 37 °C for 45 minutes.
2. Add 30 μl H_2O into the labeling mixture and purify it with a G-50 sephadex micro column.
3. Mix the 60 μl flow through with 6 μl (0.1 volume) 1 M KCl and 1 μl antisense strand oligonucleotides (0.1 nmol).
4. Add 50 μl mineral oil (Sigma) onto the top of the mixture. Then, denature at 94 °C for 10 minutes and naturally cool it down for 45 minutes to anneal the oligos using a PCR machine.
5. Dilute 2 μl labeled double-stranded oligo into 200 μl H_2O, and count the radioactivity with an LS1701 counter (Beckman).
6. Dilute 1 μl labeled double-stranded oligo into a proper volume of H_2O to get 25,000 cpm/μl.
7. *In vitro* transcription/translation was performed in a total volume of 25 μl.
8. Preincubate 4 μl *in vitro* transcription/translation protein with 15 μl 2×retardation buffer (40 mM HEPES-NaOH, pH 7.6, 8% Ficoll, 10 mM $MgCl_2$, 80 mM NaCl, 0.2 mM EDTA, 1 mM DTT), 0 μl or 8 μl 1 μg/μl His-Geminin recombinant protein, and 8 μl or 0 μl H_2O in a total volume of 27 μl on ice for 1

hour.
9. Add 2 μl 2.5 μg/μl poly[dI-dC] (Roche) and 1 μl diluted radioactive oligo (25,000 cpm) into the preincubation mixture, and incubate on ice in a total volume of 30 μl for another 1 hour.
10. Prepare a 10% polyacrylamide gel (48.1 ml H_2O, 25 ml 30% acrylamide-bisacrylamide solution, 1.5 ml 10×TBE buffer, 400 μl 10% APS, and 40 μl TEMED in a total volume of 75 ml) and prerun the gel under 150 V for 1 hour.
11. Apply 24 μl sample (20,000 cpm) from the 30 μl on the gel, and the electrophoresis was performed under 80 V overnight.
12. Fix the gel together with a support glass in the cassette, and expose to a BioMax film at –70 °C for 7.5 hours.
13. Develop the film with the Curix 60 developing machine.

Tabel 2-18: Analysis of *in vitro* protein-DNA interaction using EMSA.

2.8.2 Chromatin Immunoprecipitation (ChIP) Assay

The Chromatin Immuoprecipitation from 1.5×10^6 mouse primary cultured fibroblasts (80-90% confluence in 10 cm dishes) was performed using anti-Geminin antibodies (see 2.5.8) and ChIP Assay Kit (Upstate) (Tab. 2-19).

1. Crosslink histones to DNA by adding formaldehyde directly into culture medium to a final concentration of 1% (270 μl 37% formaldehyde into 10 ml culture medium) at 37 °C for 10 minutes.
2. Aspirate medium, and wash the cells twice with 5 ml ice cold PBS (always containing 1 mM PMSF and protease inhibitor in the ChIP assay).
3. Scrape the cells with a glass slide in 5 ml PBS, and transfer floated cells together with buffer into a 15 ml Falcon tube.
4. Wash the dish twice with 2.5 ml ice cold PBS and collect them into the same tube.
5. Pellet the cells at 2,000 rpm at 4 °C for 4 minutes. In the meantime, prewarm the SDS Lysis Buffer to room temperatute, then add 1 mM PMSF and protease inhibitor.

6. Aspirate the supernatant, and resuspend the cell pellet in 300 μl SDS Lysis Buffer (200 μl/10^6 cells) and incubate on ice for 10 minutes.

7. Sonicate the cell lysate on ice to shear DNA to lengths shorter than 500 bp using 3 mm tip under the condition of output option 3, 5 times 10 seconds continuous pulse.

8. Separate the sonicated cell lysate into two 2 ml tubes with 1.5 ml each. Centrifuge at 13,000 rpm at 4 °C for 10 minutes. Collect the supernatant and discard the pellet.

9. Dilute the supernatant 10 fold by adding 1350 μl ChIP Dilution Buffer into 150 μl supernatant. Add 1 mM PMSF and protease inhibitors, and save 7.5 μl dilution for checking shearing efficiency.

10. Preclear 1.5 ml diluted cell supernatant with 60 μl Salmon Sperm DNA/Protein A Agarose-50% Slurry at 4 °C rotating for 30 minutes.

11. Pellet the agarose by brief centrifugation and collect the supernatant fraction.

12. Add 150 μg anti-Geminin antibodies (0.8 μg/μl) to the precleared supernatant and incubate at 4 °C rotating overnight, using pre-immune serum as control.

13. Add 60 μl Salmon Sperm DNA/Protein A Agarose Slurry and incubate at 4 °C rotating for 1 hour to capture the complexes.

14. Pellet the agarose by gentle centrifugation at 700 rpm at 4 °C for 1 minute. Carefully remove the supernatant.

15. Wash with 1 ml Low Salt Immune Complex Wash Buffer at 4 °C rotating for 3-5 minutes.

16. Wash with 1 ml High Salt Immune Complex Wash Buffer at 4 °C rotating for 3-5 minutes.

17. Wash with 1 ml LiCl Immune Complex Wash Buffer at 4 °C rotating for 3-5 minutes.

18. Wash twice with 1 ml 1×TE Buffer at 4 °C rotating for 3-5 minutes each.

19. Elute the complex from antibody by adding 250 μl freshly prepared elution buffer (1% SDS, 0.1 M $NaHCO_3$) to the pelleted agarose. Vortex briefly to mix and incubate at room temperature rotating for 15 minutes.

20. Spin down the agarose, collect the supernatant, repeat elution, and combine elutions (about 500 μl).

21. Add 20 µl 5 M NaCl to the combined elution to reverse the crosslinks by incubation at 65 °C for 4 hours.
22. Add 10 µl 0.5 M EDTA, 20 µl 1 M Tris-HCl, pH 6.5, and 2 µl 10 mg/ml Proteinase K to the combined elution and incubate at 45 °C for 1 hour.
23. Recover DNA by phenol/chloroform/isoamylalcohol (25:24:1) extraction and isopropanol precipitation. Dissolve the pellet in 10 µl H_2O.
24. 1 µl of dissolved DNA was applies as template for PCR using LA Tag system and four pairs of primers (Prom: 5'-CACGAGATTGCTCAGGGCTTAG-3', 5'-CAATACTCAGCCAGCGTGGAAAC-3'; Intron: 5'-TTCAGAGCCTGCCTTGCCATC-3', 5'-CACTCTGGCCACTGAGCTAG-3'; UTR1: 5'-CCACTACAGCCTGAGGAAGAG-3', 5'-GACAGTGACTCATGCCCAAAG-3'; UTR2: 5'-CATAAGATGCACAGCAGCTCATGC-3', 5'-GTGGGTCTGGATGTATGAGCCTG-3').

Tabel 2-19: Analysis of *in vivo* protein-chromatin association using ChIP assay.

2.9 Cell Culture and Immunocytochemistry

2.9.1 Cell Culture Medium

U2-OS osteosarcoma cells were cultured in McCoy's 5A medium (Gibco BRL) containing 1.5 mM L-glutamine, 10% FCS, 100 U/ml penicillin G, and 100 µg/ml streptomycin.

A-375 melanoma cells were cultured in Dulbecco's modified Eagle's medium (DMEM, Gibco BRL) containing 4 mM L-glutamine, 10% FCS, 1.5 mg/ml sodium bicarbonate, 4.5 mg/ml glucose, 100 U/ml penicillin G, 100 µg/ml Streptomycin.

NIH/3T3 cells were cultured in DMEM medium containing 4 mM L-glutamine, 10% FCS, 1.5 mg/ml sodium bicarbonate, 4.5 mg/ml glucose, 100 U/ml penicillin G, 100 µg/ml Streptomycin.

Hela cells were cultured in DMEM medium containing 2 mM L-glutamine, 10% FCS, 4.5 mg/ml glucose, 100 U/ml penicillin G, 100 µg/ml Streptomycin.

2.9.2 Cell Revival

Cells from liquid nitrogen are revived in a 37 °C water bath as quickly as possible, then transferred into a 15 ml Falcon tube containing 5 ml proper culture medium, and centrifuged at 1,000 rpm for 5 minutes. The supernatant medium was aspirated, 5 ml

fresh medium was added to the cell pellet and pipetted up and down for at least 15 times to break cell aggregates. The, the cell resuspension was distributed in a 10 cm petridish containing 5 ml culture medium (10 ml in total). The dish was gently shaken left-right and backward-forward to achieve equally distribution of cells. Then, the cells were cultured in a BBD 6220 incubator (Heraeus) at 37 °C under 5% CO_2 concentration.

2.9.3 Cell Passage and Freeze

The medium of cultured 70-95% confluent cells in a 10 cm dish was aspirated. Cells were washed with 10 ml PBS, which was then aspirated from the dish. 2.5 ml 1×Trypsin-EDTA solution (Gibco BRL) was equally distributed onto the washed cells, and incubatd at 37 °C for about 2 minutes. The dish was shaken until all the cells became floating. 5 ml culture medium was added to stop the trypsin digestion, pipetted up and down for several times to blow the cells, and then transferred into a 15 ml Falcon tube. Centrifugation was carried out at 1,000 rpm for 5 minutes to pellet the cells, followed by aspirating the supernatant.

For passage, the cell pellet was resuspended in 6 ml culture medium by pipetting 15 to 20 times to break cell aggregates. 2 ml resuspension was finally equally distributed into a 10 cm dish containing 8 ml medium (1:3 dilution), gently shaken and incubated.

For freeze, the cell pellet was resuspended in 2 ml culture medium, and every 500 μl cell resuspension was transferred into a cryotube (Nunc) containing 500 μl culture medium and 10% DMSO, mixed well by inverting, and sequentially frozen at –20 °C overnight, at –80 °C for a week to a month, and finally in liquid nitrogen.

2.9.4 Immunocytochemistry

The antibody staining on cultured cells was performed as described below (Tab. 2-20) using antibodies against Geminin (Santa Cruz), Rae28 (Suzuki *et al.*, 2002), or Mel18 (Santa Cruz).

1. Passage cells onto a Lab-Tek Chamber slide (Nunc), and culture the cells in each chamber in 0.5-1 ml medium under 5% CO_2 at 37 °C overnight.
2. Aspirate the medium and wash the cells in each chamber with 1 ml PBS twice.

3. Fix the cells with 500 µl 4% PFA/PBS at 4 °C for 1 hour or at RT for 20 minutes.
4. Wash with 500 µl PBS 3 times for 5 minutes each.
5. Permeabilize the cells with 500 µl 0.5% Triton X-100/PBS at RT for 3-5 minutes.
6. Wash with 500 µl 0.1% Tween 20/PBS (PBT) twice for 5 minutes each.
7. Block in 500 µl 10% FCS/PBT at RT for 1-2 hours.
8. Incubate the cells with 500 µl 1:100-1:1000 diluted primary antibody in 10% FCS/PBT at 4 °C overnight (preferred) or at RT for 90 minutes.
9. Wash with 500 µl PBT twice for 5 minutes each.
10. Wash with 500 µl 10% FCS/PBT for 5 minutes.
11. Incubate the cells with 500 µl 1:2000 diluted Alexa conjugated secondary antibody (Molecular Probes) in 10% FCS/PBT at RT for 1 hour. After the application of fluorescence labeled secondary antibody, all the following steps should avoid light.
12. Wash with 500 µl PBT 3 times for 5 minutes each.
13. For nuclei staining, incubate the cells with 500 µl 0.5 µg/ml DAPI in PBT at RT for 5 minutes.
14. Wash with 500 µl PBT 3 times for 5 minutes each.
15. Rinse the slide with water briefly, and cover the specimen with 200 µl moviel and a coverslip without air bubble.
16. Apply the sample to a BX-60 fluorescence microscopy (Olympus).

Tabel 2-20: Immunocytostaining of cultured cells.

2.9.5 Cell Transfections with Plasmids or siRNAs

The cultured cells were transfected with plasmids or siRNAs using Lipofectamine 2000 transfection reagent (Invitrogen) (Tab. 2-21).

1. One day before transfection, passage cells into a 24-well cell culture plate (Nunc) with a proper dilution in order to get 80-95% confluence (50% for siRNA transfection) at the time of transfection.

2. Culture cells in each well with 500 µl proper medium without penicillin/streptomycin under 5% CO_2 at 37 °C overnight.
3. 3 hours before transfection, refresh the medium (Optional).
4. Dilute 2 µl (3 µl for siRNA transfection) Lipofectamine 2000 into 48 µl (47 µl for siRNA transfection) Opti-MEM®I medium (Gibco BRL) to a final volume of 50 µl. Mix well by gently flicking and incubate at RT for 5 minutes.
5. Dilute 0.8 µg DNA or DNA combinations (3 µl 20 µM siRNA) into Opti-MEM®I medium to a final volume of 50 µl. Mix well by gently flicking.
6. Combine the diluted Lipofectamine 2000 and the diluted DNA or RNA (total volume 100 µl). Mix well by gently flicking, and incubate at RT for 30 minutes (20 minutes for siRNA transfection) to form DNA or RNA-Lipofectamine 2000 complexes.
7. Distribute 100 µl DNA or RNA-Lipofectamine 2000 complexes to the 80-95% confluent cells (50% for siRNA transfection) in each well, mix well by gently rocking the plate and incubate at 37 °C for 24 hours (48-72 hours for siRNA transfection) in a 5% CO_2 incubator.
8. Cells in each well were trypsinized with 200 µl Trypsin-EDTA solution, spun down at 3,000 rpm at 4 °C for 4 minutes, resuspended in 25 µl PBS, mixed with 25 µl 2×SDS loading buffer and heated at 95 °C for 6-8 minutes.

Tabel 2-21: Transfection of plasmids or siRNAs into cultured cells using lipofectacmine.

2.9.6 Luciferase Assay

The luciferase assay was performed using Luciferase Assay System (Promega) (Tab. 2-22).

1. To prepare Luciferase Assay Reagent, add 10 ml Luciferase Assay Buffer to the vial containing the lyophilized Luciferase Assay Substrate.
2. 1:5 dilute 5×Reporter Lysis Buffer with H_2O.
3. Equilibrate Luciferase Assay Reagent and 1×Reporter Lysis Buffer at RT.
4. Aspirate the medium of transfected cells in 24-well plates. Wash cells in each well with 500 µl PBS once and completely aspirate PBS buffer.

5. Add 100 µl 1×Reporter Lysis Buffer into each well, and apply one freeze-thaw cycle to ensure the lysis.
6. Pipette up and down for several times, and centrifuge the lysate at 12,000×g at RT for 20 seconds.
7. Inject 100 µl Luciferase Assay Reagent into 20 µl cell lysate supernatant in a 75×12 mm tube (Sarstedt), and measure the luciferase activity for 10 seconds by a Lumat LB9501 luminometer (Berthold)

Tabel 2-22: The preparation of cell lysate and measurement of luciferase activities.

2.10 Competition Assays

2.10.1 *In Vitro* Competition Assay

The N-terminally Geminin coupled beads (see 2.5.7) was equilibrated in western buffer A, followed by preincubating 100 µl bed volume Geminin coupled beads (1.5 µg protein/µl) with 500 µg GST-Geminin recombinant or GST protein at 4 °C rotating for 2 hours. The unbound protein was washed away with 1 ml western buffer A. Then, the preincubated and 100 µl non-preincubated Geminin coupled beads were individually incubated with 1 ml 11.5 d.p.c. mouse embryonic extracts at 4 °C rotating for 2 hours. After wash once with 1 ml western buffer A and once with 1 ml western buffer A plus 50 mM NaCl, the bound proteins were eluted with 70 µl 2×SDS loading buffer by heating at 95 °C for 5 minutes. The samples were loaded on a 10% SDS-polyacrylamide gel, and western blotting was performed using anti-Cdt1 antibodies.

2.10.2 *In Vivo* Competition Assay

Primary cultured MEFs in 3.5 cm dishes were transfected with Lipofectamine 2000, and cell lysate was prepared 24 hours after transfection as described in ChIP assay (see 2.8.2). Then, an immunoprecipitation was performed as described above (see 2.7.2), and the co-precipitants were analyzed by western blotting using anti-Geminin and anti-Cdt1 antibodies.

2.11 Manipulation and Analysis of Chick Embryos

2.11.1 *In Ovo* Electroporation

Fertilized eggs were incubated at 38 °C in a humid incubator for 36-44 hours to reach stage HH9-11 (Hamburger and Hamilton, 1951), without rolling during the whole incubation time. For *in ovo* electroporation, 2-5 μg/μl plasmid or plasmid combination in PBS supplemented with 1 mM $MgCl_2$ and 25-50 ng/μl Fast Green was pipetted into a microinjection glass needle, which was subsequently connected to and held on a Pneumatic PicoPump PV820 pump system (World Precision Instruments). After incubation, an egg was held on a stander with the orientation that the embryo sits on the top of the yolk, and 2.5 ml albumin was aspirated with a 5 ml syringe (Terumo). Then, a 2 cm diameter window was opened on the shell exactly above the embryo, several drops of 1×Tyrods buffer (8 g NaCl, 0.2 g KCl, 0.271 g $CaCl_2 \cdot 2H_2O$, 0.05 g $NaH_2PO_4 \cdot 2H_2O$, 0.2 g $MgCl_2 \cdot 6H_2O$, 1 g glucose in a total volume of 1 liter, and freshly added 1×penicillin/streptomycin) were applied on the embryo proper to avoid drying, and 1:75 diluted black ink (Higgins) in 1×Tyrods buffer was injected with a 1 ml syringe (Terumo) into the yolk right beneath the embryo to visualize it. Subsequently, a small hole was broken on the vitelline membrane carefully using a 0.125 mm diameter wolfram-draht needle (Agar Scientific) to make the neural tube accessible. A parallel platinum electrode (Aldrich) with 5-6 mm length, 0.25 mm diameter, and 7 mm distance between two electrodes was placed onto the vitelline membrane flanking the embryo in parallel with neural tube, pressed down to the same horizontal level with the neural tube, and several drops of 1×Tyrods buffer were applied on each electrode. Afterwards, DNA solution was injected into the neural tube, and 5 square electric pulses were given under the condition of 33 V, 50 miniseconds/pulse with 950 miniseconds intervals by a Electro Square Porator ECM830 electroporator (BTX). Finally, the window on the shell was tightly sealed with tape, and the electroporated embryo was further incubated for 48 hours to reach stage HH18-20. The surviving embryos were dissected out from the yolk in PBS, and GFP expression was assayed with an SZX12 fluorescence microscope (Olympus).

2.11.2 DIG Labeled RNA Probe Preparation

5-10 μg plasmid DNA was linearized by incubating with 4 μl restriction enzyme at 37 °C for 3 hours, purified with PCR Purification Kit, and eluted in 30 μl H_2O. 1 μl elution was loaded on an agarose gel to check the linearization efficiency. DIG labeled antisense RNA probes were synthesized by incuabting 1 μl linearized DNA, 2

μl 10×Transcription Buffer (Roche), 2 μl DIG-Labeling Mixture (Roche), 1 μl RNasin, 1 μl T3 or T7 RNA Polymerase (Roche), and 13 μl DEPC-H_2O in a total volume of 20 μl at 37 °C for 2-2.5 hours. Then, the transcription product was supplemented with 30 μl H_2O and purified with a G-50 Sephadex Micro Column. 5 μl purified probe was checked on an agarose gel.

2.11.3 Whole-Mount *In Situ* Hybridization

48 hours after *in ovo* electroporation, the GFP positive chick embryos (HH 18-20) without head were fixed in 4% PFA/PBS at 4 °C for 4 hours to overnight, and subjected to whole-mount *in situ* hybridization (Tab. 2-23).

	Treatment and Solution	Temperature	Duration
Dehydration	1. Wash the fixed embryos with PBT 3 times, shaking.	on ice	10 minutes each
	2. 25% methanol/PBT, shaking.	on ice	10 minutes
	3. 50% methanol/PBS, shaking.	on ice	10 minutes
	4. 75% methanol/PBT, shaking.	on ice	10 minutes
	5. 100% methanol, shaking.	on ice	10 minutes
The embryos in 100% methanol can be stored in –20 °C up to 2 weeks.			
	1. 75% methanol/PBT, shaking.	on ice	10 minutes
	2. 50% methanol/PBS, shaking.	on ice	10 minutes
	3. 25% methanol/PBT, shaking.	on ice	10 minutes
	4. Wash with PBT twice, shaking.	on ice	10 minutes each
	5. Bleach with 6% H_2O_2/PBT, shaking.	on ice	30 minutes
	6. Wash with PBT 3 times, shaking.	on ice	5 minutes each
	7. Digest with 10 μg/ml Proteinase K (1:1000 dilution from stock in PBT).	on ice	10 minutes
	8. Stop the Proteinase K digestion with about 2 mg/ml glycine in PBT.	on ice	5 minutes

	9. Wash with PBT 3 times, shaing.	on ice	5-10 minutes each
Day 1	10. Treat with RIPA buffer (10 mM Tris, pH 8.0, 150 mM NaCl, 2.5 mM EDTA, 0.1% SDS, 1% NP-40, 0.05% Sodium deoxycholate) 3 times, shaking.	on ice	20 minutes each
	11. Wash with PBT 3 times, shaking.	on ice	5-10 minutes each
	12. Refix with 4% PFA, 0.2% glutaraldehyde, and 0.1% Tween20 in PBS	on ice	30 minutes
	13. Wash with PBT 3 times, shaking.	on ice	10 minutes each
	14. Prehybridize in prewarmed Prehyb solution (50% formamide, 5×SSC, pH 4.5, 1% SDS, 50 μg/ml yeast tRNA, 50 μg/ml heparin), shaking.	70 °C	3 hours
	Or before prehybridization, the embryos can be stored in store mix (50% formamide, 5×SSC, pH 4.5) at –20 °C up to 2 weeks.		
	15. 1:100 dilute a DIG labeled RNA probe into the Prehyb solution to hybridize	70 °C	overnight
	1. Incubate with prewarmed Solution 1 (50% formamide, 5×SSC, pH 4.5, 1% SDS) twice, shaking.	70 °C	30 minutes each
	2. Incubate with prewarmed Solution 3T (50% formamide, 2×SSC, pH 4.5, 0.1% Tween20) twice, shaking.	70 °C	30 minutes each

Day 2	3. Incubate with MABT (100 mM maleic acid, 150 mM NaCl, 0.1% Tween20) 3 times, shaking.	RT	5 minutes each
	4. Incubate with 2% Block Reagent (Roche) in MABT, shaking.	RT	5 minutes
	5. Block with blocking solution (2% Block Reagent, 20% FCS in MABT), shaking.	RT	5-8 hours
	6. Incubate with 1:2000 diluted Anti-DIG-AP Fab fragment (Roche) in blocking reagent, shaking.	4 °C	overnight
Day 3, 4	1. Wash with MABT 3 times.	RT	10 minutes each
	2. Transfer the embryos into a sealed 5 ml bottle and wash with MABT for 48 hours rotating. Refresh the solution once in the middle.	RT	48 hours
Day 5	1. Equilibrate with freshly prepared NTMT/Lev (100 mM NaCl, 100 mM Tris, pH 9.5, 50 mM $MgCl_2$, 1% Tween20, 2 mM Levamisol) twice, shaking.	RT	5 minutes each
	2. Incubate with NTMT/Lev.	RT	4 hours
	3. Stain with 1:50 diluted NBT/BCIP (Roche) in NTMT/Lev in a dark environment shaking. Control the staining every 10 minutes.	RT	10 minutes-2 hours
	4. Wash with PBT twice, shaking.	RT	5 minutes each
	5. Incubate with 50% glycerol/PBT, shaking.	RT	15-60 minutes
	6. Incubate with 80% glycerol/PBT, shaking.	RT	15-60 minutes

	7. Take pictures for the embryos using a binocular (Zeiss) and Ektachrome 64T film (Kodak)		
Then, the embryos can be stored in 80% glycerol/PBT at 4 °C.			

Tabel 2-23: Whole-mount *in situ* hybridization of chick embryos

3. Results

3.1 Geminin Directly Interacts with Hox Proteins and a Polycomb Group Member

In order to identify proteins that interact with Geminin during embryogenesis, a two-hybrid screen was performed using a complementary DNA library prepared from 8.5 d.p.c. mouse embryos. The MaV203 yeast strain containing *HIS3* and *lacZ* reporter genes was first transformed with pDBLeu-*Geminin*, and then with 8.5 d.p.c. mouse cDNA library in pPC86, using lithium acetate transformation. 177 independent colonies were selected out from the first round of screen on plates lacking leucine, tryptophan and histidine, and supplemented with 60 mM 3AT (Fig. 3-1A). Then, all these clones were applied to the second round of screen, in which β-galactosidase activity was assayed for every clone. Eight positive cDNA clones were finally identified to encode Geminin-binding proteins (Fig. 3-1B). Three independent cDNAs each encoded parts of the homeodomain proteins Hoxd10 and Hoxa11, respectively. One clone represented the "Sex comb on midleg homolog 1" (Scmh1) protein, the mouse homolog of the *Drosophila* Scm protein, a member of the Polycomb multiprotein complex (Bornemann *et al.*, 1996; Tomotsune *et al.*, 1999). In order to eliminate the possibility of self-activation, all the eight cDNA clones in pPC86 vector were individually transformed into MaV203 yeast and assayed for β-galactosidase activities. No self-activation was detected.

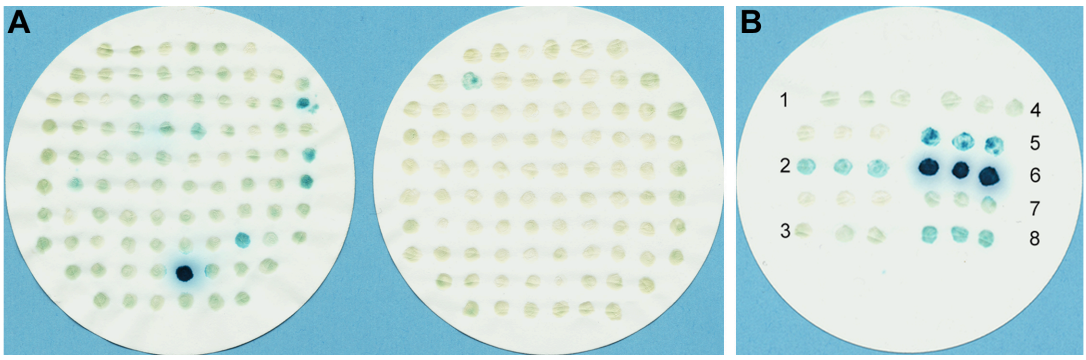

Figure 3-1: Yeast two-hybrid screen. (A) 177 independent colonies were selected out from the first round of screen on medium lacking histidine, and supplemented with 60 mM 3AT. (B) Eight positive clones were shown to encode Geminin-binding proteins, as visualized by lacZ activity in the second round of screen. Clones 1, 2, 8 encode Hoxa11, and clones 3, 4, 7 encode Hoxd10. Clone 6 encodes Scmh1.

To confirm the protein-protein interactions, full-length Hoxd10, Hoxa11 and Scmh1 proteins were synthesized by *in vitro* transcription/translation in the presence of [^{35}S]-methionine. These radiolabeled proteins were tested for binding to the recombinant GST-Geminin fusion protein, and pure GST as a control (Fig. 3-2). In such pull-down assays, Hoxd10, Hoxa11 and Scmh1 bound directly to GST-Geminin, but exhibited no appreciable binding to GST alone. By means of these pull-down assays, the interactions of Geminin with Hoxd10, Hoxa11 and Scmh1 were confirmed *in vitro*.

The interactions of Geminin with two abdominal B (Abd-B)-like Hox proteins raised the question whether it also binds to other Hox proteins. GST pull-down assays were performed with *in vitro* transcribed/translated Hoxa7, Hoxc8, Hoxc9, Hoxa10, and Msx1 proteins (Fig. 3-2). Also these full-length proteins except Msx1 were able to bind directly and specifically to GST-Geminin, but not to GST. Together, the results identify homeodomain proteins of the Hox family, as well as the Polycomb group member Scmh1, as binding partners of the cell cycle regulator Geminin.

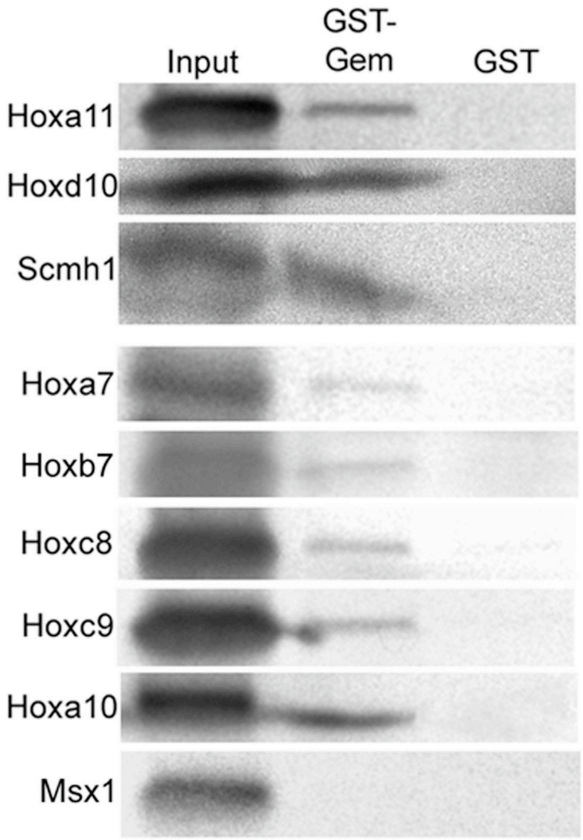

Figure 3-2: Pull-down assays. All the full-length *in vitro* transcription/translation products of the indicated genes except Msx1 were specifically bound by a GST-Geminin fusion protein but not by GST alone.

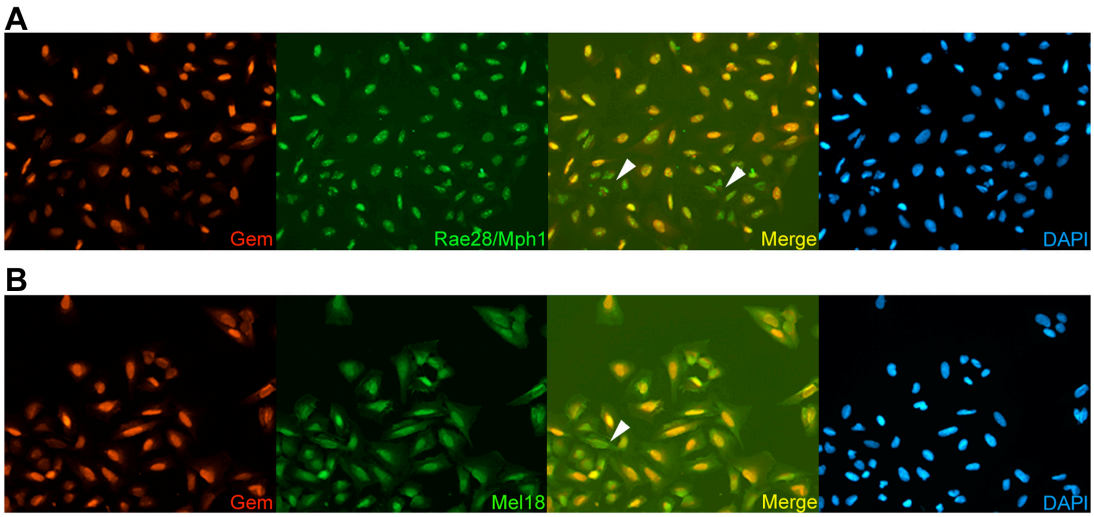

Figure 3-3: Subcellular colocalization between Geminin and Polycomb members. Double immunofluorescence stainings with antibodies against Geminin and Polycomb members Rae28 (A) or Mel18 (B) were performed on U2OS cells. DAPI indicates the nuclei of all cultured cells. Arrowheads denote cells with Polycomb member Rae28 or Mel18, but without Geminin expression.

3.2 Geminin Associates with the Polycomb Complex

The *in vitro* interaction between Geminin and the Polycomb member Scmh1 was demonstrated above. In order to test if Geminin also associates with other members of the Polycomb complex, we first analysed its *in vivo* co-localizations with Rae28 (Takihara *et al.*, 1997) and Mel18 (Akasaka *et al.*, 1996), respectively. Double immunofluorescence stainings of U2-OS cells were performed with anti-Geminin antibodies, and antibodies against Rae28 or Mel18, respectively (Fig. 3-3). The endogenous Geminin colocalized with Rae28 or Mel18 in the nuclei of the cultured cells. However, whereas the two Polycomb proteins were detected in the nuclei of all observed cells, several nuclei were significantly negative for Geminin (Fig. 3-3, arrow heads). A close inspection of these U2-OS cells revealed that the expression of Geminin depended on the phase of the cell cycle (Fig. 3-4). Geminin protein was not detectable during the interphase. Then, it accumulated in the nucleus and persisted throughout mitosis until the anaphase-telophase transition. On the contrary, the expression of Rae28 or Mel18 was continuous in all phases of the cell cycle.

Direct evidence for an *in vivo* association between Geminin and a Polycomb protein was obtained by immunoprecipitation from 11.5 d.p.c. mouse embryonic extracts using anti-Geminin antibodies. A pre-immune rabbit serum was used as a negative control. A band with a mobility corresponding to 120 kDa in the precipitated

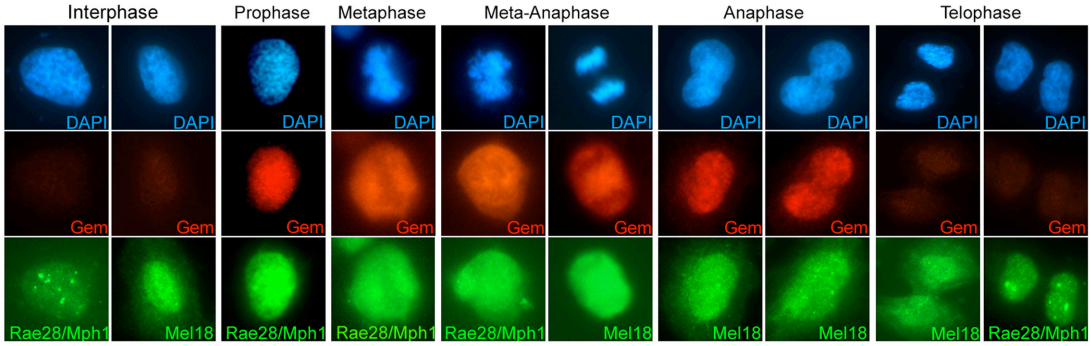

Figure 3-4: The cell cycle dependent expression of Geminin. Geminin protein was not detectable during the interphase. Then, it accumulated in the nucleus and persisted throughout mitosis until the anaphase-telophase transition. On the contrary, the expression of Rae28 or Mel18 was continuous in all phases of the cell cycle.

materials was recognized by anti-Rae28 antibodies (Fig. 3-5), which indicates that the protein complex isolated from mouse embryos containing Geminin, in addition also contained Rae28. Together, these data demonstrate the association of Geminin and the Polycomb complex *in vivo*. However, this association is cell cycle dependent, since Geminin is absent in some phases of cell cycle in contrast to the Polycomb members.

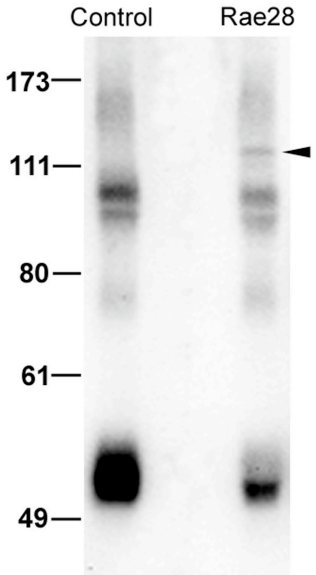

Figure 3-5: Co-immunoprecipitation of Geminin and Rae28 from 11.5 d.p.c. mouse embryonic extracts. The arrowhead indicates that Rae28 was specifically co-precipitated by anti-Geminin antibodies, but not by the pre-immune serum as control.

3.3 Geminin Associates with *Hox* Regulatory DNA Elements *In Vivo*

The Polycomb complex was previously demonstrated to associate with *Hox* regulatory DNA elements on the chromatin (Barna *et al.*, 2002). A fraction of

Geminin was also proved to be chromatin-associated previously (Kulartz *et al.*, 2003). To further investigate whether Geminin associates with these *Hox* regulatory elements *in vivo*, chromatin immunoprecipitation (ChIP) assays were performed to isolate DNA fragments bound by Geminin-including protein complexes in primary cultured mouse embryonic fibroblasts. Four *Hox* regulatory elements within the *Hoxd11* gene bind to Plzf, a protein that associates with Polycomb complex members and mediates transcriptional repression of *Hox* genes (Fig. 3-6A, Barna *et al.*, 2002). Three of these Plzf binding sites, located within the *Hoxd11* intron or 3' UTR, were specifically co-precipitated by Geminin antibodies but not by pre-immune serum (Fig. 3-6B). These results demonstrate that Geminin substantially associates *in vivo* with the *Hox* regulatory DNA elements that anchor Plzf together with Polycomb members.

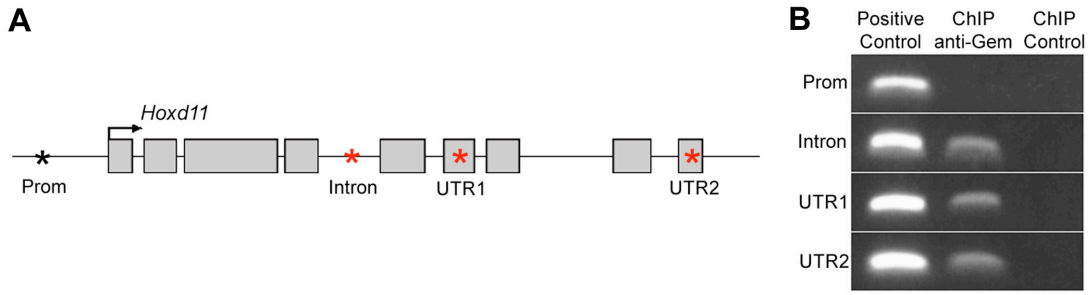

Figure 3-6: Chromatin immunoprecipitation assays using anti-Geminin antibodies. (A) The genomic organization of *Hoxd11* gene. The gray boxes indicate the exons of *Hoxd11* gene, and the asterisks indicate four Plzf-binding *Hox* regulatory elements within *Hoxd11* gene. (B) Three of these *Hox* regulatory DNA elements within the *Hoxd11* intron and 3'UTR (red asterisks) were identified by ChIP assays to be associated with Geminin protein. The *Hox* regulatory element in the promoter region (black asterisk) was not detected.

3.4 Overexpression of Geminin Represses *Hox* Gene Transcription

From the results depicted above, Geminin was elucidated to associate *in vivo* with the Polycomb complex, together with which Geminin further associates with *Hox* regulatory elements on the chromatin. These associations raised the question whether Geminin is involved in *Hox* gene transcriptional repressions by the Polycomb complex. To characterize the effect of ectopically expressed Geminin on *Hox* gene transcription, we overexpressed Geminin unilaterally in the neural tube of chicken embryos by *in ovo* electroporation, a strategy previously applied to Polycomb members (Suzuki *et al.*, 2002). For these experiments, expression vectors were

applied, driving either the murine *Geminin* cDNA, or an *EGFP-Geminin* fusion by the cytomegalovirus (CMV) enhancer/promoter. CMV-*EGFP-Gem* plus pCMV-*Gem* or the control vector CMV-*EGFP* were injected into the neural tube of HH9-11 stage chicken embryos, that is, at an embryonic time, when *Abd-B* related *Hox* genes like *Hoxb9* become activated in the posterior body region. The plasmids were electroporated to the right side of the neural tube, where the expression of GFP was confirmed after 24 hours of incubation by *in vivo* green fluorescence and recorded (Fig. 3-7A,B). Then, embryos were incubated for another 24 hours, fixed at about stage HH18-20, and submitted to whole-mount *in situ* hybridization. The *Hoxb9* anterior transcription boundary was posteriorly shifted by one to two somites length on the electroporated, right side (Fig. 3-7C, 5/8). By contrast, there was no posterior shift of the endogenous *Hoxb9* transcription domain in those control embryos, where only CMV-*EGFP* was electroporated (Fig. 3-7D, 6/6). This result demonstrates that overexpressed Geminin represses *Hox* gene transcription, which suggests a Polycomb like activity of Geminin.

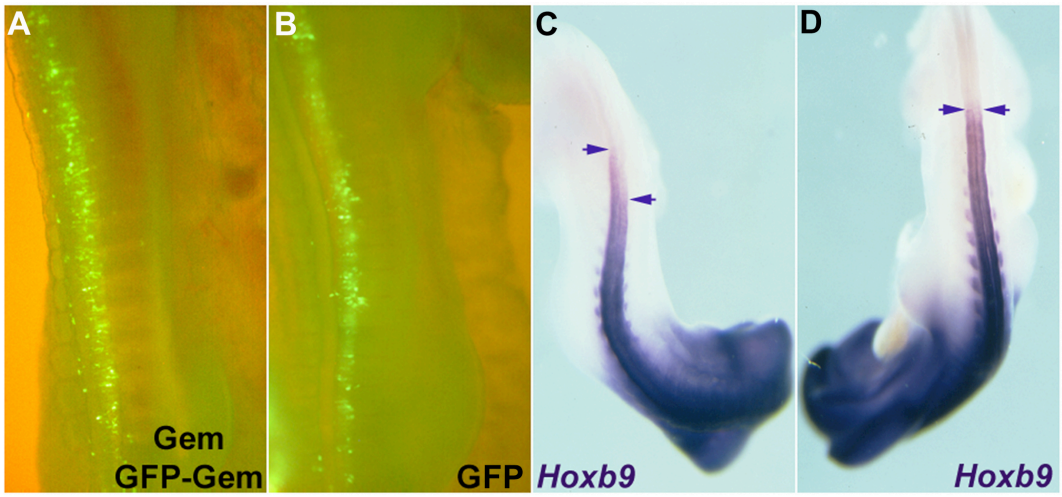

Figure 3-7: Overexpression of Geminin inhibits endogenous *Hoxb9* transcription. (A, B) GFP expressions were documented 24 hours after unilateral electroporation of expression plasmids to the right side of the neural tube of HH9-11 stage chick embryos. (C, D) Endogenous *Hoxb9* transcripts were detected by whole-mount *in situ* hybridization in the same embryos depicted in (A) and (B), respectively, at stage HH18-19. Arrowheads indicate the anterior transcription boundary of *Hoxb9*.

3.5 Loss of Geminin Function Derepresses *Hox* Gene Transcription

To ensure that the inhibition of *Hox* gene transcription by Geminin is really due to a Geminin-Polycomb interaction and better characterize the role of Geminin in the Polycomb complex, the Geminin-binding domains of Scmh1 was delineated precisely. The amino acids sequence of Scmh1 was subdivided into 20-amino acid-length peptides from N- to C-terminus, with 17 amino acids overlapping between adjacent peptides. All these peptides were synthesized and arrayed onto a cellulose membrane. Binding of recombinant His-Geminin protein to arrayed Scmh1 peptides revealed a basic amino acid rich domain of Scmh1 (amino acids 540-568) as the Geminin-binding region lying outside the SPM domain (Fig. 3-8A), through which Scmh1 associates with other Polycomb members (Tomotsune *et al.*, 1999). From this information a dominant-negative form of Scmh1 (amino acids 508-585, dnScmh1), which included the Geminin-binding domain but not the SPM domain, was designed (Fig. 3-8B). The binding of dnScmh1 to Geminin was confirmed using a pull-down assay (Fig. 3-8C).

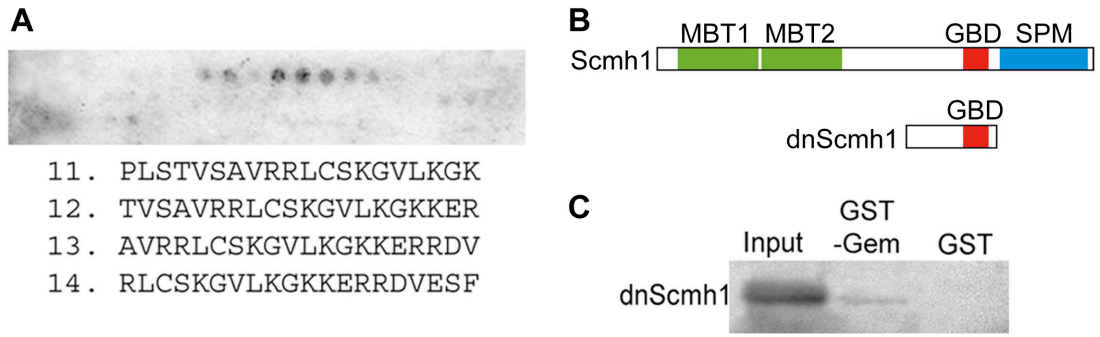

Figure 3-8: The design of a dominant-negative Scmh1 (dnScmh1) molecule. (A) Binding of His-tagged Geminin to a Scmh1 peptide array. Below, His-Geminin bound peptides are listed (number 11-14). Amino acids 540-568 of Scmh1 comprise the Geminin-binding domain. (B) Amino acids 508-585 of Scmh1 protein was designed as a dnScmh1 protein, including the Geminin-binding domain (GBD) but not the SPM domain. (C) Confirmation of dnScmh1-Geminin binding through a GST-Geminin pull-down assay.

The introduction of abundant dnScmh1 protein into cells was supposed to compete for Geminin binding with endogenous Scmh1 protein, and remove Geminin out of the Polycomb complex (Fig. 3-9). *In ovo* co-electroporations of a *dnScmh1* expression vector and CMV-*EGFP* to the right side of the neural tube (Fig. 3-10A), controlled by

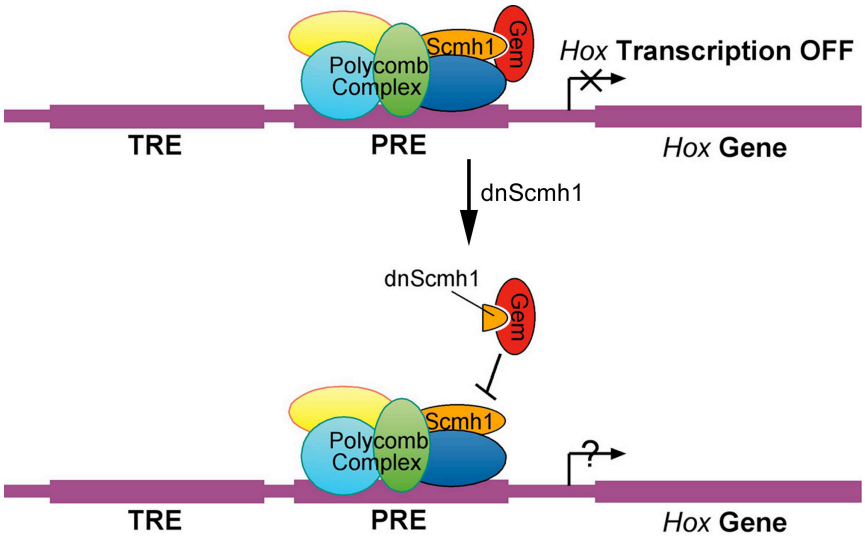

Figure 3-9: Schematic representation of the dominant negative inactivation of Geminin by dnScmh1.

single electroporations of CMV-*EGFP* (Fig. 3-10B), and whole-mount *in situ* hybridization to *Hoxb9* (Fig. 3-10C,D) were performed as described above. In contrast to the control (Fig. 3-10D, 5/5), a derepression of *Hoxb9* transcription, one somite length anterior of the normal expression boundary (Fig. 3-10C, 6/8), was observed. This result demonstrates that the inhibition of *Hox* gene transcription by Geminin is due to a Geminin-Polycomb interaction, that is, that Geminin behaves like a Polycomb protein *in vivo*.

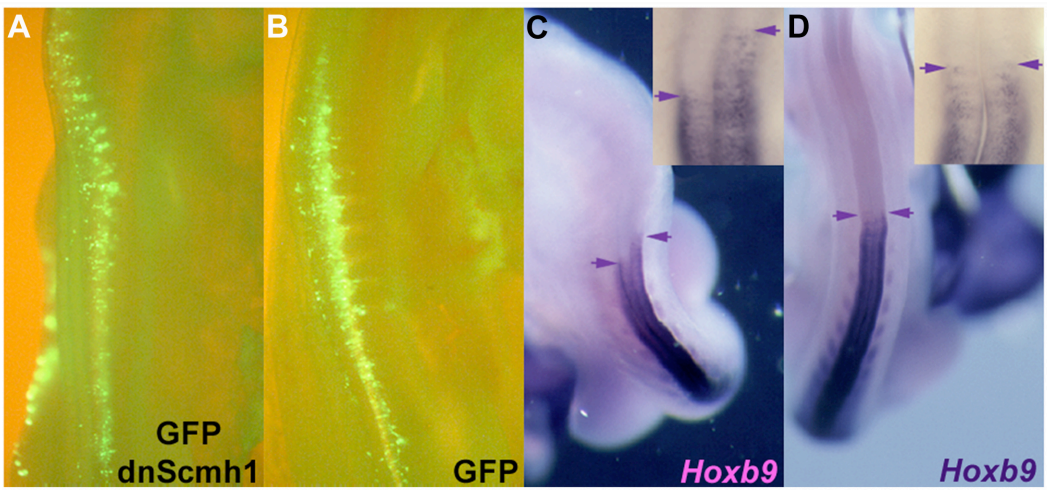

Figure 3-10: *In vivo* Geminin loss-of-function by a dominant-negative Scmh1 derepresses *Hoxb9* transcription. (A, C) Ectopically expressed dnScmh1 derepresses the *Hoxb9* transcription and shifts its transcription domain anteriorly in the right side of the neural tube, but not in the control embryo shown in (B, D). Arrowheads indicate the anterior transcription boundary of *Hoxb9*.

A direct elimination of Geminin was carried out by the co-electroporation of siRNA against chick *Geminin* (siGem) and CMV-*EGFP*, controlled by siRNA against luciferase (siLuc; Fig 3-11). Similarly, a pronounced derepression of *Hoxb9* transcription by one and a half to two somites length was observed (Fig. 3-11C, 5/7). This finding indicates that the downregulation of endogenous Geminin derepresses *Hoxb9* transcription, further confirming that Geminin behaves like a Polycomb protein *in vivo*.

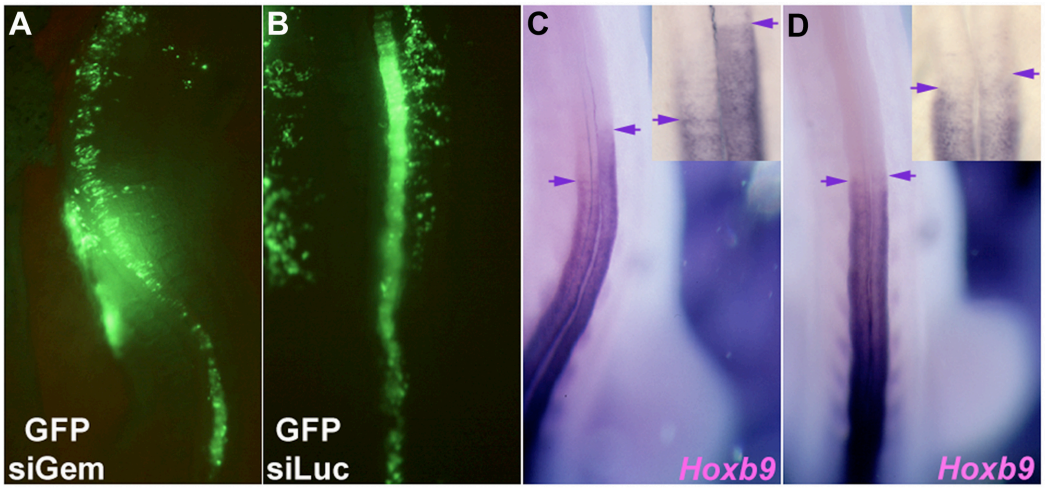

Figure 3-11: Direct elimination of endogenous Geminin by siRNA derepresses *Hoxb9* transcription. (A, C) The *Hoxb9* anterior transcription boundary was anteriorly shifted by siRNA against Geminin, but not by the control siRNA against luciferase (B, D). Arrowheads indicate the anterior transcription boundary of *Hoxb9*.

3.6 Geminin Directly Interacts with the Homeodomain of Hox Proteins

From the yeast two-hybrid screen and GST pull-down assays, Geminin not only binds to the *Hox* repressive Polycomb member Scmh1, but also interacts direcly with Hox proteins. Through the application of peptide arrays, the homeodomain of Hoxa11 protein was identified as the Geminin binding region, with two clusters of basic amino acids as the core binding sequences (Fig. 3-12A,B, red frames).

The N-terminus of Hoxa11 had a slightly positive influence on Geminin binding, as indicated in lacZ activities in two-hybrid screen (Fig. 3-1B). Clone 1, 2 and 8 all indicated the interaction between Geminin and Hoxa11, but the lacZ activity that reflected the binding affinity in clone 1 was weaker than the others. Further investigations of Hoxa11 encoding sequences in these three clones revealed that the

Hoxa11 complementary DNA sequence in clone 1 encoded a truncated Hoxa11 protein with the N-terminal 163 amino acids missing. Therefore, the N-terminal region of Hox proteins regulates their interactions with Geminin, although the C-terminal homeodomain is the direct Geminin biniding site. This N-terminal effect also explains why the homeobox protein Msx1 does not interact with Geminin. The deletion of N-terminal 90 or 140 amino acids resulted in two truncated Msx1 proteins. In contrast to the full-length Msx1, both of the truncated Msx1 proteins were detected to interact with Geminin using a GST pull-down assay. In addition, the longer sequence deleted from the N-terminus, the stronger the interaction was (Fig. 3-12C). Thus, N-terminal Msx1 sequences inhibited the interaction of Geminin with the Msx1 homeodomain, which lead to the loss of affinity between Geminin and full-length Msx1 proteins. From these results, I conclude that the N-terminus has an influence on the binding of Geminin to a homeodomain protein.

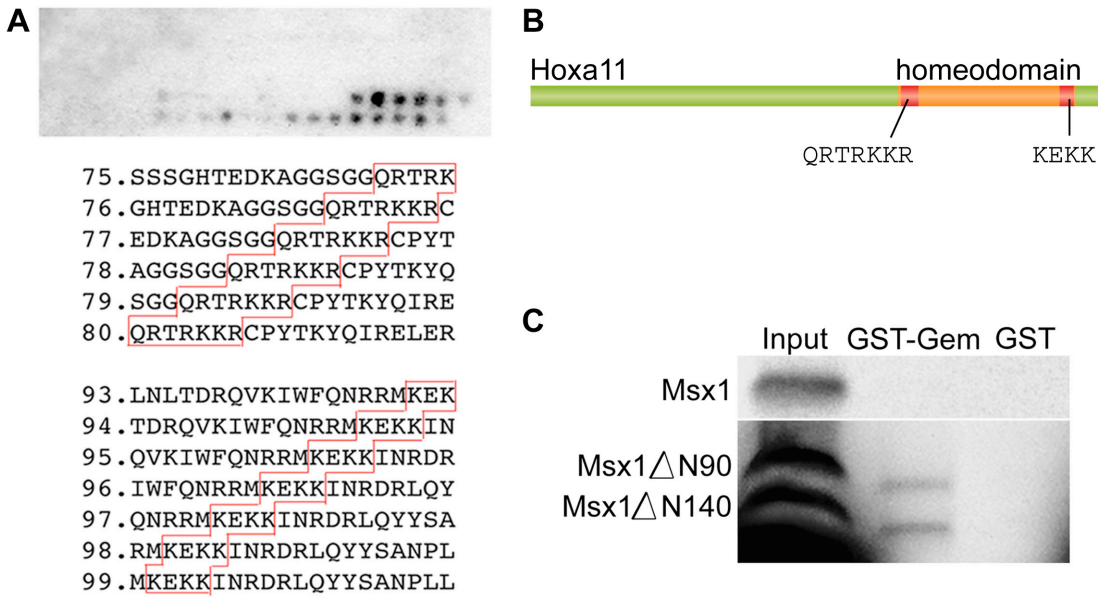

Figure 3-12: Geminin binds to the homeodomain of Hox proteins. (A) Binding of His-Geminin to a Hoxa11 peptide array. Bound peptides are listed, and the common core sequences are framed in red. (B) The Geminin binding domains of Hoxa11 are localized inside its homeodomain (orange), with the core binding sequences marked with red. (C) N-terminal sequences affect the Geminin-homeodomain interaction. Full-length Msx1 does not interact with Geminin, whereas the two N-terminal truncated forms of Msx1 do interact with Geminin. The longer sequence deleted from the N-terminus, the stronger the interaction was. Msx1Δ90 or Msx1Δ140 represents truncated Msx1 proteins with N-terminal 90 or 140 amino acids deleted.

3.7 The Interaction with Geminin Inhibits the DNA Binding of Hox Proteins

Since the homeodomain is the DNA binding domain of Hox protein, this finding suggest that Geminin might represent a specific antagonist of DNA binding by the Hox homeodomains. We performed electrophoretic mobility shift assays (EMSA), applying *in vitro* transcribed/translated Hoxd10, Hoxa11, Hoxb7 and Msx1 proteins, radioactive labeled double-stranded oligonucleotides including their respective, consensus binding sequences, and recombinant His-Geminin protein. The Hox proteins led to prominent shifts of oligonucleotide bands during electrophoresis (Fig. 3-13, lane 2,4,6,9). Pre-incubations of Geminin with Hox proteins resulted in the release of free probe, hence a significant reduction of the shifted bands (Fig. 3-13, lane 3,5,7,10). In contrast, the binding of Msx1 to its target sequence was not attenuated by Geminin (Fig. 3-13, lane 11,12). In summary, Geminin inhibits the binding of Hox proteins to their target DNA sequences as a result of interacting with, and thus blocking, their homeodomains.

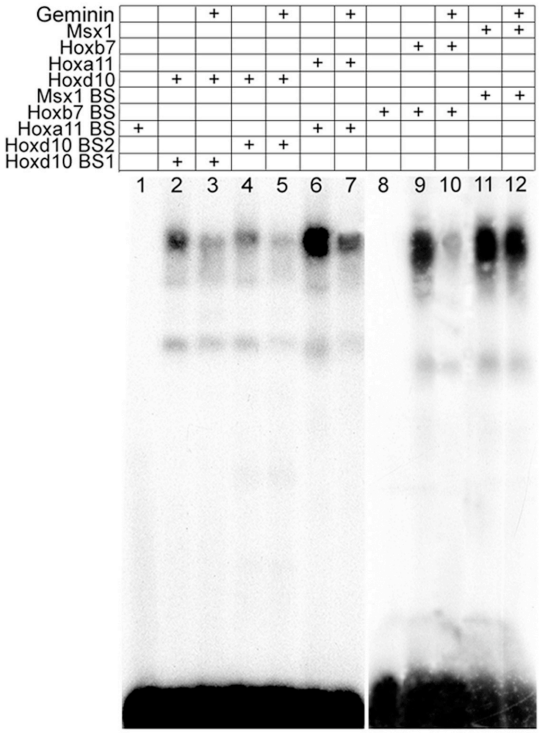

Figure 3-13: Geminin interferes with the binding of Hox proteins to specific double stranded DNAs *in vitro*. In the EMSAs, His-Geminin recombinant protein, *in vitro* transcribed/translated Hoxb7, Hoxd10, Hoxa11, and Msx1 proteins, and five different binding sites (BS) were applied.

3.8 Geminin Inhibits Hox Dependent Transcriptional Activations of Reporter Gene

Since Geminin blocks Hox homeodomains, in order to examine whether Geminin inhibits the transcriptional activation promoted by Hox *in vivo*, a reporter construct

was designed by inserting a triple Hoxa11 binding sequence before a SV40 basic promoter, followed by a luciferase reporter gene (Fig. 3-14A, a11Luc). As expression vectors, CMV-*Hoxa11* and CMV-*Gem* were applied. A positive control was represented by pGL3-Control, where the SV40 promoter is driven by the SV40 enhancer. Different combinations of expression vectors were co-transfected with a11Luc into NIH/3T3 cells and luciferase activities were measured 24 hours after transfection. Expression of the reporter gene was 10-fold enhanced by the overexpression of Hoxa11. This increased level was reduced by 60% if in addition to Hoxa11 also Geminin was overexpressed (Fig. 3-14B). Similarly, another reporter plasmid was constructed by inserting a 500 bp FGF2 promoter fragment including a Hoxb7 binding site (Care *et al.*, 1996) before the luciferase gene (Fig. 3-15A, FgfLuc). The luciferase activity was increased dramatically by the overexpressed Hoxb7 in Hela cells, and this increment was reduced by 40% by Geminin (Fig. 3-15B, column 1-3). No appreciable change of the luciferase activity was observed, when a control DNA fragment with mutated Hoxb7 binding site was inserted and applied (ConLuc; Fig. 3-15B, column 4-6). Together, these data show that the Geminin-Hox interaction interferes with the role of Hox proteins as transcriptional activators.

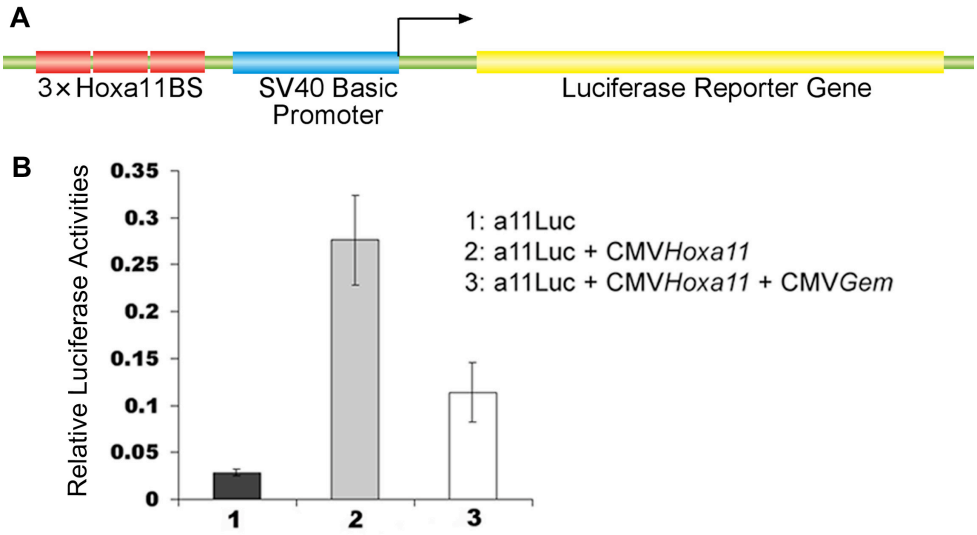

Figure 3-14: Geminin inhibits Hoxa11 dependent transcriptional activation of luciferase reporter gene. (A) Schematic representation of the a11Luc luciferase reporter construct with a triple Hoxa11 binding site (BS) inserted before an SV40 basic promoter. (B) The transcriptional activation of luciferase reporter gene promoted by Hoxa11 was inhibited by Geminin. The values of measured luciferase activities were brought to ratios of the positive control pGL3-Control, which was set as "1" in arbitrary units.

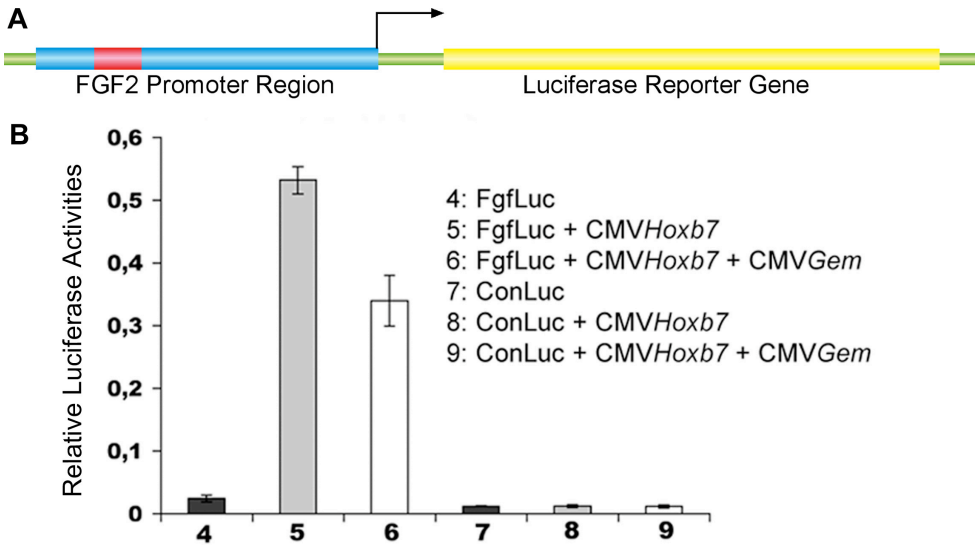

Figure 3-15: Geminin inhibits Hoxb7 dependent transcriptional activation of luciferase reporter gene. (A) Schematic representation of the FgfLuc luciferase reporter construct with an FGF2 promoter region including a Hoxb7 binding site (red) inserted before the luciferase reporter gene. (B) The transcriptional activation of luciferase reporter gene promoted by Hoxb7 was inhibited by Geminin, but not the control reporter construct with the Hoxb7 binding site mutated. The values of measured luciferase activities were brought to ratios of the positive control pGL3-Control, which was set as "1" in arbitrary units.

3.9 Geminin Inhibits Hox Dependent Transcriptional Activation of Endogenous Downstream Target Gene

FGF2 is a downstream target gene of Hoxb7 in the melanoma cell line A375 (Care *et al.*, 1996). This well defined system was used to study the influence of Geminin on the function of Hox proteins. CMV-*Gem*, a siRNA targeting human *Geminin* mRNA (sihGem), or siLuc were transfected into cultured A375 cells. Subsequently, Geminin, FGF2 or Vimentin levels were detected by western blotting (Fig. 3-16). We observed a decrease of FGF2 level in parallel with an elevated level of Geminin, and an increase of FGF2 in parallel to the suppression of Geminin caused by specific siRNA. These results suggest that the level of Geminin modulates the function of the Hoxb7 protein *in vivo*, as detected here by measuring the product of its direct target FGF2. In addition, the FGF2 promoter region could not be detected, when a ChIP assay was performed using an A375 cell extract and Geminin antibodies (data not shown), indicating that Geminin is not recruited with Hoxb7 to its DNA target. Taken together, Geminin binds to the homeodomain of Hox proteins, blocks their DNA

binding, and inhibits Hox dependent transcriptional activations of reporter and endogenous downstream target genes.

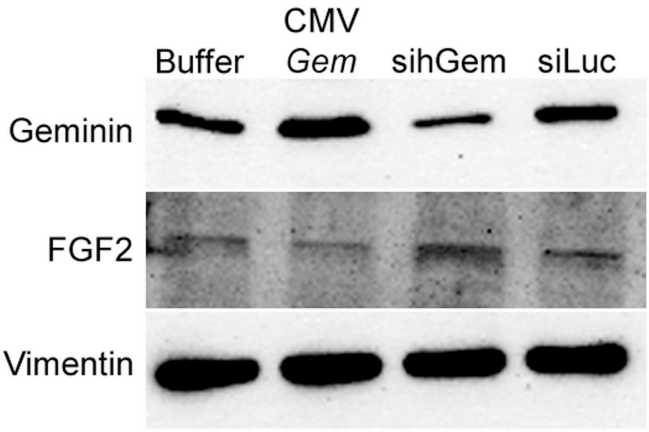

Figure 3-16: Geminin inhibits the expression of the Hoxb7 downstream target FGF2 in A375 cells. Note that overexpression or siRNA downregulation of Geminin leads to reciprocal changes in FGF2 levels. Vimentin served as an internal control.

3.10 Hox and Cdt1 Compete for Geminin Binding

Since the Hox binding regions of Geminin partially overlap with its coiled-coil domain, which is also the Cdt1 binding domain, I further investigated whether Hox proteins compete for the binding of Cdt1 to Geminin. The Cdt1 protein in the 11.5 d.p.c. mouse embryonic extracts was pulled-down with Geminin-coupled beads. The pull-down of Cdt1 was prominently decreased by a pre-incubation of the Geminin-coupled beads with GST-Hoxa11 recombinant protein, but not with GST alone (Fig. 3-17A). This result indicated the competition of Hoxa11 and Cdt1 proteins for Geminin binding *in vitro*.

The *in vitro* result was further supported *in vivo* using primary cultured MEFs. When Hoxb7 or Hoxa11 was overexpressed, the amount of Cdt1 co-precipitated by Geminin antibodies was significantly reduced in contrast to the control cells transfected with empty vector, whereas the level of Geminin itself was not affected (Fig. 3-17B). This result indicated that the overexpressed Hox proteins in the cells competed with endogenous Cdt1 for Geminin binding, thus leading to reductions of co-precipitated Cdt1 with Geminin. Together, these data indicate that Hox proteins can compete with Cdt1 for Geminin binding and displace Geminin from the Cdt1-Geminin complex.

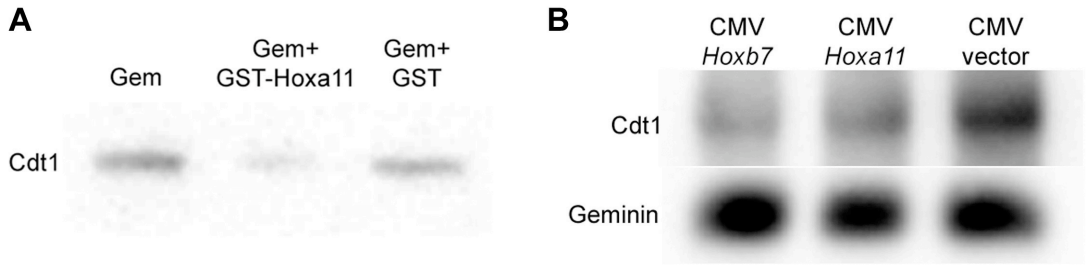

Figure 3-17: Competition for Geminin binding between Cdt1 and Hox proteins. (A) Competition for Geminin binding between Cdt1 and Hoxa11 *in vitro*. Note that the binding of endogenous Cdt1 was significantly reduced when GST-Hoxa11, but not GST alone, was pre-bound to immobilized Geminin. (B) Competition for Geminin binding between Cdt1 and Hox proteins *in vivo*. Note that the co-precipitated endogenous Cdt1 was significantly reduced when Hoxb7 or Hoxa11 was overexpressed in the cells, whereas the level of Geminin itself was not affected.

4. Discussion

4.1 The Roles of Hox and Polycomb Proteins in Cell Cycle Regulation and the Involvement of Geminin

Embryonic growth and patterning along an axis and the colinear activation of *Hox* genes have to be precisely coordinated during development. Positive or negative controls of proliferation must feed back on *Hox* gene activation or repression in order to guarantee proper formations of morphologic structures and to prevent homeosis (Duboule, 1995). Thus, it is not surprising that several indications were reported for roles of Hox as well as Polycomb proteins in proliferation, cell cycle control, and transformation.

In many cases, Hox proteins themselves are involved in proliferation, cell cycle regulation, and transformation. For an instance, Hoxb7 is constitutively expressed in many proliferating melanoma cell lines, but not in normal quiescent melanocytes. To better understand the mechanisms underlying this phenomenon, mechanistic investigations of one of the melanoma cell line demonstrated that basic fibroblast growth factor (*FGF2*) is one of the Hoxb7 direct downstream target genes. Hoxb7 protein transactivates *FGF2* gene transcription through direct binding to its promoter region. Antisense oligonucleotides targeting *Hoxb7* mRNA specifically abolish *FGF2* mRNA transcription and markedly inhibit cell proliferation (Care *et al.*, 1996). Other examples include Hoxb3 or Hoxb4, which can induce cellular proliferation and transformation in Rat-1 cells in cooperation with Pbx homeodomain protein (Krosl *et al.*, 1998). Primary bone marrow cells, retrovirally engineered to overexpress Hoxa9 and co-factors, induce growth factor-dependent leukemic transformation (Kroon *et al.*, 1998). Furthermore, the upregulation of AP-1 activity was identified as one of the molecular mechanisms underlying Hox-induced cellular proliferation and transformation (Krosl and Sauvageau, 2000). Here, my work suggests another possible mechanism through interacting with Geminin thereby releasing Cdt1 by Hox proteins. Then, the released Cdt1 is available for the licensing process, thus promoting DNA replication and cell proliferation.

Not only the Hox proteins, but also the Polycomb complex members are involved in proliferation and cell cycle regulation. Bmi-1 has a key role in regulating the proliferative activity of normal stem and progenitor cells. The proliferative potential of leukemic cells lacking Bmi-1 is compromised, so that these cells finally undergo

proliferation arrest, and show signs of differentiation and apoptosis. These proliferative defects can be completely rescued by Bmi-1 replenishment (Lessard and Sauvageau, 2003). Ring1B deficiency leads to cell cycle inhibition and gastrulation arrest during murine development (Voncken *et al.*, 2003). Obviously, these proliferative effects of Polycomb complex members are probably not achieved through their *Hox* transcription inhibition pathway, since the Hox proteins also play positive roles in cellular proliferation as described above. Nevertheless, if we consider that the Geminin-Polycomb association plausibly resembles Geminin-Hox interaction to reduce the availability of Geminin to Cdt1 binding, cellular proliferation can also be promoted by Polycomb members through a similar mechanism like Hox proteins.

4.2 The Association between Geminin and the Polycomb Complex

In the study, an overexpression or a loss-of-function of Geminin along the whole right side of neural tube resulted in a shift of *Hoxb9* anterior transcription boundary only within one or two segments instead of the whole neural tube (Fig. 3-7, 10, 11). Similarly in previous studies, despite the ubiquitous presence of *PcG* and *trxG* mRNAs during development, global alterations of *Hox* gene transcription have not been observed in the *PcG* or *trxG* mutant mice (Schumacher and Magnuson, 1997). The shiftes in *Hox* gene expression boundaries and skeletal transformations involve only one to two segments, and are neither fully penetrant nor observed in all tissues. This restricted boundary shifts within normal target tissues implies several possibilities. First, the distribution of and the interplay between repressors and activators vary regionally. Second, only *Hox* expression boundaries are sensitive to the presence of absence of these upstream regulators. Third, functional redundancy among trans-acting proteins masks the loss of a single component outside of expression boundaries, which is substantiated by the exacerbated phenotypes of homozygous mutant for two Polycomb members. These three possibilities can serve as the explanations of the limited shift of *Hoxb9* anterior transcription boundary in my study and mild homeotic transformations in mutant mice, alone of synergically.

Three findings on Geminin could help to define the functional phase of the Polycomb complex during the cell cycle. Firstly, Geminin is only available from the early S phase to the end of the mitosis. Secondly, this transient association with Geminin is crucial for Polycomb to inhibit *Hox* gene transcription, since a loss of Geminin function in the embryo by either dominant-negative Scmh1 or siRNA leads

to a de-repression of *Hox* gene transcription (Luo *et al.*, 2004) Thirdly, the mitotic phase is not the functional phase, since the complete Polycomb complex does not remain at its target site all the way through mitosis, although individual members could remain associated with the mitotic chromosome (Buchenau *et al.*, 1998). Therefore, the repression of *Hox* genes by the Polycomb complex plausibly takes place at the S and G2 phase of the cell cycle (Luo and Kessel, 2004a). This is exactly coincident with a previously reported result, demonstrating that *Hoxc10* gene expression is initiated at the late G1 phase of the cell cycle (Gabellini *et al.*, 2003).

Geminin seems not to contribute to the transcriptional memory, the "memory body", epigenetically maintained by Polycomb complexes (Francis and Kingston, 2001), since it is absent from the nucleus in some phases of cell cycle. However, Geminin definitively contributes to the "functional body" of the complex, since its removal from the complex, either by dominant-negative titration or by siRNA-mediated knock-down, de-represses *Hox* gene transcription. The componential difference between the "memory body" and the "functional body", and thus the mechanism underlying the maintenance of Polycomb repression throughout replication or mitosis still remains unclear. But, apparently, to perform its transcriptional repression function through each cell division, the "memory body" will recruit many transient components, including Geminin, to form the functional Polycomb complex (Luo and Kessel, 2004a).

4.3 The Direct Interaction between Geminin and Hox Proteins

Geminin not only inhibits *Hox* gene transcription through Polycomb-mediated interaction, but also binds to the homeodomains of Hox proteins directly. This direct interaction blocks the Hox homeodomain, inhibits its binding to DNA, and thus prohibits a regulatory function in downstream transcription, as was demonstrated in biochemical assays. Surprisingly little is known about downstream targets of vertebrate *Hox* genes, be it in an embryonic context or in tissue culture cells. However, as depicted above, a relatively well characterized example is the relationship between Hoxb7 as an activator, and *FGF2* in a melanoma cell line. In this experimental system it was shown that a modulation of the Geminin level led to reciprocal changes in the level of FGF2. Thus, the sequestration of a Hox protein and the consequent transcriptional inhibition of its downstream target *FGF2* by Geminin correlated with the deceleration of cell cycle and cell proliferation, adding a second

mechanism of action, besides the well-defined Cdt1 binding pathway (Luo and Kessel, 2004a).

The involvement of Geminin in the function of *Hox* genes accentuates its role as a regulator of embryonic processes. A different evidence for such a role was previously pointed out, when a function in the neuralization of ectodermal cells was shown in the frog Xenopus (Kroll *et al.*, 1998). During eye development of the Medaka fish, Geminin directly interacts and antagonizes the role of another homeobox protein, Six3. Different over-doses of Geminin in the embryo result in smaller eyes, cyclopia, or loss of the entire forebrain, phenotypes resembling those after a loss of Six3 function (Del Bene *et al.*, 2004; Carl *et al.*, 2002). Mechanistically, this shows that by means of direct binding and inhibiting Six3, Geminin can induce cellular proliferation inhibition accompanied by premature neural induction and apoptosis. Since *Hox* genes and *Six3* all belong to the homeobox family, the question arises, if and how other homeodomain proteins might interact with Geminin.

4.4 The Coordination of Cell Cycle and Developmental Control by Geminin

The Hox interaction regions of Geminin partly overlap with its coiled-coil domain that has been demonstrated to be the Cdt1 binding and re-replication inhibition domain. Hence, there is a competition between the Hox-Geminin, and the Cdt1-Hox interaction (Fig. 4-1). If Cdt1 binds to Geminin, Hox proteins can be expected to be released from the Geminin inhibition. They would then be free to recognize and bind to enhancer sequences of their downstream target genes, and to activate their transcription. In the meantime, Cdt1 would be available to bind to Geminin, and not for the initiation of replication. This sequestration of Cdt1 during embryonic development would impede proliferation and, in effect, promote differentiation. Vice versa, if the Geminin-Hox association is dominant and Cdt1 is available for DNA replication, the transcriptional activation of Hox downstream target genes and the subsequent cell differentiation will be hampered, while proliferation will be favoured. These Geminin-mediated, competitive interactions establish an equilibratory system in the cells between Cdt1 and Hox proteins, or, more generally, between proliferation and differentiation (Fig. 4-1). It is most likely, that further factors are involved in the establishment of this equilibrium, and Polycomb complex members appear to be likely candidates. Post-translational polyubiquitination of Geminin can influence its interaction with Cdt1 (Li and Blow, 2004), and other modifications like

phosphorylation of Geminin have also been demonstrated (Kulartz *et al.*, 2003). However, the role of protein modifications for the affinity of Geminin to Hox proteins, and thus for the Hox-Geminin-Cdt1 equilibrium, are still not known. The qualitative and quantitative differences of the components in this system will finally decide, whether a cell will continue its proliferation, or start to undergo differentiation.

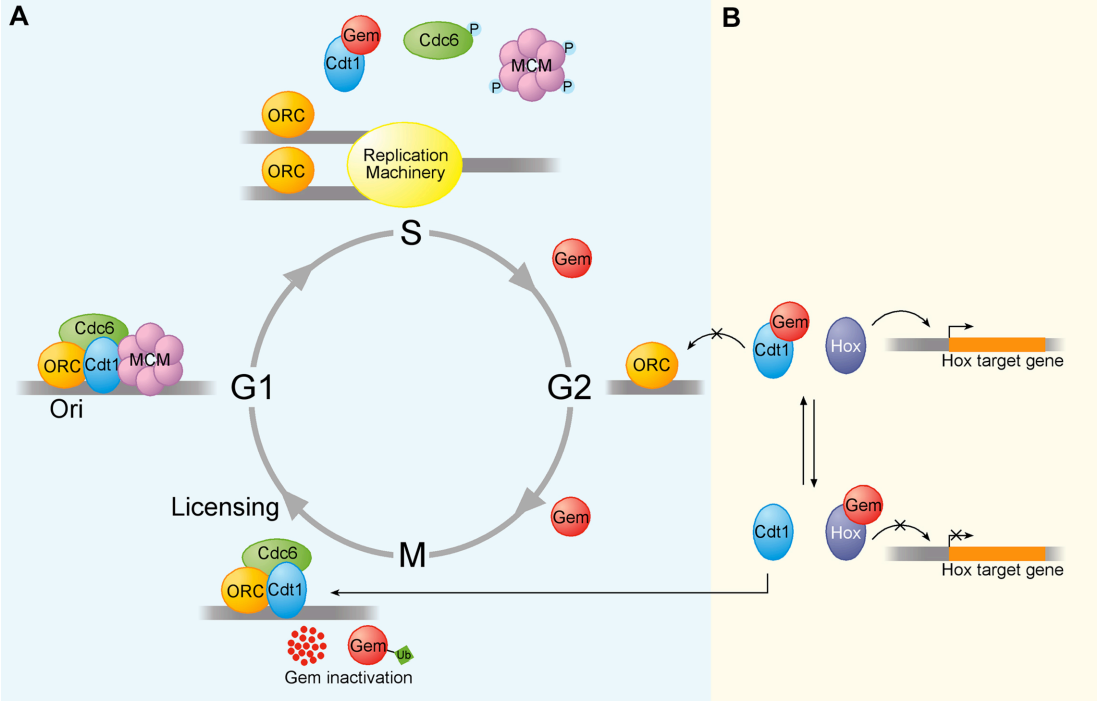

Figure 4-1: (A) The role of Geminin in cell cycle regulation through Cdt1 sequestration. (B) The competition of Hox and Cdt1 for Geminin binding. These competitive interactions establish an equilibratory system to decide on cellular proliferation or differentiation. P: phosphorylation. Ub: ubiquitination (Lygerou and Nurse, 2000; Luo and Kessel, 2004a).

A coordination between proliferative and differential controls is essential for embryonic development. This is particularly evident in the patterning of the antero-posterior axis controlled by the colinear activation of *Hox* genes. Positive or negative controls of proliferation must feed back on *Hox* gene activation or repression in order to guarantee proper formations of anatomical structures. If proliferation and *Hox* gene activation run out of register, a proper structure will be generated at a wrong place. Such a modification would perfectly fit a type of natural variation defined as "homeosis". In vertebrates, homeotic transformations are especially apparent along

the vertebral column, when for example the base of the skull develops as a vertebra, or ribs develop in the cervical or lumbar regions of the vertebral column (Kessel and Gruss, 1991). Geminin is involved both in the regulation of proliferation by arresting Cdt1 and inhibiting rereplication during cell cycle, and in the regulation of Hox- and Polycomb-dependent embryonic patterning. Through its participation in both multiprotein machineries, Geminin could be a key element in the coordination of cell cycle and developmental control.

5. Summary and Conclusions

In the work, I have shown that murine Geminin associates transiently with members of the *Hox*-repressing Polycomb complex dependent on the cell cycle, with the chromatin of *Hox* regulatory DNA elements, and with Hox proteins. Gain- and loss-of-function experiments in the chick neural tube demonstrate that Geminin modulates the anterior boundary of *Hoxb9* transcription, indicating a Polycomb-like activity. The interaction between Geminin and Hox homeodomains blocks the binding of Hox proteins to DNA, inhibits the Hox dependent transcriptional activation of reporter and endogenous downstream target genes, and displaces Cdt1 from its complex with Geminin. Thus, the work suggests that Geminin is involved in two processes controlled by multiprotein complexes. One is the specification of cellular identity during embryogenesis, which is controlled by Hox proteins and the Polycomb complex, including Scmh1 (Fig. 5-1A,B). The other is the replication initiation of DNA during the cell cycle, which is controlled by ORC, Cdc6, Cdt1, and MCM complex (Fig. 5-1C). The participations of Geminin in these two processes are competitive with each other (Fig. 5-1C). Therefore, by establishing this competitive regulation, Geminin functions as a coordinator between developmental and proliferative control (Luo *et al.*, 2004).

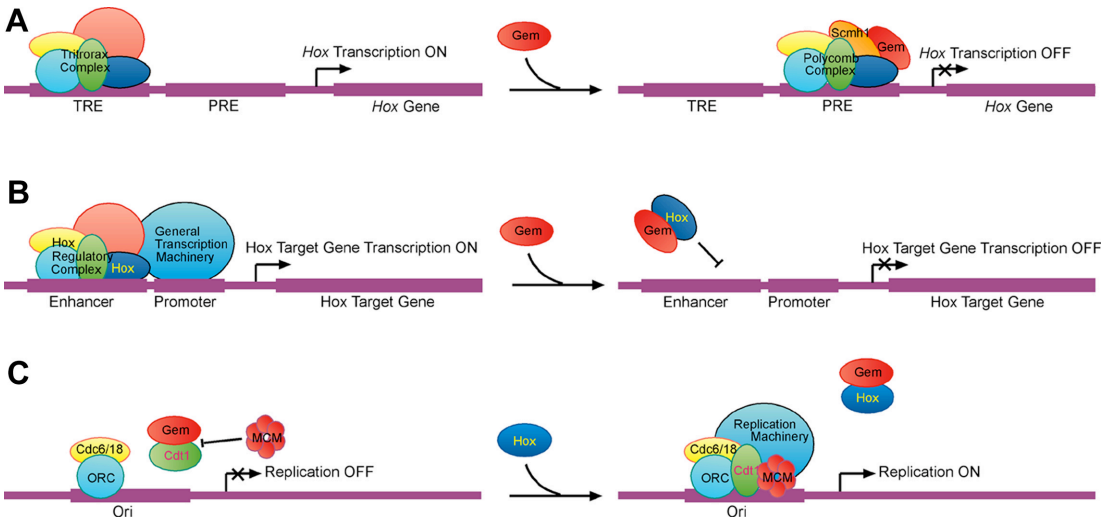

Figure 5-1: Geminin is involved in two processes controlled by multi-protein complexes and establishes their competitive regulation. (A, B) Geminin is involved in the specification of cellular identity during embryogenesis, which is controlled by Hox proteins and the Polycomb complex. (C) Geminin plays an important role in the replication initiation of DNA and preventing rereplication

during the cell cycle. The participations of Geminin in these two processes are competitive with each other (Luo and Kessel, 2004b).

References:

Akam M. The molecular basis for metameric pattern in the Drosophila embryo. *Development*, **101:** 1-22 (1987).

Akasaka T, Kanno M, Balling R, Mieza MA, Taniguchi M and Koseki H. A role for mel-18, a Polycomb group-related vertebrate gene, during the anteroposterior specification of the axial skeleton. *Development*, **122:** 1513-22 (1996).

Barna M, Merghoub T, Costoya JA, Ruggero D, Branford M, Bergia A, Samori B and Pandolfi PP. Plzf mediates transcriptional repression of HoxD gene expression through chromatin remodeling. *Dev. Cell*, **3:** 499-510 (2002).

Bateson W. Materials for the study of variation treated with special regard to discontinuity in the origin of species. London: Macmillan (1894).

Bell SP and Dutta A. DNA replication in eukaryotic cell. *Annu. Rev. Biochem.*, **71:** 333-74 (2002).

Bell SP and Stillman B. ATP-dependent recognition of eukaryotic origins of DNA replication by a multiprotein complex. *Nature*, **357:** 128-34 (1992).

Blow JJ and Laskey RA. A role for the nuclear envelope in controlling DNA replication within the cell cycle. *Nature*, **332:** 546-8 (1988).

Bornemann D, Miller E and Simon J. The Drosophila Polycomb group gene Sex comb on midleg (Scm) encodes a zinc finger protein with similarity to polyhomeotic protein. *Development*, **122:** 1621-30 (1996).

Buchenau P, Hodgson J, Strutt H and Arndt-Jovin DJ. The distribution of polycomb-group proteins during cell division and development in Drosophila embryos: impact on models for silencing. *J. Cell Biol.*, **141:** 469-81 (1998).

Burke AC, Nelson CE, Morgan BA and Tabin C. Hox genes and the evolution of vertebrate axial morphology. *Development*, **121:** 333-46 (1995).

Calzada A, Sanchez M, Sanchez E and Bueno A. The stability of the Cdc6 protein is regulated by cyclin-dependent kinase/cyclin B complexes in Saccharomyces cerevisiae. *J. Biol. Chem.*, **275:** 9734-41 (2000).

Care A, Silvani A, Meccia E, Mattia G, Stoppacciaro A, Parmiani G, Peschle C and Colombo MP. HOXB7 constitutively activates basic fibroblast growth factor in melanomas. *Mol. Cell Biol.*, **16:** 4842-51 (1996).

Carl M, Loosli F and Wittbrodt J. Six3 inactivation reveals its essential role for the formation and patterning of the vertebrate eye. *Development*, **129:** 4057-63 (2002).

Carpenter PB, Mueller PR and Dunphy WG. Role for a Xenopus Orc2-related protein in controlling DNA replication. *Nature*, **379:** 357-60 (1996).

Casanova J, Sanchez-Herrero E, Busturia A and Morata G. Double and triple mutant combinations of bithorax complex of Drosophila. *EMBO J.*, **6:** 3103-9 (1987).

Chesnokov I, Remus D and Botchan M. Functional analysis of mutant and wild-type Drosophila origin recognition complex. *Proc. Natl. Acad. Sci. USA*, **98:** 11997-2002 (2001).

Chong JP, Mahbubani HM, Khoo CY and Blow JJ. Purification of an MCM-containing complex as a component of the DNA replication licensing system. *Nature*, **375:** 418-21 (1995).

Coleman TR, Carpenter PB and Dunphy WG. The Xenopus Cdc6 protein is essential for the initiation of a single round of DNA replication in cell-free extracts. *Cell*, **87:** 53-63 (1996).

Cook JG, Chasse DA and Nevins JR. The regulated association of Cdt1 with minichromosome maintenance proteins and Cdc6 in mammalian cells. *J. Biol. Chem.*, **279:** 9625-33 (2004).

Coré N, Bel S, Gaunt SJ, Aurrand-Lions M, Pearce J, Fisher A and Djabali M. Altered cellular proliferation and mesoderm patterning in Polycomb-M33-deficient mice. *Development*, **124:** 721-9 (1997).

Dahmann C, Diffley JF and Nasmyth KA. S-phase-promoting cyclin-dependent kinases prevent re-replication by inhibiting the transition of replication origins to a pre-replicative state. *Curr. Biol.*, **5:** 1257-69 (1995).

Dekker EJ, Pannese M, Houtzager E, Boncinelli E and Durston A. Colinearity in the Xenopus laevis Hox-2 complex. *Mech. Dev.*, **40:** 3-12 (1993).

Del Bene F, Tessmar-Raible K and Wittbrodt J. Direct interaction of geminin and Six3 in eye development. *Nature*, **427:** 745-9 (2004).

Detweiler CS and Li JJ. Ectopic induction of Clb2 in early G1 phase is sufficient to block prereplicative complex formation in Saccharomyces cerevisiae. *Proc. Natl. Acad. Sci. USA*, **95:** 2384-9 (1998).

Drury LS, Perkins G and Diffley JF. The Cdc4/34/53 pathway targets Cdc6p for proteolysis in budding yeast. *EMBO J.*, **16:** 5966-76 (1997).

Duboule D. Patterning in the vertebrate limb. *Curr. Opin. Genet. Dev.*, **1:** 211-6 (1991).

Duboule, D. Vertebrate Hox genes and proliferation: an alternative pathway to homeosis? *Curr. Opin. Genet. Dev.*, **5:** 525–528 (1995).

Duboule D. Vertebrate hox gene regulation: clustering and/or colinearity? *Curr. Opin. Genet. Dev.*, **8:** 514-8 (1998).

Duboule D and Dollé P. The structural and functional organization of the murine HOX gene family resembles that of Drosophila homeotic genes. *EMBO J.*, **8:** 1497-505 (1989).

Dubrulle J, McGrew MJ and Pourquié O. FGF signaling controls somite boundary position and regulates segmentation clock control of spatiotemporal Hox gene activation. *Cell*, **106:** 219-32 (2001).

Dutta A and Bell SP. Initiation of DNA replication in eukaryotic cells. *Annu. Rev. Cell Dev. Biol.*, 13: 293-332 (1997).

Elbashir SM, Harborth J, Lendeckel W, Yalcin A, Weber K and Tuschl T. Duplexes of 21-nucleotide RNAs mediate RNA interference in cultured mammalian cells. *Nature*, **411:** 494-8 (2001).

Elsasser S, Chi Y, Yang P and Campbell JL. Phosphorylation controls timing of Cdc6p destruction: A biochemical analysis. *Mol. Biol. Cell*, **10:** 3263-77 (1999).

Findeisen M, El-Denary M, Kapitza T, Graf R and Strausfeld U. Cyclin A-dependent kinase activity affects chromatin binding of ORC, Cdc6, and MCM in egg extracts of Xenopus laevis. *Eur. J. Biochem.*, **264:** 415-26 (1999).

Francis NJ and Kingston RE. Mechanisms of transcriptional memory. *Nature Rev. Mol. Cell Biol.*, **2:** 409-21 (2001).

Francis NJ, Saurin AJ, Shao Z and Kingston RE. Reconstitution of a functional core polycomb repressive complex. *Mol. Cell*, **8:** 545-56 (2001).

Fujita M, Yamada C, Tsurumi T, Hanaoka F, Matsuzawa K and Inagaki M. Cell cycle- and chromatin binding state-dependent phosphorylation of human MCM heterohexameric complexes. A role for cdc2 kinase. *J. Biol. Chem.* **273:** 17095-101 (1998).

Gabellini D, Colaluca IN, Vodermaier HC, Biamonti G, Giacca M, Falaschi A, Riva S and Peverali FA. Early mitotic degradation of the homeoprotein HOXC10 is potentially linked to cell cycle progression. *EMBO J.*, **22:** 3715-24 (2003).

Gould A. Functions of mammalian Polycomb group and trithorax group related genes. *Curr. Opin. Genet. Dev.*, **7:** 488-94 (1997).

Graham A, Papalopulu N and Krumlauf R. The murine and Drosophila homeobox gene complexes have common features of organization and expression. *Cell*, **57:** 367-78 (1989).

Greer JM, Puetz J, Thomas KR and Capecchi MR. Maintenance of functional equivalence during paralogous Hox gene evolution. *Nature*, **403:** 661-5 (2000).

Hamburger V and Hamilton HL. A series of normal stages in the development of the chick embryo. *J. Morphol.*, **88:** 49-92 (1951).

Harding K, Wedeen C, McGinnis W and Levine M. Spatially regulated expression of homeotic genes in Drosophila. *Science*, **229:** 1236-42 (1985).

Hartwell LH. Three additional genes required for deoxyribonucleic acid synthesis in Saccharomyces cerevisiae. *J. Bacteriol.*,**115:** 966-74 (1973).

Hendrickson M, Madine M, Dalton S and Gautier J. Phosphorylation of MCM4 by cdc2 protein kinase inhibits the activity of the minichromosome maintenance complex. *Proc. Natl. Acad. Sci. USA*, **93:** 12223-8 (1996).

Hodgson B, Li A, Tada S and Blow JJ. Geminin becomes activated as an inhibitor of Cdt1/RLF-B following nuclear import. *Curr. Biol.*, **12:** 678-83 (2002).

Hofmann JF and Beach D. Cdt1 is an essential target of the Cdc10/Sct1 transcription factor: requirement for DNA replication and inhibition of mitosis. *EMBO J.*, **13:** 425-34 (1994).

Horan GS, Ramirez-Solis R, Featherstone MS, Wolgemuth DJ, Bradley A and Behringer RR. Compound mutants for the paralogous hoxa-4, hoxb-4, and hoxd-4 genes show more complete homeotic transformations and a dose-dependent increase in the number of vertebrae transformed. *Genes Dev.*, **9:** 1667-77 (1995).

Hua XH and Newport J. Identification of a preinitiation step in DNA replication that is independent of origin recognition complex and cdc6, but dependent on cdk2. *J. Cell Biol.* **140:** 271-81 (1998).

Hua XH, Yan H and Newport J. A role for Cdk2 kinase in negatively regulating DNA replication during S phase of the cell cycle. *J. Cell Biol.*, **137:** 183-92 (1997).

Hunt P and Krumlauf R. Deciphering the Hox code: clues to patterning branchial regions of the head. *Cell*, **66:** 1075-8 (1991).

Ishimi Y. A DNA helicase activity is associated with an MCM4, -6, and -7 protein complex. *J. Biol. Chem.*, **272:** 24508-13 (1997).

Ishimi Y and Komamura-Kohno Y. Phosphorylation of Mcm4 at specific sites by cyclin-dependent kinase leads to loss of Mcm4,6,7 helicase activity. *J. Biol. Chem.*, **276:** 34428-33 (2001).

Ishimi Y, Komamura-Kohno Y, You Z, Omori A and Kitagawa M. Inhibition of Mcm4,6,7 helicase activity by phosphorylation with cyclin A/Cdk2. *J. Biol. Chem.*, **275:** 16235-41 (2000).

Izpisua-Belmonte JC, Falkenstein H, Dollé P, Renucci A and Duboule D. Murine genes related to the Drosophila AbdB homeotic genes are sequentially expressed during development of the posterior part of the body. *EMBO J.*, **10:** 2279-89 (1991).

Jiang W, Wells NJ and Hunter T. Multistep regulation of DNA replication by Cdk phosphorylation of HsCdc6. *Proc. Natl. Acad. Sci. USA*, **96:** 6193-8 (1999).

Kal AJ, Mahmoudi T, Zak NB and Verrijzer CP. The Drosophila brahma complex is an essential coactivator for the trithorax group protein zeste. *Genes Dev.*, **14:** 1058-71 (2000).

Kaufman TC, Seeger MA and Olsen G. Molecular and genetic organization of the antennapedia gene complex of Drosophila melanogaster. *Adv. Genet.*, **27:** 309-362 (1990).

Kelly TJ and Brown GW. Regulation of chromosome replication. *Annu. Rev. Biochem.*, 69: 829-80 (2000).

Kessel M. Respecification of vertebral identities by retinoic acid. *Development*, **115:** 487-501 (1992).

Kessel M. Reversal of axonal pathways from rhombomere 3 correlates with extra Hox expression domains. *Neuron*, **10:** 379-93 (1993).

Kessel M and Gruss P. Homeotic transformations of murine vertebrae and concomitant alteration of Hox codes induced by retinoic acid. *Cell*, **67:** 89-104 (1991).

Klemm RD, Austin RJ and Bell SP. Coordinate binding of ATP and origin DNA regulates the ATPase activity of the origin recognition complex. *Cell*, **88:** 493-502 (1997).

Klemm RD and Bell SP. ATP bound to the origin recognition complex is important for preRC formation. *Proc. Natl. Acad. Sci. USA*, **98:** 8361-7 (2001).

Kmita M, Fraudeau N, Herault Y and Duboule D. Serial deletions and duplications suggest a mechanism for the collinearity of Hoxd genes in limbs. *Nature*, **420:** 145-50 (2002).

Kmita M, van der Hoeven F, Zákány J, Krumlauf R and Duboule D. Mechanisms of *Hox* gene colinearity: transposition of the anterior *Hoxb1* gene into the posterior *HoxD* complex. *Genes Dev.*, **14:** 198-211 (2000).

Kondo T and Duboule D. Breaking colinearity in the mouse HoxD complex. *Cell*, **97:** 407-17 (1999).

Kreitz S, Ritzi M, Baack M and Knippers R. The human origin recognition complex protein 1 dissociates from chromatin during S phase in HeLa cells. *J. Biol. Chem.*, **276:** 6337-42 (2001).

Kroll KL, Salic AN, Evans LM and Kirschner MW. Geminin, a neuralizing molecule that demarcates the future neural plate at the onset of gastrulation. *Development*, **125:** 3247-58 (1998).

Kroon E, Krosl J, Thorsteinsdottir U, Baban S, Buchberg AM and Sauvageau G. Hoxa9 transforms primary bone marrow cells through specific collaboration with Meis1a but not Pbx1b. *EMBO J.*, **17:** 3714-25 (1998).

Krosl J, Baban S, Krosl G, Rozenfeld S, Largman C and Sauvageau G. Cellular proliferation and transformation induced by HOXB4 and HOXB3 proteins involves cooperation with PBX1. *Oncogene*, **16:** 3403-12 (1998).

Krosl J and Sauvageau G. AP-1 complex is effector of Hox-induced cellular proliferation and transformation. *Oncogene*, **19:** 5134-41 (2000).

Krumlauf R. Hox genes in vertebrate development. *Cell*, **78:** 191-201 (1994).

Kubota Y, Mimura S, Nishimoto S, Masuda T, Nojima H and Takisawa H. Licensing of DNA replication by a multi-protein complex of MCM/P1 proteins in Xenopus eggs. *EMBO J.* **16:** 3320-31 (1997).

Kulartz M, Kreitz S, Hiller E, Damoc EC, Przybylski M and Knippers R. Expression and phosphorylation of the replication regulator protein geminin. *Biochem. Biophys. Res. Commun.*, **305:** 412-20 (2003).

Labib K and Diffley JF. Is the MCM2-7 complex the eukaryotic DNA replication fork helicase? *Curr. Opin. Genet. Dev.*, **11:** 64-70 (2001).

Labib K, Diffley JF and Kearsey SE. G1-phase and B-type cyclins exclude the DNA-replication factor Mcm4 from the nucleus. *Nature Cell Biol.*, **1:** 415-22 (1999).

Labib K, Tercero JA and Diffley JF. Uninterrupted MCM2-7 function required for DNA replication fork progression. *Science*, **288:** 1643-7 (2000).

Lagos-Quintana M, Rauhut R, Meyer J, Borkhardt A and Tuschl T. New microRNAs from mouse and human. *RNA*, **9:** 175-9 (2003).

Lawrence PA and Morata G. Homeobox genes: their function in Drosophila segmentation and pattern formation. *Cell*, **78:** 181-189 (1994).

Lessard J and Sauvageau G. Bmi-1 determines the proliferative capacity of normal and leukaemic stem cells. *Nature*, **423:** 255-60 (2003).

Lewis EB. A gene complex controlling segmentation in Drosophila. *Nature*, **276:** 565-70 (1978).

Li A and Blow JJ. Non-proteolytic inactivation of geminin requires CDK-dependent ubiquitination. *Nature Cell Biol.*, **6:** 260-7 (2004).

Li X, Zhao Q, Liao R, Sun P and Wu X. The SCF (Skp2) ubiquitin ligase complex interacts with the human replication licensing factor Cdt1 and regulates Cdt1 degradation. *J. Biol. Chem.*, **278:** 30854-8 (2003).

Liu E, Li X, Yan F, Zhao Q and Wu X. Cyclin-dependent kinases phosphorylate human Cdt1 and induce its degradation. *J. Biol. Chem.*, **279:** 17283-8 (2004).

Luo L and Kessel M. Geminin coordinates cell cycle and developmental control. *Cell Cycle*, **3:** 711-4 (2004a).

Luo L and Kessel M. Coordination between patterning and cell cycle control by Geminin. *MPIbpc News*, **10(5):** 1-4 (2004b).

Luo L, Yang X, Takihara Y, Knoetgen H and Kessel M. The cell-cycle regulator geminin inhibits Hox function through direct and polycomb-mediated interactions. *Nature*, **427:** 749-53 (2004).

Lygerou Z and Nurse P. Cell cycle. License withheld--geminin blocks DNA replication. *Science*, **290:** 2271-3 (2000).

Madine MA, Khoo CY, Mills AD and Laskey RA. MCM3 complex required for cell cycle regulation of DNA replication in vertebrate cells. *Nature*, **375:** 421-4 (1995).

Maiorano D, Moreau J and Mechali M. XCDT1 is required for the assembly of pre-replicative complexes in Xenopus laevis. *Nature*, **404:** 622-5 (2000).

McGarry TJ. Geminin deficiency causes a Chk1-dependent G2 arrest in Xenopus. *Mol. Biol. Cell*, **13:** 3662-71 (2002).

McGarry TJ and Kirschner MW. Geminin, an inhibitor of DNA replication, is degraded during mitosis. *Cell*, **93:** 1043-53 (1998).

McGinnis W, Levine MS, Hafen E, Kuroiwa A and Gehring WJ. A conserved DNA sequence in homoeotic genes of the Drosophila Antennapedia and bithorax complexes. *Nature*, **308:** 428-33 (1984a).

McGinnis W, Garber RL, Wirz J, Kuroiwa A and Gehring WJ. A homologous protein-coding sequence in Drosophila homeotic genes and its conservation in other metazoans. *Cell*, **37:** 403-08 (1984b).

Mihaylov IS, Kondo T, Jones L, Ryzhikov S, Tanaka J, Zheng J, Higa LA, Minamino N, Cooley L and Zhang H. Control of DNA replication and chromosome ploidy by geminin and cyclin A. *Mol. Cell Biol.*, **22:** 1868-80 (2002).

Mizushima T, Takahashi N and Stillman B. Cdc6p modulates the structure and DNA binding activity of the origin recognition complex in vitro. *Genes Dev.*, **14:** 1631-41 (2000).

Nguyen VQ, Co C, Irie K and Li JJ. Clb/Cdc28 kinases promote nuclear export of the replication initiator proteins Mcm2-7. *Curr. Biol.*, **10:** 195-205 (2000).

Nguyen VQ, Co C and Li JJ. Cyclin-dependent kinases prevent DNA re-replication through multiple mechanisms. *Nature*, **411:** 1068-73 (2001).

Nishitani H, Lygerou Z, Nishimoto T and Nurse P. The Cdt1 protein is required to license DNA for replication in fission yeast. *Nature*, **404:** 625-8 (2000).

Nishitani H, Taraviras S, Lygerou Z and Nishimoto T. The human licensing factor for DNA replication Cdt1 accumulates in G1 and is destabilized after initiation of S-phase. *J. Biol. Chem.*, **276:** 44905-11 (2001).

Ogawa Y, Takahashi T and Masukata H. Association of fission yeast Orp1 and Mcm6 proteins with chromosomal replication origins. *Mol. Cell Biol.*, **19:** 7228-36 (1999).

Pak DT, Pflumm M, Chesnokov I, Huang DW, Kellum R, Marr J, Romanowski P and Botchan MR. Association of the origin recognition complex with heterochromatin and HP1 in higher eukaryotes. *Cell*, 91: 311-23 (1997).

Pereverzeva I, Whitmire E, Khan B and Coue M. Distinct phosphoisoforms of the Xenopus Mcm4 protein regulate the function of the Mcm complex. *Mol. Cell Biol.*, **20:** 3667-76 (2000).

Perkins G and Diffley JF. Nucleotide-dependent prereplicative complex assembly by Cdc6p, a homolog of eukaryotic and prokaryotic clamp-loaders. *Mol. Cell*, **2:** 23-32 (1998).

Petersen BO, Wagener C, Marinoni F, Kramer ER, Melixetian M, Denchi EL, Gieffers C, Matteucci C, Peters JM and Helin K. Cell cycle- and cell growth-regulated proteolysis of mammalian CDC6 is dependent on APC-CDH1. *Genes Dev.*, **14:** 2330-43 (2000).

Petruk S, Sedkov Y, Smith S, Tillib S, Kraevski V, Nakamura T, Canaani E, Croce CM and Mazo A. Trithorax and dCBP acting in a complex to maintain expression of a homeotic gene. *Science*, **294:** 1331-4 (2001).

Pflumm MF and Botchan MR. Orc mutants arrest in metaphase with abnormally condensed chromosomes. *Development*, **128:** 1697-707 (2001).

Quinn LM, Herr A, McGarry TJ and Richardson H. The Drosophila Geminin homolog: roles for Geminin in limiting DNA replication, in anaphase and in neurogenesis. *Genes Dev.*, **15:** 2741-54 (2001).

Ramirez-Solis R, Zheng H, Whiting J, Krumlauf R and Bradley A. Hoxb-4 (Hox-2.6) mutant mice show homeotic transformation of a cervical vertebra and defects in the closure of the sternal rudiments. *Cell*, **73:** 279-94 (1993).

Riddihough G. Homing in on the homeobox. *Nature*, **357:** 643-4 (1992).

Romanowski P, Madine MA, Rowles A, Blow JJ and Laskey RA. The Xenopus origin recognition complex is essential for DNA replication and MCM binding to chromatin. *Curr. Biol.*, **6:** 1416-25 (1996).

Rowles A, Chong JP, Brown L, Howell M, Evan GI and Blow JJ. Interaction between the origin recognition complex and the replication licensing system in Xenopus. *Cell*, **87:** 287-96 (1996).

Rowles A, Tada S and Blow JJ. Changes in association of the Xenopus origin recognition complex with chromatin on licensing of replication origins. *J. Cell Sci.*, **112:** 2011-8 (1999).

Saha P, Chen J, Thome KC, Lawlis SJ, Hou ZH, Hendricks M, Parvin JD and Dutta A. Human CDC6/Cdc18 associates with Orc1 and cyclin-cdk and is selectively eliminated from the nucleus at the onset of S phase. *Mol. Cell Biol.*, **18:** 2758-67 (1998).

Sakai Y, Meno C, Fujii H, Nishino J, Shiratori H, Saijoh Y, Rossant J and Hamada H. The retinoic acid-inactivating enzyme CYP26 is essential for establishing an uneven distribution of retinoic acid along the anterio-posterior axis within the mouse embryo. *Genes Dev.*, **15:** 213-25 (2001).

Sánchez-Herrero E, Vernos I, Marco R and Morata G. Genetic organization of Drosophila bithorax complex. *Nature*, **313:** 108-13 (1985).

Schock F, Reischl J, Wimmer E, Taubert H, Purnell BA and Jäckle H. Phenotypic suppression of empty spiracles is prevented by buttonhead. *Nature*, **405:** 351-4 (2000).

Schumacher A and Magnuson T. Murine Polycomb- and trithorax-group genes regulate homeotic pathways and beyond. *Trends Genet.*, **13:** 167-70 (1997).

Scott MP and Weiner AJ. Structural relationships among genes that control development: sequence homology between the Antennapedia, Ultrabithorax, and fushi tarazu loci of Drosophila. *Proc. Natl. Acad. Sci.*, **81:** 4115-9 (1984).

Seki T and Diffley JF. Stepwise assembly of initiation proteins at budding yeast replication origins in vitro. *Proc. Natl. Acad. Sci. USA*, 97: 14115-20 (2000).

Sharpe J, Nonchev S, Gould A, Whiting J and Krumlauf R. Selectivity, sharing and competitive interactions in the regulation of *Hoxb* genes. *EMBO J.*, **17:** 1788-1798 (1998).

Shreeram S, Sparks A, Lane DP and Blow JJ. Cell type-specific responses of human cells to inhibition of replication licensing. *Oncogene*, **21:** 6624-32 (2002).

Simeone A, Acampora D, Arcioni L, Andrews PW, Boncinelli E and Mavilio F. Sequential activation of HOX2 homeobox genes by retinoic acid in human embryonal carcinoma cells. *Nature*, **346:** 763-6 (1990).

Simon JA and Tamkun JW. Programming off and on states in chromatin: mechanisms of Polycomb and trithorax group complexes. *Curr. Opin. Genet. Dev.*, **12:** 210-8 (2002).

Spitz F, Gonzalez F and Duboule D. A global control region defines a chromosomal regulatory landscape containing the HoxD cluster. *Cell*, **113:** 405-17 (2003).

Sugimoto N, Tatsumi Y, Tsurumi T, Matsukage A, Kiyono T, Nishitani H and Fujita M. Cdt1 phosphorylation by cyclin A-dependent kinases negatively regulates its function without affecting geminin binding. *J. Biol. Chem.*, **279:** 19691-7 (2004).

Suzuki M, Mizutani-Koseki Y, Fujimura Y, Miyagishima H, Kaneko T, Takada Y, Akasaka T, Tanzawa H, Takihara Y, Nakano M, Masumoto H, Vidal M, Isono K and Koseki H. Involvement of the Polycomb-group gene Ring1B in the specification of the anterior-posterior axis in mice. *Development*, **129:** 4171-83 (2002).

Tada S, Li A, Maiorano D, Mechali M and Blow JJ. Repression of origin assembly in metaphase depends on inhibition of RLF-B/Cdt1 by geminin. *Nature Cell Biol.*, **3:** 107-13 (2001).

Takihara Y, Tomotsune D, Shirai M, Katoh-Fukui Y, Nishii K, Motaleb MA, Nomura M, Tsuchiya R, Fujita Y, Shibata Y, Higashinakagawa T and Shimada K. Targeted disruption of the mouse homologue of the Drosophila polyhomeotic gene leads to altered anteroposterior patterning and neural crest defects. *Development*, **124:** 3673-82 (1997).

Tanaka T, Knapp D and Nasmyth K. Loading of an Mcm protein onto DNA replication origins is regulated by Cdc6p and CDKs. *Cell*, **90:** 649-60 (1997).

Tomotsune D, Takihara Y, Berger J, Duhl D, Joo S, Kyba M, Shirai M, Ohta H, Matsuda Y, Honda BM, Simon J, Shimada K, Brock HW and Randazzo F. A novel member of murine Polycomb-group proteins, Sex comb on midleg homolog protein, is highly conserved, and interacts with Rae28/Mph1 in vitro. *Differentiation*, **65:** 229-39 (1999).

van der Vlag J and Otte AP. Transcriptional repression mediated by the human polycomb-group protein EED involves histone deacetylation. *Nature Genet.*, **23:** 474-8 (1999).

van den Akker E, Fromental-Ramain C, de Graaff W, Le Mouellic H, Brulet P, Chambon P and Deschamps J. Axial skeletal patterning in mice lacking all paralogous group 8 Hox genes. *Development*, **128:** 1911-21 (2001).

Vas A, Mok W and Leatherwood J. Control of DNA rereplication via Cdc2 phosphorylation sites in the origin recognition complex. *Mol. Cell Biol.*, **21:** 5767-77 (2001).

Voncken JW, Roelen BA, Roefs M, de Vries S, Verhoeven E, Marino S, Deschamps J and van Lohuizen M. Rnf2 (Ring1b) deficiency causes gastrulation arrest and cell cycle inhibition. *Proc. Natl. Acad. Sci. USA*, **100:** 2468-73 (2003).

Wakimoto BT, Turner FR and Kaufman TC. Defects in embryogenesis in mutants associated with the antennapedia gene complex of Drosophila melanogaster. *Dev. Biol.*, **102:** 147-72 (1984).

Weinreich M, Liang C and Stillman B. The Cdc6p nucleotide-binding motif is required for loading mcm proteins onto chromatin. *Proc. Natl. Acad. Sci. USA*, **96:** 441-6 (1999).

Wellik DM and Capecchi MR. Hox10 and Hox11 genes are required to globally pattern the mammalian skeleton. *Science*, **301:** 363-7 (2003).

Whittaker AJ, Royzman I and Orr-Weaver TL. Drosophila double parked: a conserved, essential replication protein that colocalizes with the origin recognition complex and links DNA replication with mitosis and the down-regulation of S phase transcripts. *Genes Dev.*, **14:** 1765-76 (2000).

Wohlschlegel JA, Dwyer BT, Dhar SK, Cvetic C, Walter JC and Dutta A. Inhibition of eukaryotic DNA replication by geminin binding to Cdt1. *Science*, **290:** 2309-12 (2000).

Wohlschlegel JA, Kutok JL, Weng AP and Dutta A. Expression of geminin as a marker of cell proliferation in normal tissues and malignancies. *Am. J. Pathol.*, **161:** 267-73 (2002).

Yamaguchi R and Newport J. A role for Ran-GTP and Crm1 in blocking re-replication. *Cell*, **113:** 115-25 (2003).

Yanagi K, Mizuno T, You Z and Hanaoka F. Mouse geminin inhibits not only Cdt1-MCM6 interactions but also a novel intrinsic Cdt1 DNA binding activity. *J. Biol. Chem.*, **277:** 40871-80 (2002).

Yekta S, Shih IH and Bartel DP. MicroRNA-directed cleavage of HOXB8 mRNA. *Science*, **304:** 594-6 (2004).

Yoshida K, Oyaizu N, Dutta A and Inoue I. The destruction box of human Geminin is critical for proliferation and tumor growth in human colon cancer cells. *Oncogene*, **23:** 58-70 (2004).

You Z, Komamura Y and Ishimi Y. Biochemical analysis of the intrinsic Mcm4-Mcm6-mcm7 DNA helicase activity. *Mol. Cell Biol.*, **19:** 8003-15 (1999).

Zàkàny J, Kmita M, Alarcon P, de la Pompa JL and Duboule D. Localized and transient transcription of Hox genes suggests a link between patterning and the segmentation clock. *Cell*, **106:** 207-17 (2001).

Zhong W, Feng H, Santiago FE and Kipreos ET. CUL-4 ubiquitin ligase maintains genome stability by restraining DNA-replication licensing. *Nature*, **423:** 885-9 (2003).

Abbreviations:

APS: ammonium persulphate
3AT: 3-amino-1,2,4-triazole
BMP: bone morphogenetic protein
bp: base pair
BSA: bovine serum albumin
CDK: cyclin dependent kinase
ChIP: chromatin immunoprecipitation
cpm: counts per minute
DAPI: 4,6-diamidino-2-phenylindol
DEPC: diethyl pyrocarbonate
DIG: digoxigenin
DMEM: Dulbecco's modified Eagle's medium
DMFA: dimethylformamide
DMSO: dimethylsulfoxide
dnScmh1: dominant negative sex comb on midleg homolog 1
d.p.c.: days post coitum
EDTA: ethylenediaminetetraacetic acid
EGFP: enhanced green fluorescence protein
EMSA: electrophoretic mobility shift assays
FCS: fetal calf serum
FGF: fibroblast growth factor
GFP: green fluorescence protein
GST: glutathione sulfur transferase
HOM-C: homeotic complex
HRP: horseradish peroxidase
IPTG: isopropylthio-β-D-galactoside
kDa: kilo Dalton
MCM: minichromosome maintenance
MEF: mouse embryonic fibroblast
O.D.: optical density
ORC: origin recognition complex
PBS: phosphate buffered saline

PCR: polymerase chain reaction

PFA: paraformaldehyde

Plzf: promyelocytic leukemia zinc finger

PMSF: phenylmethylsulfonyl fluoride

PRC1: polycomb repressive complex 1

PRE: polycomb response element

pre-RC: pre-replicative complex

rpm: round per minute

RT-PCR: reverse transcription-polymerase chain reaction

Scmh1: sex comb on midleg homolog 1

SDS: sodium dodecyl sulfate

siRNA: small interference RNA

TAC: trithorax acetyltransferase complex

TBE: Tris-borate-EDTA

TCA: trichloride acetate

TEMED: N,N,N',N'-tetramethyl-ethylenediamine

Tm: melting temperature

TRE: trithorax response element

U: units

V: volts

UTR: untranslated region

YY1: yin yang 1

Curriculum Vitae

Personal Data:

Surname:	Luo
Forename:	Lingfei
Nationality:	P. R. China
Birth:	November 4th, 1977; Chongqing, China
Age:	26
Marital Status:	Married
Private Address:	Room 520 Robert-Koch-Str. 38 37075 Göttingen Germany
Telephone:	0049-551-3791655
Work Address:	Department of Molecular Cell Biology Max-Planck-Institute for Biophysical Chemistry Am Fassberg 11 37077 Göttingen Germany
Telephone:	0049-551-2011752
Fax:	0049-551-2011504
E-mail:	lluo@gwdg.de, luolingfei@hotmail.com
Position at Work:	Ph.D.

Scientific Education:

Oct. 2001-Present	Department of Molecular Cell Biology Max-Planck-Institute for Biophysical Chemistry Doctor of Philosophy (Ph.D.)
Oct. 2000-Aug. 2001	International M.Sc./Ph.D. Program "Molecular Biology" Georg August University Göttingen and Max-Planck Research School Master of Science (M.Sc.)
Sep. 1999-Jul. 2000	Shanghai Institute of Biochemistry, Chinese Academy of Sciences

Sep. 1995-Jun. 1999	Department of Biochemistry, Nanjing University Bachelor of Science (B.Sc.)

Publications:

Lingfei Luo, Xiaoping Yang, Yoshihiro Takihara, Hendrik Knoetgen and Michael Kessel. The cell-cycle regulator geminin inhibits Hox function through direct and polycomb-mediated interactions. *Nature*, **427(6976):** 749-753 (2004).

Lingfei Luo and Michael Kessel. Geminin coordinates cell cycle and developmental control. *Cell Cycle*, **3(6):** 711-714 (2004).

Lingfei Luo and Michael Kessel. Coordination between patterning and cell cycle control by Geminin. *MPIbpc News*, **10(5):** 1-4 (2004).

Erzsebet Mernyak, Janos Wolfling, Gabor Bunkoczi, Lingfei Luo, Thomas R. Schneider and Gyula Schneider. Stereoselective Synthesis of the Two *trans*-(16-Hydroxymethyl)-3-methoxy-13a-estra-1,3,5(10)-trien-17-ol Isomers. *Collect. Czech. Chem. Commun.*, **68(6):** 1141-1148 (2003).

Honor:

Gruss-Jäckle-Prize 2003: Awarded by the Gruss-Jäckle foundation on May 6th, 2004 at the Max-Planck-Institute for Biophysical Chemistry in Göttingen.